

**AMINOSILANE-FUNCTIONALIZED CELLULOSIC POLYMERS
FOR INCREASED CARBON DIOXIDE SORPTION**

A Thesis
Presented to
The Academic Faculty

by

Diana Marisol Pacheco Rodriguez

In Partial Fulfillment
of the Requirements for the Degree
Master of Science in Chemical Engineering

Georgia Institute of Technology

December, 2010

Copyright © 2010 by Diana Marisol Pacheco Rodriguez

Aminosilane-Functionalized Cellulosic Polymers
for Increased Carbon Dioxide Sorption

Approved by:

Dr. William J. Koros, Advisor
School of Chemical & Biomolecular Engineering
Georgia Institute of Technology

Dr. Christopher W. Jones
School of Chemical & Biomolecular Engineering
Georgia Institute of Technology

Dr. James Mulholland
School of Civil & Environmental Engineering
Georgia Institute of Technology

Date Approved: August 13, 2010

ACKNOWLEDGEMENTS

I sincerely want to thank my advisor, Dr. William J. Koros, for his advice, his support, his patience and for giving me the great opportunity to work with him. I am deeply grateful for his understanding at all times and his continuous encouragement even for small achievements. I also want to thank Dr. Christopher W. Jones and Dr. James Mulholland for his presence in my Thesis Advisory Committee. Many thanks to our lab manager, J. R. Johnson, for his assistance on every technical problem in the development of my experiments, for his patience and support sharing his knowledge of polymer sorption. The help of my lab mate Dhaval Bhandari performing SEM analysis and discussing results, and the assistance of Dr. Ryan Adams performing IR analysis have been invaluable and are deeply appreciated.

Special thanks to the sponsors of my research project, the King Abdullah University of Science and Technology (KAUST) in Saudi Arabia and the Mexico's National Council on Science and Technology (CONACYT) for their financial support in my studies and research.

Finally, I want to thank God, my parents Carlos and Idalia, my sister Rocío and her family, my brother Carlos, and very specially my lovely husband Pablo, for understanding, listening, supporting and encouraging me at all times.

TABLE OF CONTENTS

Acknowledgements.....	iii
List of Tables.....	vi
List of Figures.....	viii
Summary.....	xii
Chapter 1: Introduction.....	1
Chapter 2: Literature Review.....	6
Chapter 3: Problem Definition and Proposed Approaches.....	12
3.1 Problem Definition.....	12
3.2 Proposed Approaches.....	16
Chapter 4: Humid Grafting of Aminosilanes on High-acetyl Content Cellulose Acetate.....	21
4.1 Background Theory.....	21
4.2 Experimental.....	35
4.3 Results.....	43
4.4 Discussion.....	54
Chapter 5: Anhydrous Grafting of Aminosilanes on Low-acetyl Content Cellulose Acetate.....	64
5.1 Background Theory.....	65
5.2 Experimental.....	68
5.3 Results.....	72
5.4 Discussion.....	87

Chapter 6: Preparation of Cellulose Acetate/Titanium(IV) Oxide Hybrid Polymer.....	94
6.1 Background Theory.....	96
6.2 Experimental.....	99
6.3 Results.....	107
6.4 Discussion.....	136
Chapter 7: Grafting of Aminosilanes on High-acetyl Content Cellulose Acetate Under Optimum Reaction Conditions.....	145
7.1 Experimental.....	146
7.2 Results.....	150
7.3 Discussion.....	165
Chapter 8: Summary, Conclusions and Recommendations for Further Work.....	172
8.1 Summary.....	172
8.2 Conclusions.....	176
8.3 Recommendations for Further Work.....	179
References.....	181

LIST OF TABLES

Table 1	Sigma-Aldrich cellulose acetate typical physical chemical properties.....	35
Table 2	Gelest, Inc. N-(2-aminoethyl)-3-aminoisobutyldimethylmethoxysilane typical properties.....	36
Table 3	Gelest, Inc. aminopropyldimethylethoxysilane typical properties.....	36
Table 4	Reaction conditions for wet amination of high-acetyl cellulose acetate.....	38
Table 5	EA of pure and selected samples of amine-grafted cellulose acetate by a wet grafting procedure.....	46
Table 6	Densities of pure and selected samples of amine-grafted cellulose acetate by wet grafting	47
Table 7	Reaction conditions for dry aminosilanes grafting of low-acetyl content cellulose acetate films.....	71
Table 8	EA of high-acetyl content CA, low-acetyl content CA and aminated low-acetyl content CA films	75
Table 9	Densities of high-acetyl content CA, low-acetyl content CA and aminated LACA films.....	76
Table 10	Titanium tetrachloride typical properties as provided by Sigma-Aldrich....	100
Table 11	Reaction conditions for low-acetyl content cellulose acetate films and high-acetyl content cellulose acetate powder during TiCl_4 reactions....	103
Table 12	Reaction conditions for aminosilane grafting of cellulose acetate/titanium(IV) oxide films.....	106
Table 13	Elemental Analysis of LACA/Ti(IV) oxide films and silanated LACA/Ti(IV) oxide films.....	112
Table 14	Densities of LACA/Ti(IV) oxide films and silanated LACA/Ti(IV) oxide films.....	114
Table 15	Reaction conditions for aminosilane-grafting of high-acetyl content cellulose acetate powder.....	148

Table 16	EA of pure and aminated cellulose acetate powder at dry and wet grafting optimum conditions	154
Table 17	Densities of high-acetyl content cellulose acetate and aminated cellulose acetate samples.....	156

LIST OF FIGURES

Figure 1	Cellulose molecular structure.....	21
Figure 2	Cellulose acetate molecular structure.....	22
Figure 3	CO ₂ sorption isotherms for cellulose acetate grafted samples <i>B</i> , <i>C</i> , and <i>D</i> with C ₉ H ₂₄ N ₂ OSi.....	44
Figure 4	CO ₂ sorption isotherms for cellulose acetate grafted samples <i>E</i> , <i>F</i> , and <i>G</i> with C ₇ H ₁₉ NOSi.....	44
Figure 5	ATR spectrum for high-acetyl content cellulose acetate and wet-grafted cellulose acetate with C ₉ H ₂₄ N ₂ OSi, sample <i>C</i>	50
Figure 6	ATR spectrum for high-acetyl content cellulose acetate and wet-grafted cellulose acetate with C ₇ H ₁₉ NOSi, sample <i>F</i>	50
Figure 7	TG curve for cellulose acetate and wet-grafted cellulose acetate with C ₉ H ₂₄ N ₂ OSi, sample <i>C</i>	52
Figure 8	TG curve for cellulose acetate and wet-grafted cellulose acetate with C ₇ H ₁₉ NOSi, sample <i>F</i>	52
Figure 9	SEM images of (a) and (b): wet-grafted cellulose acetate with C ₉ H ₂₄ N ₂ OSi, sample <i>C</i> ; (c) and (d): wet-grafted cellulose acetate with C ₇ H ₁₉ NOSi, sample <i>F</i>	53
Figure 10	Humid grafting reaction of aminosilanes with hydroxylated species.....	54
Figure 11	Types of bonding and interactions between different aminosilane molecules and cellulose acetate polymer chains.....	59
Figure 12	Reversible equilibrium showing Brönsted protonation of the amino groups by the presence of water and hydrogen-bonded aminosilanes in its absence.....	59
Figure 13	CO ₂ sorption isotherms for low-acetyl content cellulose acetate dense film sample <i>I</i> and aminosilane-grafted samples <i>J</i> and <i>K</i>	73
Figure 14	ATR-IR spectra of high-acetyl content and low-acetyl content cellulose acetate powders.....	80
Figure 15	FT-IR spectra of high-acetyl content and low-acetyl content cellulose acetate films	80

Figure 16	FT-IR spectra of low-acetyl content cellulose acetate film and anhydrous grafted film with $C_9H_{24}N_2OSi$82
Figure 17	FT-IR spectra of low-acetyl content cellulose acetate film and grafted film with $C_7H_{19}NOSi$83
Figure 18	TG curves of high-acetyl and low-acetyl content cellulose acetate Powder.....84
Figure 19	TG curves of high-acetyl, low-acetyl content cellulose acetate powder, and low-acetyl content cellulose acetate film grafted with $C_9H_{24}N_2OSi$ 85
Figure 20	TG curves of high-acetyl, low-acetyl content cellulose acetate powder, and low-acetyl content cellulose acetate film grafted with $C_7H_{19}NOSi$86
Figure 21	SEM images of (a): sample <i>I</i> ; (b): sample <i>J</i> ; (c): sample <i>K</i>87
Figure 22	Ideal anhydrous grafting of aminosilanes on low-acetyl content cellulose acetate films.....88
Figure 23	Possible physisorption mechanisms of CO_2 in low-acetyl content cellulose acetate films.....92
Figure 24	Structure of cellulose/titanium(IV) hydroxide modified with CTSN.....98
Figure 25	Main experimental steps in the preparation of cellulose acetate/titanium(IV) oxide hybrid polymers.....104
Figure 26	CO_2 sorption isotherms for high-acetyl and low-acetyl content cellulose acetate films, cellulose acetate/titanium(IV) oxide film samples <i>L–P</i>108
Figure 27	CO_2 sorption isotherms for cellulose acetate powder and cellulose acetate/titanium(IV) oxide powder, sample <i>Q</i>110
Figure 28	CO_2 sorption isotherms for silanated cellulose acetate/titanium(IV) oxide films, samples <i>R</i> and <i>S</i>111
Figure 29	FT-IR spectra of LACA film and LACA/Ti(IV) oxide film, 0.25 mL $TiCl_4$ for 5h, sample <i>L</i>116
Figure 30	FT-IR spectra LACA film and LACA/Ti(IV) oxide film, 0.25 mL $TiCl_4$, 48h reaction, sample <i>M</i>117

Figure 31	FT-IR spectra of LACA film and LACA/Ti(IV) oxide film, 2.00 mL TiCl ₄ for 5h, sample <i>N</i>	118
Figure 32	FT-IR spectra of LACA film and LACA/Ti(IV) oxide film, 2.00 mL TiCl ₄ for 48h, sample <i>O</i>	119
Figure 33	FT-IR spectra of LACA film and LACA/Ti(IV) oxide film, 0.40 mL TiCl ₄ for 5h, sample <i>P</i>	120
Figure 34	ATR spectra of CA powder and CA/Ti(IV) oxide powder, 0.40 mL TiCl ₄ , 5h reaction, sample <i>Q</i>	121
Figure 35	FT-IR spectra of LACA film and LACA/Ti(IV) oxide film grafted with C ₉ H ₂₄ N ₂ OSi, sample <i>R</i>	122
Figure 36	FT-IR spectra of LACA film and LACA/Ti(IV) oxide film grafted with C ₇ H ₁₉ NOSi, sample <i>S</i>	122
Figure 37	LACA/Titanium(IV) oxide film prepared with 0.25 mL TiCl ₄ /g LACA and 5 h reaction.....	123
Figure 38	LACA/Titanium(IV) oxide film prepared with 0.25 mL TiCl ₄ /g LACA and 48 h reaction.....	124
Figure 39	LACA/Titanium(IV) oxide film prepared with 2.00 mL TiCl ₄ /g LACA and 5 h reaction.....	125
Figure 40	LACA/Titanium(IV) oxide film prepared with 2.00 mL TiCl ₄ /g LACA and 48 h reaction.....	126
Figure 41	LACA/Titanium(IV) oxide film prepared with 0.40 mL TiCl ₄ /g LACA and 5 h reaction.....	127
Figure 42	CA/Titanium(IV) oxide powder prepared with 0.40 mL TiCl ₄ /g CA and 5 h reaction	128
Figure 43	LACA/Ti(IV) oxide film prepared with 0.40 mL TiCl ₄ /g LACA for 5h, grafted with C ₉ H ₂₄ N ₂ OSi.....	129
Figure 44	LACA/Ti(IV) oxide film prepared with 0.40 mL TiCl ₄ /g LACA for 5h, grafted with C ₇ H ₁₉ NOSi.....	130
Figure 45	SEM images of sample <i>L</i> , <i>M</i> , <i>N</i> , <i>O</i> , <i>P</i> , cross-sectional cut sample <i>P</i>	133
Figure 46	SEM images of sample <i>R</i> and <i>S</i>	135

Figure 47	TiCl ₄ reaction with cellulose acetate.....	137
Figure 48	Formation of C–O–Ti–(OEt) ₃ intermediate species through immersion in ethanol.....	137
Figure 49	Main experimental steps in the preparation of aminosilane-functionalized cellulose acetate.....	149
Figure 50	CO ₂ sorption isotherms for samples <i>T</i> , <i>U</i> , <i>V</i> and <i>W</i>	152
Figure 51	CO ₂ sorption isotherms for samples <i>T</i> , <i>X</i> and <i>Y</i>	153
Figure 52	ATR-IR of CA and anhydrous grafting of CA with C ₉ H ₂₄ N ₂ OSi, sample <i>T</i>	157
Figure 53	ATR-IR of CA and humid grafting of CA with C ₉ H ₂₄ N ₂ OSi, sample <i>U</i>	158
Figure 54	ATR-IR of CA and anhydrous grafting of CA with C ₇ H ₁₉ NOSi, sample <i>V</i>	159
Figure 55	ATR-IR of CA and humid grafting of CA with C ₇ H ₁₉ NOSi, sample <i>W</i>	159
Figure 56	TG curves of CA, anhydrous and wet grafting of CA with C ₉ H ₂₄ N ₂ OSi and sample <i>Y</i>	161
Figure 57	TG curves of CA, anhydrous and wet grafting of CA with C ₇ H ₁₉ NOSi.....	162
Figure 58	SEM images of sample <i>T</i> , <i>U</i> , <i>V</i> , and <i>W</i>	164

SUMMARY

Improvement of the efficiency of carbon dioxide (CO₂) separation from flue gases has been identified as a high-priority research area to reduce the total energy cost of carbon capture and sequestration technologies in coal-fired power plants. Efficient CO₂ removal from flue gases by adsorption systems requires the design of novel sorbents capable of capturing, concentrating and recovering CO₂ on a cost-effective basis. The preparation of a novel aminosilane-functionalized cellulosic polymer sorbent by grafting of aminosilanes showed promising performance for CO₂ separation and capture. A strategy for the introduction of N-(2-aminoethyl)-3-aminoisobutyldimethylmethoxysilane functionalities into cellulose acetate backbone by anhydrous grafting is described in this study. The dry sorption capacity of the aminosilane-functionalized cellulosic polymer reached 27 cc (STP) CO₂/ cc sorbent at 1 atm and 39 cc (STP) CO₂/ cc sorbent at 5 atm and 308 K. Exposure to water vapor slightly increased the sorption capacity of the sorbent, suggesting its potential for rapid cyclic adsorption processes under humid feed conditions. In addition, a strategy for the preparation of a cellulose acetate-titanium(IV) oxide sorbent by the reaction of cellulose acetate with titanium tetrachloride is presented. The organic-metal hybrid sorbent presented a sorption capacity of 14 cc (STP) CO₂/ cc sorbent at 1 atm and 49 cc (STP) CO₂/ cc sorbent at 5 atm and 308 K. The novel CO₂ sorbents were characterized in terms of chemical composition, density changes, molecular structure, thermal stability, and surface morphology.

CHAPTER 1

INTRODUCTION

Carbon dioxide (CO₂), a main by-product of fossil fuel combustion processes, has become a major environmental concern due to the gradual increase of its global atmospheric concentration in recent decades. Since the beginning of the age of industrialization, human activities have caused the CO₂ atmospheric concentration to increase by about 35% [1]. This increment has speeded up during the last decades. As of June 2010, the CO₂ concentration in Earth's atmosphere was measured as 392 ppm by volume, while 50 years ago the average atmospheric concentration was about 316 ppm by volume [2]. After water vapor, CO₂ is considered to be the largest contributor to the greenhouse effect by transmitting solar radiation through the atmosphere, but strongly absorbing the infrared and near infrared radiation reflected from Earth's surface. Although in reality there are several factors that contribute to the greenhouse effect, CO₂ has received by far the most attention because of its abundant as flue gas in many industrial processes.

One of the major point sources of CO₂ emissions are coal-fired power plants, since the combustion of coal emits almost twice as much CO₂ per unit of heat energy as does the combustion of natural gas, while the amount emitted from crude oil combustion falls in between that of coal and natural gas [3]. Therefore, the control of CO₂ emissions from coal-fired power plants is an urgent concern that has attracted significant attention

from governments, energy companies, and scientific researchers. Different carbon capture and storage (CCS) strategies have been proposed as a means of mitigating the contribution of CO₂ emissions to global warming from power stations. However, the costs of capture and sequestration of CO₂ has been the main hurdle to overcome for the deployment of many emerging technologies. The separation of CO₂ from flue gases of coal-fired power plants can account for as much as 70-80% of the total energy cost for CO₂ CCS [4]. Therefore, the importance to develop new energy-efficient techniques for CO₂ separation has driven vast efforts from the scientific community for the development of materials and processes that can efficiently and economically capture and isolate CO₂ from flue gases.

Several techniques have been proposed for CO₂ separation and recovery, including chemical absorption and adsorption, physical adsorption and membrane separation. Among these techniques, chemical absorption with aqueous solutions of alkanolamines (monoethanolamine and diethanolamine, among others) is already commercially used for large scale purification of industrial gases (natural gas, syngas, etc.) and in some life support gas purifying systems in submarines, spacecrafts, etc. [5]. The absorption is carried out in packed scrubbing columns where the CO₂ stream and aqueous amine solution are injected in a countercurrent way, allowing the reaction of CO₂ with amines and regenerating the CO₂-containing amine solution at high temperatures [6]. Despite its popularity, several concerns are associated with liquid amine absorption, including high energy requirements for solvent regeneration, extensive corrosion of the equipment [7, 8], and the impact that amine solutions have on the

surrounding ecosystems [9]. The use of membranes for CO₂ separation mainly involves the use of polymeric membranes or amine-modified inorganic membranes [10, 11]. The separation is based on the high permeability of CO₂ through the membranes compared to that of nitrogen gas. This process is efficient in separating CO₂ from gas streams with high volumetric flow rates and high CO₂ concentrations [10]. For applications that fit these characteristics, membrane separation technologies are one of the most realistic and lowest energy consuming CO₂ capture methods. On the other hand, pressure swing adsorption and/or temperature swing adsorption systems consisting of packed beds of novel solid sorbents are emerging technologies with great potential to reduce carbon capture costs in coal-fired power plants. They are suitable for low CO₂ concentration gas streams with large volumetric flow rates, and emerging systems using packed beds of hollow fiber hybrid sorbents have low flue gas pressure drops and low regeneration thermal requirements, allowing to reduce operational and overall CCS costs [12]. However, the success of this and other emerging adsorption technologies relies upon the creation of novel sorbents with high CO₂ sorption efficiencies and low manufacture costs that allow favorable industrial processes economics and the offset of high CO₂ capture costs in coal-fired power plants.

Conventional adsorbents such as zeolite molecular sieves, activated carbons, silica gels, and carbon molecular sieves have been not effective for CO₂ capture from low concentrated gaseous mixtures. Therefore, significant scientific research is in progress to produce suitable adsorbents for different CO₂ emitting sources applications by using all kind of classic and novel materials. Efforts are underway in different directions, ranging

from new approaches of using well known adsorbents as zeolites [12, 13] and activated carbons [14, 15] in the design of complex hybrid materials, to the exploration of totally new materials such as periodic mesoporous silicas [4, 11, 16-21] and metal organic frameworks (MOFs) [22, 23].

With the aim to exploit the efficient amine-CO₂ interactions that has brought liquid amine CO₂ scrubbing to its current status of commercial technology, but avoiding the aforementioned drawbacks of this absorption system, a new generation of amine functionalized mesoporous silica adsorbents have emerged during the last years. This class of materials exhibits large surface area and pore volume, with pore size distribution in the nanometer scale that allow the introduction of amine functionalities on its surface by conventional grafting methods [21]. Due to their ordered mesoporous structure and the possibility to tailor their internal pore system, these materials have attracted the attention of researchers in many fields other than adsorption. However, certain drawbacks have been associated with amine-functionalized mesoporous silicas, like a typical non-homogeneous amine surface coverage and the lost of its mesoscopic ordering. Perhaps even more important is the fact that a significant fraction of the amine groups may be inaccessible to CO₂ when embedded in the silica network [24]. Therefore, it has been found that amine groups only efficiently interact with the gas when the materials maintain an open pore structure after the grafting reactions [25].

Therefore, the development of efficient, reliable, thermally stable and cost-effective sorbents for CO₂ capture from power plant flue gases is still a challenge that

needs to be addressed. In order to reduce the cost of CO₂ capture and sequestration, sorbents with high sorption and long-term regeneration capacities in power-plant flue gas environments, and with low energy requirements for regeneration are needed. The use of these novel adsorbents in periodic cyclic adsorption processes is certainly a potential low-cost carbon capture alternative technology that could meet the present and future economic and environmental constraints placed on CO₂ capture from coal-fired power plants.

CHAPTER 2

LITERATURE REVIEW

Several researchers have investigated the CO₂ sorption properties of cellulose acetate. Jung and coworkers studied the sorption behavior of pyrolyzed cellulose acetate membranes when exposed to helium, carbon dioxide, oxygen and nitrogen [26]. They found that cellulose acetate membranes exhibited intermediate behavior between Knudsen diffusion and molecular sieving gas permeation behavior with a selectivity slightly greater than unity. The removal of CO₂ from natural gas streams using cellulose acetate membranes has also been studied [27], discovering a loss in selectivity due to plasticization of the polymer caused by the sorption of higher hydrocarbons present in natural gas. An effective plasticization-resistant cellulose acetate membrane coated with a fluoropolymer reduced the sorption of higher hydrocarbons. On a different report, a gas chromatographic method was applied to obtain sorption data at low pressures of hydrogen, nitrogen, oxygen, carbon monoxide, carbon dioxide, methane, and propane on cellulose acetate and triacetate [28]. The sorption isotherm for CO₂ was almost linear and a Henry's constants for the different supports were calculated from it. The sorption of CO₂, hydrogen sulfide, and vapors of acetone on di- and tri-acetate cellulose films was studied under static and dynamic conditions by Denisova and coworkers [29]. The CO₂ is first separated using a cellulose acetate hollow fiber membrane separation device and secondarily concentrated by a pressure swing adsorption device loaded with alumina pellets or synthetic zeolites. The CO₂ capture via a rapid temperature swing adsorption

system from power plant flue gases has been developed by Lively et al. [12]. The system uses cellulose acetate hollow fibers with sorbent particles embedded in the porous fiber wall and runs cooling water through the bores of the fibers during adsorption and switches to steam when desorbing the CO₂. A dense lumen layer is coated in the interior of the fiber wall to avoid mass transfer between the core and the fiber sheath. On another study, sorption isotherms for CO₂ in homogeneous dense cellulose acetate membrane were measured by the pressure decay method and described in terms of the dual-mode sorption model [30]. In addition, the pressure dependant mean permeability coefficient was obtained for asymmetric and homogeneous dense cellulose acetate membranes and interpreted by the total immobilization model. The solubility isotherms of carbon dioxide in cellulose acetate were described as a dual-sorption model by Stern et al. [31]. The tests were run at temperatures between 0–60 °C and elevated pressures and the results suggested that a large fraction of the CO₂ penetrant molecules got immobilized predominantly in cellulose acetate microcavities.

On the other hand, permeability measurements of carbon dioxide on cellulose acetate membranes have been reported by different authors. For instance, Seoane et al. have published the permeability coefficients for hydrogen, helium, methane, nitrogen, air, argon and carbon dioxide at 30 – 70 °C and 0.1 – 150 torr in cellulose acetate membranes [32]. Gas permeation measurements on homogeneous cellulose acetate membranes were also conducted by Pusch and Tanioka. They reported the permeabilities, diffusion coefficients, and solubilities of helium, nitrogen and carbon dioxide through the cellulose acetate membranes as a function of pressure and temperature [33]. Raucher and

coworkers reported on the increasing permeability of CO₂ with pressure in cellulose acetate at 30 °C. It was found that the matrix model expressions that predict sorption-transport modes of gases in glassy polymers described well the experimental data, while the dual-mode model was incompatible with it [34]. CO₂ and methane separation from natural gas streams using selective hollow fiber membranes at low pressures in enhanced oil recovery processes was investigated by Daus et al. [35]. The separation and recovery of CO₂ from boiler flue gases using cellulose acetate hollow fiber membrane modules has also been reported [36].

An alternative approach to improve, modify or confer additional properties to cellulose acetate without destroying its intrinsic characteristics has been the incorporation of functional groups on its surface. Mansson and coworkers have reported on the grafting of cellulose acetate with low-molecular-weight polystyrene to form copolymers with different properties of interest [37]. Nie and Narayan have worked on the grafting of cellulose acetate with styrene maleic anhydride to form a compatible blend that improves the dimensional stability of the original polymer and achieves a better performance in fibers and film applications [38]. The homogeneous grafting copolymerization of dichlorodimethylsilane onto cellulose acetate was achieved by Abdel-Razik et al. with the aim to improve its heat and acid resistance and adhesion properties [39]. Surface modification with polycaprolacton to achieve internal plasticization that led to a biodegradable polymer with lower glass transition temperature was investigated by Vidéki and coworkers [40]. The graft copolymerization of methyl acrylate and methyl

methacrylate on cellulose acetate was performed by Guruprasad et al. to improve its biodegradation properties [41].

However, the surface modification of cellulose acetate by introduction of amine functionalities has been little explored so far. Most of the research performed on this area has been focused on the improvement of specific properties of cellulose acetate for a variety of industrial applications not related to the separation and capture of CO₂. For instance, the synthesis of water-soluble cellulose acetate with tertiary amino groups was prepared by Liesiene by simultaneous hydrolysis and aminoalkylation of cellulose acetate with N,N-diethylepoxypropylamine [42]. The objective of this functionalization was the development of a biodegradable cationic polyelectrolyte for further use as carrier in drug delivery systems. Khidoyatov et al. explored the grafting of cellulose acetate with polymers containing tertiary amino groups, like poly(diethylaminoethyl methacrylate) [43]. However, the resulting copolymer was insoluble in a wide variety of solvents and therefore could not be used for preparation of fibers or films. On a patented work, the treatment of cellulose acetate with solutions of mono- and bifunctional amino compounds like ammonia, hydroxylamine and ethylenediamine was performed to make the polymers waterproof, dyeable and durable [44]. Enzyme immobilization on cellulose and cellulose acetate membranes was achieved by introducing amino groups on it as described by Zhao et al. [45]. Glucose oxidase enzyme was fixed on the polymer membranes functionalized with 1, 6-hexanediamine solution and characterized with scanning electrochemical microscopy. On a different study, the reaction of mixed unsaturated esters of cellulose

acetate with amines was investigated with the objective to determine the decrease in elasticity, plasticity, and glass transition temperature on the modified polymer [46].

Research has also been conducted on the area of amine functionalization of cellulose acetate membranes for improvement of ultrafiltration and reverse osmosis processes. The improvement on heavy metal sorption capacity, kinetics and selectivity from aqueous solutions has been achieved by the functionalization of cellulose acetate membranes with polyaminoacids [47]. The grafting of poly(ethylenimine) onto mesylated cellulose acetate by nucleophilic displacement of mesylate groups by amine groups was presented by Biermann et al. [48]. The modify polymer was useful to produce crosslinked resins with high ion-exchange capacity for water softening and water purification purposes. Arockiasamy and collaborators have prepared and characterized a cellulose acetate/aminated polysulfone and cellulose acetate/aminated poly(ether imide) blend ultrafiltration membranes for heavy metal ion separation in aqueous streams [49, 50]. The preparation of an amine-containing cellulose acetate material with enhanced flocculating activity through the used of a triethylenetetramine copolymer was proposed by Lapenko et al. [51].

Some research work has been found regarding the functionalization of cellulose acetate as way to improve its selectivity in gas separation applications. A recent patent published by Liu et al. describes the crosslinking and functionalization of cellulose acetate membranes to improve their performance on gas separations by incorporating different types of functionalities [52]. An older patent filed by Friesen et al. shows the

grafting of an asymmetric cellulose acetate membrane with a siloxane containing functional group. The membrane was used for the separation of CO₂ from methane with better selectivity and flux stability [53]. However, no previous work has been found in the literature so far focused on the modification of cellulose acetate with amine functionalities for improvement of its CO₂ sorption capacity.

CHAPTER 3

PROBLEM DEFINITION AND PROPOSED APPROACHES

3.1 Problem Definition

Conventional sorbents for CO₂ capture from power plant flue gases have not been cost-effective enough to be used reliably in the power industry under practical conditions. Although adsorption technologies have attracted researchers' attention for a long time already, sorbents like zeolites molecular sieves, activated carbons, silica gels, and carbon molecular sieves, among others, have not been effective for the large-scale capture of CO₂ from flue gases. The major obstacle to overcome for the existing sorption technologies is the improvement of the dynamic efficiency of the separation material being employed. Research around the world is developing a new generation of sorbents with great potential to meet the present and future economic, operational and environmental constraints placed by power plants to CO₂ capture. New materials like amine-functionalized mesoporous silicas, metal organic frameworks, and hollow polymeric fibers sorbents are under research and development, but still with several technological challenges to solve. Significant progress has been made during recent years, but the overall sorption process economics is still not favorable enough to offset the CO₂ capture and sequestration costs.

Effective CO₂ removal from power plant flue gases by adsorption requires the design and development of novel sorbents capable of capturing CO₂ on a cost-effective fashion. For the capture system to succeed, it must be able to perform effective and efficient removal, concentration and recovery of CO₂ from the complex mixture of gaseous components present in power plant flue gas. Periodic cyclic adsorption processes have the potential to overcome these process requirements and reduce carbon capture costs if a suitable adsorbent is available.

A novel adsorbent is desired with a set of important properties. Among the specific tasks that a competent adsorbent should be able to achieve are:

- High CO₂ sorption capacity suitable for concentrations in the range of 10-15 %, at high volumetric flow rates and low pressure feeds
- Rapid adsorption and desorption rates that allow its use in cyclic adsorption/desorption processes
- Long-term regeneration capacity with low energy requirements under mild process conditions
- High thermal stability over adsorption/desorption cycles
- Low mass transfer resistance and high diffusion constant
- High resistance to humid and acid gas environments
- Economical post-combustion CO₂ capture
- Environmentally benign performance

A solid sorbent capable of completely satisfying all the previous demands is certainly a promising way for achieving effective adsorption of CO₂; however, it has not been created yet. The technological challenges represented by each of the desired properties still need research to successfully overcome present complications, but every technological improvement achieved significantly enhances the potential of this new class of materials for industrial application.

The necessity of deeper scientific research to develop a material with a set of unique properties that allow its successful employment as CO₂ sorbent has inspired the development of a new strategy to design a novel sorbent for CO₂ capture. The selection of the starting material was determined both by its chemical properties and its potential to significantly reduce carbon capture costs. The proposed experimental methodology is based on classical methods and reaction conditions typically used for surface modification. However, during the course of the investigation the procedure has been tailored in order to produce the desired results according to the specific chemical and physical nature of the species involved.

Cellulose acetate has been a material used for many years in a wide variety of industrial applications for its great versatility and unique physical-chemical properties. It is a relatively inexpensive cellulosic, thermoplastic and non-hazardous polymer easy to work with. It has a selective adsorption and removal of low levels of certain organic species. Cellulose acetate is soluble in many common solvents. It comes from wood pulp, a renewable resource, and may be biodegradable. It is one of the few polymers currently

being used in commercial gas separations as asymmetric membrane. Moreover, its sorption properties as CO₂ sorbent and transport properties as CO₂ separation membrane have been previously investigated and fully characterized [54]. The results have shown great potential for this material to evolve into a promising CO₂ sorbent if treated chemically properly in order to enhance its sorption properties. Therefore, commercial high-acetyl content cellulose acetate was chosen as the starting material for the development of a novel CO₂ sorbent with enhanced sorption capacity.

The objective of the present research has been to design and develop a strategy to improve the CO₂ sorption capacity of high-acetyl content cellulose acetate. During the progress of the study, different specific objectives were outlined in order to overcome unexpected challenges and fulfill the general objective. The specific objectives chronologically achieved included:

- The evaluation of the improvement of the CO₂ sorption capacity of cellulose acetate after introduction of amine functionalities into the polymer backbone using a humid grafting method and literature-based reaction conditions
- The evaluation of the improvement of the CO₂ sorption capacity of the polymer after an increase in its degree of hydroxylation and the introduction of amine functionalities through an anhydrous grafting procedure
- The evaluation of the improvement of the CO₂ sorption capacity of cellulose acetate after the introduction of metal hydroxide and amine functionalities into the polymer backbone

- The evaluation of the improvement of the CO₂ sorption capacity of the polymer after introduction of amine functionalities into the polymer backbone using a set of optimum reaction conditions
- The characterization of the novel sorbents in terms of chemical composition, density changes, molecular structure, thermal stability, and surface morphology

The work described here contains the essential elements of the chemical design strategies for transforming high-acetyl content cellulose acetate into promising novel sorbents for CO₂ capture from power plant flue gases and its main physical-chemical characterization. The sorbents developed during the present research are not final products, but rather novel sorbent materials with enhanced CO₂ sorption capacities and a high potential for further development. The best attempt has been made to accomplish the greatest improvement of the material sorption properties in order to fulfill most of the desired requirement for state-of-the-art CO₂ sorbents.

3.2 Proposed Approaches

In order to achieve the research objective, the starting point for the study consisted in the selection from the literature of a suitable experimental procedure for a chemical species compatible with the characteristics of cellulose acetate. The selected method was then adapted to the particular chemical properties of high-acetyl content

cellulose acetate and to the available equipment in the laboratory. The criteria for the selection of each experimental method was influenced by its use and success in achieving the desired goal among the scientific community working on similar research areas, as well as by its simplicity and adaptability to the equipment at hand in our laboratories.

The first experimental approach selected consisted in the introduction of amine functionalities into the polymer backbone of high-acetyl content cellulose acetate via the wet grafting of aminosilanes. The conventional wet grafting procedure was selected for its popularity and degree of success among different research groups working on amine functionalization of mesoporous silica supports for CO₂ adsorption. The method has been widely used as a simple and useful reaction scheme to modify the chemical structure of porous *inorganic* materials by attaching amine groups into the material's surface and conferring it new properties. Recent work on aminosilanes grafting on mesoporous silica supports have reported improved yields of grafted amines in the presence of water than in its absence [21, 34, 35]. Therefore, the humid grafting procedure was chosen to be tested first employing the most common reaction conditions used in the literature. The starting material was a commercial high-acetyl content cellulose acetate in its powdered form. All reactants were used as received. The characterization analyses to evaluate the physical-chemical properties of the modified polymer consisted in Elemental Analysis (EA), absolute density, Fourier-Transformed and Attenuated Total Reflection Infrared Spectroscopy (FT-IR, ATR-IR), Thermogravimetric Analysis (TGA), and Scanning Electron Microscopy (SEM). The CO₂ sorption capacity characterization was performed by using a pressure decay method developed for polymers [55].

The analysis of the results obtained from the first experimental approach led the present research to test a second experimental pathway. With the aim to increase the reactivity of cellulose acetate polymer macromolecules toward aminosilanes, a method to decrease its degree of acetylation was applied. The replacement of acetyl groups by reactive hydroxyl functionalities was achieved by acidic hydrolysis of commercial cellulose acetate powder (~39.8 wt% acetyl content). The resulting material had an acetyl content in the range of 14–19 wt% and water-solubility properties. The low-acetyl content polymeric material was subsequently dissolved in water, cast into dense films and subjected to an anhydrous aminosilane grafting procedure in order to introduce amine functionalities into the modified polymer chains. The dry grafting method was employed due to the water solubility of the polymer after de-acetylation. The CO₂ sorption capacity of the sorbent was characterized using the aforementioned pressure decay method and its physical and chemical features were also evaluated using Elemental Analysis, absolute density, Fourier Transformed-Infrared Spectroscopy, Thermogravimetric Analysis, and Scanning Electron Microscopy techniques.

A third reaction pathway was followed motivated by the lack of satisfactory results from the previous experimental approaches. It was inspired by successful literature reports on the improvement of cellulose reactivity by introduction of metal hydroxides functionalities on its surface [56, 57]. The titanium(IV) oxide-coated cellulose material from literature reports exhibited good sorption properties toward metal ions. It was envisioned that some adaptations of the published experimental method for cellulose

could be the key to successfully increase the surface reactivity of cellulose acetate towards aminosilanes. In order to start with a polymeric material with similar characteristics to cellulose, high-acetyl content cellulose acetate powder was subjected to the aforementioned de-acetylation procedure and dense films were cast out of it. The hydroxylated cellulose acetate films were then reacted with titanium tetrachloride (TiCl_4) in order to introduce titanium hydroxide functionalities into the polymer backbone. The water-solubility of the cellulose acetate films after the TiCl_4 reaction did not allow the hydroxylation with water for the introduction of titanium hydroxide functionalities into the polymer backbone. Instead, titanium oxide functionalities were obtained. Different reaction conditions were tested in order to determine the optimum amount of chemical reactants and reaction times. The low-acetyl content cellulose acetate/titanium(IV) oxide films were characterized by the analytical techniques used in previous approaches. The results showed a significant improvement of the CO_2 sorption capacity for films with the highest titanium loadings.

The learning curve experienced during the course of the present study guided the research towards its final approach. It consisted in the grafting of aminosilanes on high-acetyl content cellulose acetate under a set of optimum reaction conditions similar to those employed in the TiCl_4 reaction. Rigorous anhydrous conditions, a lower temperature, longer reaction times, an inert atmosphere and different solvent rinsing procedures allowed the greatest increase in amine loading and the best improvement in CO_2 sorption capacity for this class of materials. The controlled addition of minimum amounts of water was also tested, and the improvement or worsening of the amine

loadings and sorption capacities depended on the reactivity of the aminosilane species used in the presence of water. The samples were characterized as before. In addition, the sorbent with highest amine loading and greatest improvement in sorption capacity was exposed to water vapor in order to determine its chemical stability under humid conditions. Additional dry sorption cycles were also applied to the aforementioned sorbent.

CHAPTER 4

HUMID GRAFTING OF AMINOSILANES ON HIGH-ACETYL CONTENT CELLULOSE ACETATE

4.1 Background Theory

4.1.1 Cellulose Acetate

Cellulose acetate is the acetate ester of cellulose, a natural polymer made up of a linear chain of several hundred to over ten thousands linked glucoside units. Figure 1 shows the molecular structure of cellulose. The multiple hydroxyl groups on a glucoside unit from one chain form hydrogen bonds with oxygen atoms on the same or on a neighbor chain, firmly holding the chains together side by side. These inter chain links produce a rigid structure that imparts a great strength to cellulose, promotes its crystallinity and makes it insoluble in water and most organic solvents [58].

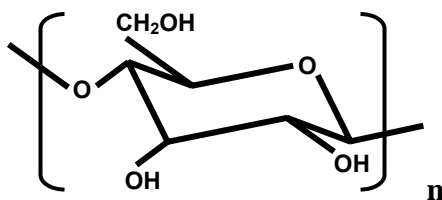


Figure 1. Cellulose molecular structure

Cellulose acetate is prepared from cellulose by an acetylation reaction. Good quality, purified cellulose is reacted with acetic acid and acetic anhydride in the presence of sulfuric acid. The sulfate and excess acetate groups are then removed by partial hydrolysis. Figure 2 presents the molecular structure of cellulose acetate's fundamental repeating unit. Cellulose acetate is an amorphous polymer, that is, its molecules are oriented randomly and intertwined. As a polymer, it is characterized by its degree of substitution or degree of acetylation, the degree of polymerization and the distribution of its hydroxyl groups. The degree of substitution refers to the average number of acetyl groups per glucoside unit. The degree of polymerization refers to the average number of glucoside units per molecule or polymer chain. On the other hand, the distribution of unesterified hydroxyl groups among the primary (6th position) and secondary (2nd and 3rd) carbon positions is also important in cellulose acetate characterization [59].

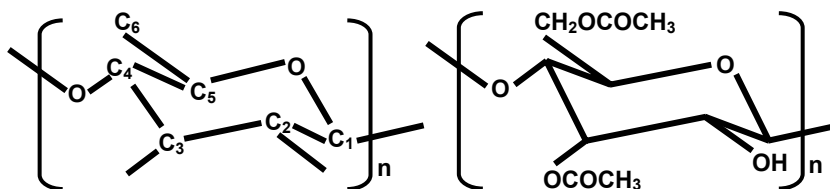


Figure 2. Cellulose acetate molecular structure

The acetyl groups in cellulose acetate reduce the amount of intermolecular hydrogen bonding present in cellulose, suppress its crystallinity and increase its flexibility and mobility [60]. The most common form of cellulose acetate has acetate groups on 2–2.5 of the 3 available positions for substitution, receiving the name of secondary acetate. Cellulose triacetate is a complete acetylated polymer in which at least

92% of the hydroxyl groups are acetylated [61]. The presence of both acetyl and hydroxyl functionalities in cellulose acetate allows different types and degrees of intra and intermolecular interactions that produce a polymer with useful properties. Among the main physical and chemical characteristics of cellulose acetate are the selective adsorption and removal of organic chemicals, its hydrophilicity, and its solubility in common organic solvents that allows the manufacture of fibers, membranes or films. These are used in a variety of applications as reverse osmosis, ultrafiltration and dialysis membranes, fabrics, plastic frames, cigarettes filters, diapers and surgical products, toys, magnetic computer tapes, adhesives, among others.

Cellulose acetate is an inexpensive polymer that has been used for adsorption of a variety of chemical species, including phenyl compounds and polynuclear aromatic hydrocarbons (PAHs) in membrane separations [62], N-methylcarbamates and lactose in ultrafiltration [63, 64], N-isopropylacrylamide and N-*n*-butyl-acrylamide in for membrane-based biochemistry immunoassay [65], among many others.

4.1.2 Aminosilanes

Organosilanes are compounds containing silicon bonded to a carbon atom. Aminosilanes are a particular type of organosilanes containing primary, secondary, and tertiary amines. This family of compounds can be used as adhesion promoters, coupling agents, resin additives and surface modifiers. The utilization of aminosilanes has been greatly directed toward surface modification, since they possess a hydrolytically sensitive

center that reacts with hydroxyl groups from a surface to form stable covalent bonds. The organic substituent remains available for interaction with other species and allows permanent property modification of the substrate. This reaction with hydroxylated surfaces then results in a substitution reaction at the silicon atom and the formation of a silylated surface where the silicon is covalently bonded to the surface via an oxygen atom. It can occur by hydrolytic deposition or under anhydrous conditions. Surface treatment with aminosilanes are influenced by different factors, like concentration of surface hydroxyl groups, the type of surface hydroxyl groups, the hydrolytic stability of the bond formed and the substrate features, among others [66].

4.1.3 Humid Grafting of Aminosilanes in High-Acetyl Content Cellulose Acetate

Experiments have shown that solid adsorbents with grafted amine functionalities are promising for CO₂ sorption [4, 11, 13, 16, 17, 19-21, 34, 47-49]. Therefore, the first attempt to improve the CO₂ sorption properties of cellulose acetate consisted of its functionalization with amines. Grafting reactions are chemical procedures where one or more functionalities are connected to the main chain of a macromolecule as side chains, resulting on a polymer with different physical and chemical properties than the original. Aminosilanes are commercial surface modifiers that provide primary amino functionalities available for CO₂ fixation.

In this work, the conventional humid grafting procedure of aminosilanes was primarily used in order to introduce amine groups into the backbone of cellulose acetate

and enhance its CO₂ sorption properties. The selection of the method was based upon its wide use and success in the amination of silica-based supports for preparation of CO₂ sorbents. To the best of our knowledge, the method has not been tested yet on organic polymers like cellulose acetate for enhancement of its CO₂ sorption properties.

Although the grafting of aminosilanes is not a complicated procedure from a technical perspective, several variables directly affect the course of the reaction and therefore the amount of grafted amines. On one hand, the chemical characteristics of the substrate have a deep impact on the efficiency of the grafting reaction. Particularly, the amount of active hydroxyl groups available for aminosilane grafting is of prime importance. On the other hand, the chemical properties of the surface modifier also largely determine the course of the reaction. In addition, grafting conditions like water presence, temperature, aminosilane concentration, and reaction times are critically important.

Hydroxyl functionalities are hydrogen donating groups that enter into hydrogen bonding interactions with the electron rich amine center of aminosilanes. The basic chemical nature of amine groups facilitates their protonation. The mixing of the aminosilane species with cellulose acetate in an adequate solvent allows the adsorption of the amine groups by hydrogen bonding to the available hydroxyl groups on cellulose acetate surface. After adsorption, the amine groups catalyze the condensation of the silicon side of the molecule with a surface C–OH group. Therefore, siloxyl bonds (Si–O–C) are formed with interaction of the polymer backbone in the absence of water for some

aminosilanes or with an initial hydrolysis of the alkoxy groups for others. It is clear then that the hydroxyl groups are the main reactive centers for chemical bonding in the grafting reaction, whatever the reaction conditions may be. This way, the amount of free hydroxyl groups on the cellulose acetate surface is a key factor on the success of the amine grafting. The larger the amount of free hydroxyl groups pending from the surface, the higher the amount of aminosilane molecules grafted [67].

On the other hand, the grafting density of amine functionalities over cellulose acetate surface is also a function of the properties of the aminosilane species used. Aminosilanes that carry one or more amine groups in their organic chain are commonly used for surface modifications because the amino functionality gives them unique properties. The amino groups catalyze inter or intra-molecularly the reaction between the aminosilane molecules and cellulose acetate surface hydroxyl groups, leading to the formation of siloxyl bonds (Si-O-C). This way, the amine side of the molecule should be of special attention.

In addition, Harlick et al. have proposed that the addition of a controlled amount of water prior to the grafting reaction can increase the amount of fixed amines functionalities on silica-based supports [21]. The presence of water would increase the number of hydroxyl groups over the surface of the support material and start the hydrolysis of the unreacted aminosilane alkoxy groups with the free silanes still present in the solvent phase. Water may facilitate silane polymerization and generate a degree of silane condensation in the solution phase prior to the grafting reaction. This phenomenon

may enhance the amount of aminosilane grafted onto the silica surface either directly or through the attachment of the silane polymers present in solution phase. On this regard, Harlick and coworkers suggest that some aminosilane molecules do not get attached directly to the surface, but rather to other grafted aminosilanes through Si–O–Si bridges. This phenomenon is acceptable as long as it increases the density of free amine functionalities available for CO₂ capture and does not block the sites available for direct surface grafting. According to Engelhardt et al. it is necessary that some water may be present at the surface of silica in order to form aminosilane layers using organic solvents [68]. Caravajal et al. has showed that increasing the amount of water on a silica support surface decreases the amount of unreacted alkoxy moieties from the aminosilane molecule [69]. A series of grafting experiments with different amounts of relative humidity and anhydrous supports samples showed the elimination of unreacted alkoxy groups through the wet grafting procedure. They attributed the complete cleavage of the Si–O–R bond in aminosilanes to the presence of excess water. Therefore, different research groups have agreed on the importance of a desirable amount of surface water on silica-based supports to promote the cleavage of siloxyl bonds in the aminosilane molecule and allow further grafting to the support surface.

Among the additional grafting conditions that directly affect the amount of grafted amine groups on cellulose acetate is the amount of aminosilane species used in the reaction. A series of amine grafting studies on mesoporous silica MCM-41 carried out by Harlick et al. showed that there is an optimum amount of aminosilane added to the reaction and higher amounts of aminosilane did not increase the quantity of amine grafted

or the CO₂ sorption capacity of the sorbent [21]. For the preparation of a smooth aminosilane layer over the support surface, Zhang et al. have found that a low aminosilane concentration and anhydrous solvents with a trace amount of water was desirable for silicon dioxide surfaces [70].

On the other hand, the temperature of the reaction also plays an important role. It has been found that higher molecular mobility is favored by high temperature reactions in solution, overcoming hydrogen bonding interactions between amine groups and surface hydroxyl groups from silica surfaces [71]. Vapor phase silanization has also been reported to produce a smooth aminosilane monolayer over silica surfaces [72]. However, vapor phase grafting favors the presence of horizontal positioned aminosilanes over the inorganic support surface.

4.1.4 Adsorption

Adsorption is the attraction and binding of atoms and molecules from an adjacent fluid to an exposed solid surface. The adsorbed chemical species is called adsorbate, while the adsorbent or surface is sometimes denominated substrate. The process can be driven by long (weak) and short (strong) range atomic and molecular forces. Long distance interactions can initiate the attraction and short range forces may finalize the setting of a new layer or layers onto the solid surface. The most common weak forces are the Van der Waals and London dispersion interactions. Van der Waals are attractive or repulsive interactions between molecules or between atoms of a molecule due to

permanent and induced dipoles. They do not include those forces due to covalent bonds or electrostatic interactions of ions (ionic bonds). Instantaneous induced dipole-dipole forces or London dispersion forces are another type of weak interactions. On the other hand, strong or short range forces may include ionic or metallic forces [73].

Physisorption, or physical adsorption, is a sorption process involving weak forces (Van der Waals and London forces, for example) which do not change significantly the electronic configuration of the species involved. Its main features include its general nature, the minimal perturbation of the species electronic states, its reversibility, the lack of activation energy, the fact that usually increases with pressure and decreases with temperature, and the possibility of adsorbate multilayer formation [73].

Chemisorption, or chemical adsorption, is the type of sorption process where the interactions involved are valence forces driven by a chemical reaction occurring at the exposed solid surface. Therefore, a new chemical species is generated at the substrate. Strong interactions between the surface and the sorbed species create a new chemical bond, either ionic or covalent. It is characterized by chemical specificity, an activation energy, a change in the electronic state of the species involved, the formation of a monolayer, the fact that may not be reversible, and that may be endothermic or exothermic [73].

The adsorption of CO₂ onto solid substrates is often a chemisorption process. Therefore, it is useful to review the main factors affecting this type of adsorption.

Generally, the fraction of collisions that result in chemisorption is influenced by the activation energy, the steric factor, the efficiency of energy transfer, the heterogeneity of the surface, and the fraction of occupied sites. As chemisorption can be an activated process, only those molecules having the required activation energy can be chemisorbed. However, not all the molecules having the necessary activation energy will chemisorb, but only those having the particular configuration associated with the activated complex will do so. In addition, in order for gaseous species to chemisorb, they must lose a fraction of their original thermal energy when colliding with the substrate, avoiding their immediate desorption. Inelastic collisions are desired in order to effectively transfer thermal energy from the adsorbate to the substrate. The acidic or basic properties of the adsorbate molecules also have to oppose those of the active site for chemisorption to occur. The adsorption of gaseous molecules onto the surface can be molecular or dissociative, depending on the basic or acid character of the adsorbate and the substrate. Finally, heterogeneous surfaces have different chemisorption capacities from site to site and collisions with occupied sites decrease chemisorption activity, although some molecules can weakly chemisorb on occupied sites and migrate over until a vacant site is found [74].

Adsorption is usually described by an isotherm or the amount of adsorbate on the adsorbent as a function of its pressure (if gas) or concentration (if liquid) at a constant temperature. The amount of adsorbate is usually normalized by the mass or volume of the adsorbent to allow comparisons. A sorption isotherm represents an equilibrium adsorption process. There are several models in the literature describing the process of

adsorption. The main ones are the Langmuir, Freundlich, Henry, Temkin, BET, Kisliuk, among others. In 1916 Langmuir published a model for adsorption of gases onto ideal solid surfaces. The semi-empirical formula represents an equilibrium adsorption based on a series of assumptions related to an ideal uniform surface. The Langmuir model assumes that adsorption occurs only at vacant identical sites and only one species is adsorbed per active vacant site (only a monolayer could be formed). In addition, all adsorption occurs through the same mechanism and the heat of adsorption is constant and independent of coverage, implying no interaction between adsorbed species. In 1926, a new mathematical fit to an isotherm was published by Freundlich. It was a purely empirical formula for gaseous adsorbates on solid, non-uniform surfaces. On the other hand, many experimental isotherms display a behavior similar to the Henry isotherm, the simplest adsorption model. This model may work for adsorption systems at high temperatures and/or low pressures. Its mathematical formulation is identical to the well-known Henry's law for gas adsorption in liquids. Basically, the Henry isotherm states that the surface coverage depends linearly on the pressure of the system [74].

For amorphous polymers like cellulose acetate above its glass transition temperature (189 °C), the equilibrium sorption of CO₂ would follow Henry sorption model. The equation describing the process is

$$C_D = k_D p \quad (4.1)$$

where C_D is the Henry's concentration of CO₂ adsorbed on the polymer at equilibrium, k_D is the Henry's solubility coefficient and p is the applied pressure of the system at equilibrium. However, amorphous polymers in the glassy state (below their glass transition temperatures) have a micro heterogeneous molecular structure. These heterogeneities can be categorized in two components: the usual matrix and the microvoid region. Gas sorption into these different regions is therefore represented by different sorption mechanisms. Henry sorption is the dominant mechanism in the matrix component, while Langmuir sorption dominates the microvoid region. The sum of both contributions is described by the dual-mode sorption model. The total concentration of sorbed gas in the polymer C is equal to the sum of the concentrations from the Henry sorption model (C_D) and Langmuir sorption model (C_H), as described by the equation

$$C = C_D + C_H = k_D p + \frac{C'_H b p}{1 + b p} \quad (4.2)$$

where C'_H is the Langmuir saturation or capacity constant and b is the Langmuir site affinity constant. The dual-mode sorption model provides a good description of the sorption process in most glassy polymers, like cellulose acetate [75].

4.1.5 CO₂ Adsorption Behavior in Cellulose Acetate

Puleo et al. have studied CO₂ gas transport and sorption behavior in cellulose acetate polymers with different degrees of acetylation [54]. The CO₂ sorption and transport in cellulose acetate occur in the amorphous fraction of the polymer. Sorption

isotherms measured at 35 °C fit the dual-mode sorption model and present typical non-linear concave shape characteristic of glassy polymers. Cellulose acetate films exposed to high CO₂ pressures are plasticized or “conditioned”, affecting sorption properties. Plasticization and swelling by CO₂ exposure causes the rigid small microvoids between the polymer chains to redistribute. Sorption at extreme high gas pressures causes swelling of the polymer chains and a change in volume that may not return to the original value only after very long times. Therefore, swelling generates semi-permanent changes in the cellulose acetate microstructure that result in the increment of the Langmuir capacity constant C'_H and the total sorption capacity. This is explained by the increase and redistribution on the sites where Langmuir sorption occurs. After CO₂ desorption, the extremely slow relaxation time of the cellulose acetate prevents return to the polymer’s original state for long periods of time. In addition, the Henry’s solubility coefficient k_D increases after plasticization due to changes in the packing efficiency of the polymer chains or to changes in the interaction with CO₂ after conditioning. Therefore, the elevated solubility of CO₂ in cellulose acetate makes it a highly soluble penetrant [54].

CO₂ sorption into cellulose acetate chains is significantly affected by the acetyl content of the polymer. The higher the acetylation degree of cellulose acetate, the higher its intrinsic CO₂ solubility and susceptibility to CO₂ plasticization. Conditioning swells the polymer and modifies intermolecular interactions, increasing the mobility of functional groups and small-scale polymer chain motions. High acetyl content cellulose acetate shows higher increments in CO₂ sorption capacity after plasticization than low

acetyl content films. Generally, CO₂ sorption capacity of high acetyl content cellulose acetate tends to increase with time [54].

Intermolecular interactions of functional groups in cellulose acetate vary according to its degree of acetylation. In low-acetyl content cellulose acetates the dominant interactions are hydroxyl-hydroxyl, which are strong interactions due to hydrogen bonding. Hydroxyl-acetyl interactions are weaker, but still of comparable strength to hydrogen bonding. Acetyl-acetyl interactions are the weakest ones and the most common in high-acetyl content cellulose acetates. These interactions are more susceptible to be completely solvated and plasticized by a polar adsorbate like CO₂ [54].

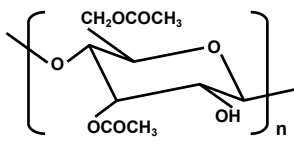
Commercial cellulose acetate is usually a high-acetyl content polymer in which CO₂ gets adsorbed through the carbonyl group C=O, part of the acetyl functionality. Different IR studies have demonstrated that exposure to CO₂ produces a shift in the carbonyl peak of the spectra, attributed to a weakening of the functionality due to disruptions in the dipolar interaction between acetyl groups. In addition, the presence of CO₂ in cellulose acetate also affects the intermolecular and intramolecular hydrogen bonding interactions. That is, CO₂ can also get sorbed on the free hydroxyl functionalities.

4.2 Experimental

4.2.1 Materials

All materials were used as received from the different suppliers. Cellulose acetate, anhydrous toluene, and methanol were supplied by Sigma-Aldrich (St. Louis, MO, USA). N-(2-aminoethyl)-3-aminoisobutyldimethylmethoxysilane and aminopropyldimethylethoxysilane were purchased from Gelest, Inc. (Morrisville, PA, USA). For practical reasons, from now on we will refer to the aforementioned aminosilane species by its molecular formulas, that is, $C_9H_{24}N_2OSi$ and $C_7H_{19}NOSi$, respectively. Table 1 shows the typical physical and chemical properties of the cellulose acetate.

Table 1. Sigma-Aldrich cellulose acetate typical physical chemical properties

CELLULOSE ACETATE (Product Code: 419028)	
Typical Properties	Typical Values
Acetyl content	39.8 wt%
Hydroxyl content	3.5 wt%
Average molecular weight	50,000 GPC
Acidity as acetic acid	0.2 wt % max.
Viscosity	114 poise
Moisture content	3 wt%
Ash content	< 0.05 wt%
Specific gravity (wt/vol)	1.4205 kg/L*
Bulk density, tapped	432 kg/m ³
Bulk density, poured	320 kg/m ³
Melting point	230 – 250 °C
Glass transition temperature (T _g)	189 °C
Refractive Index	1.475
Dielectric strength	669 kv/cm (1.7 kv/mil)
Molecular structure	

*Obtained by gas pycnometry analysis at Micromeritics Analytical Services.

The values provided by Sigma-Aldrich for the properties of cellulose acetate are literature-based values and not experimental data, with the exception of absolute density, obtained by gas pycnometry at Micromeritics Analytical Services (Norcross, GA, USA).

Typical values for some physical properties of $C_9H_{24}N_2OSi$ and $C_7H_{19}NOSi$ as provided by Gelest, Inc. are summarized on Table 2 and Table 3.

Table 2. Gelest, Inc. N-(2-aminoethyl)-3-aminoisobutyldimethylmethoxysilane typical properties

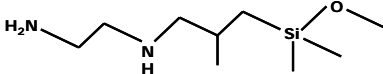
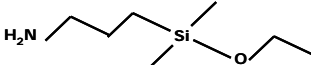
N-(2-AMINOETHYL)-3-AMINOISOBUTYLDIMETHYLMETHOXSILANE <i>(Product Code: SIA0587.2)</i>	
Typical Properties	Typical Values
Molecular weight	204.39 g/mol
Boiling point	85 – 9 °C at 24 mmHg
Specific gravity	0.9 g/cm ³
Purity	95 %
Vapor density (air = 1)	> 1
Volatiles content	< 5 %
Freezing point	< 0 °C
Vapor pressure	< 1 mmHg at 25 °C
Solubility in water	Reacts
Refractive index	1.4513 at 25 °C
Appearance and color	Clear to straw liquid with amine (ammonia – like)
Molecular formula	odor $C_9H_{24}N_2OSi$
Molecular structure	

Table 3. Gelest, Inc. aminopropyldimethylethoxysilane typical properties

AMINOPROPYLDIMETHYLETHOXSILANE <i>(Product Code: SIA0603.0)</i>	
Typical Properties	Typical Values
Molecular weight	161.32 g/mol
Boiling point	78 – 9 °C at 24 mmHg
Specific gravity	0.857 g/cm ³
Vapor density (air = 1)	> 1
Freezing point	< 0 °C
Solubility in water	Reacts
Refractive index	1.4276 at 25 °C
Appearance and color	Clear to straw liquid with amine (ammonia – like)
Molecular formula	odor $C_7H_{19}NOSi$
Molecular structure	

4.2.2 Humid Grafting of Aminosilanes on High-acetyl Content Cellulose Acetate

It is well known that the humid grafting of amine functionalities on inorganic silica supports enhances its CO₂ sorption capabilities [5, 21, 34, 35]. In order to introduce amine groups into the polymer backbone of pure cellulose acetate, a conventional wet grafting technique with aminosilanes was used as initial experimental approach. The selection of the method was based on the most recent investigations on the area of inorganic supports amine functionalization, using a wet grafting approach in order to enhance results from classical dry grafting procedures. The reaction conditions employed were those most widely utilized by different researchers and considered as baseline for the aminosilanes grafting reaction.

The wet grafting reactions were carried out using commercial, high-acetyl content cellulose acetate in its powder form, two different types of liquid aminosilanes in order to determine their degree of reactivity and the effect of single and multiple amine groups per aminosilane molecule, deionized water, anhydrous toluene as solvent and methanol as washing species.

As received, high-acetyl content cellulose acetate powder was dried in a vacuum oven at 120 °C overnight. Cellulose acetate is a hydrophilic material, so the drying step was necessary to make sure that any water on its surface was due only to the controlled addition during the reaction and not from physically adsorbed water during storage. 1

gram of dried cellulose acetate was introduced into a three-neck flask with a magnetic stirrer. 150 mL of anhydrous toluene were added and the system was closed afterwards. The mixture was stirred for 30 minutes at room temperature. After this time, 1 mL of deionized water was added to the solution using a syringe and continuous stirring. The resulting solution was allowed to equilibrate for 3 h under the same temperature and stirring conditions. Afterwards, the system was connected to a condenser, immersed into an oil bath at 110 °C and a specific amount of the corresponding aminosilane was added. 1.5, 3.0 and 4.5 mL of each aminosilane species were tested in different experimental runs. The system was held under reflux conditions for 16 h. After this time, the reaction solution was filtrated using a Büchner funnel under vacuum and washed with 400 mL of anhydrous toluene, 400 mL of methanol and 400 mL of deionized water. The product was dried under vacuum at 80 °C and store in capped vials until further use. Table 4 identifies the different samples obtained by varying the amount and species of aminosilane used.

Table 4. Reaction conditions for wet amination of high-acetyl cellulose acetate

Sample	Cellulose Acetate (g)	Toluene (mL)	Aminosilane Species	Aminosilane (mL)	H ₂ O (mL)	Amination Time (h)	Amination Temperature (°C)
<i>B</i>	1	150	C ₉ H ₂₄ N ₂ OSi	1.5	1	16	110
<i>C</i>	1	150	C ₉ H ₂₄ N ₂ OSi	3.0	1	16	110
<i>D</i>	1	150	C ₉ H ₂₄ N ₂ OSi	4.5	1	16	110
<i>E</i>	1	150	C ₇ H ₁₉ NOSi	1.5	1	16	110
<i>F</i>	1	150	C ₇ H ₁₉ NOSi	3.0	1	16	110
<i>G</i>	1	150	C ₇ H ₁₉ NOSi	4.5	1	16	110

4.2.3 Sorbent Sorption Characterization

To characterize the sorption of CO₂ in the resulting sorbents as a function of CO₂ pressure at a constant temperature, a pressure decay method developed for polymers has been used [55]. The system allows the determination of the sorption isotherms of sorbents, as well as the estimation of preliminary kinetic and equilibrium data. Accurate sorption kinetics measurements can not be possible with this system since sorption generated heat effects are not taken into account. The time required for the sorbent to reach equilibrium can be measured to provide an insight of the sorbent response time. The system is useful to test the sorption properties of the sorbents when exposed to pure gases only. Therefore, the effects of competitive adsorption and humidity in the feed stream could not be evaluated using this apparatus [12].

Each sample was introduced and held inside a porous stainless steel filter and capped with aluminum foil. The foil cap was fastened in place using a tight stainless steel coil around it. The sorbent samples were introduced into a sample cell, which was tightly closed afterwards. The closed sorption system was immersed into a constant temperature oil bath at 35 °C. After the sample was loaded, vacuum was pulled on the sample cell for one day to completely evacuate and dry the cell and the sorbent sample before the beginning of the test. After the drying step, CO₂ was introduced to a reservoir cell at a controlled low pressure and allowed to equilibrate. After thermal equilibrium was achieved, the sample cell valve was opened rapidly to introduce the CO₂ into the sample cell. As the stainless steel filter is porous, the gas easily reached the sample. The pressure

decay over time was recorded until equilibrium was attained. When the sample reached sorption saturation at a particular pressure, the data recording was stopped and an additional amount of CO₂ was introduced into the reservoir cell. The same procedure was repeated for this new pressure value. The recorded data allow the determination of the sorption isotherms and preliminary sorption kinetics. The design of the system complicates the temperature control of the local thermal heat effects inside the sample cell. Desorption was carried out by exposing the samples to temperatures of about 130 °C under vacuum for 24 h.

4.2.4 Instrumental Characterization of Sorbents

The composition and properties of the modified cellulose acetate was characterized by Elemental Analysis (EA), density analysis, Attenuated Total Reflection Infrared Spectroscopy (ATR – IR), Thermogravimetric Analysis (TGA) and Scanning Electron Microscopy (SEM).

Elemental Analysis was used to determine the percentage weights of the main elements present in each sample. The results can help to find out the amount of amine functionalities grafted to the polymer chains of cellulose acetate. The elements analyzed for the grafted samples comprised carbon, hydrogen, oxygen, nitrogen and silicon. The analyses were carried out by Galbraith Laboratories, Inc. (Knoxville, TN, USA). Carbon, hydrogen and nitrogen weight percentages were determined by a combustion technique. Silicon was measure by Inductively Coupled Plasma – Optical Emission Spectroscopy

(ICP-OES). The presence of silicon in amounts greater than 1.0 wt% difficulties the measurement of oxygen due to the formation of oxides. Therefore, on those cases the oxygen content was estimated by difference.

Density measurements were also performed in order to determine the change in mass per unit volume of a modified material. The knowledge of the absolute density of the samples was very important to accurately evaluate their CO₂ sorption capacity. The absolute density is the mass divided by the absolute volume, which is the volume occupied by a material excluding all pores and voids. The measurements were carried out by Micromeritics Analytical Services (Norcross, GA, USA) using an AccuPyc II 1340 pycnometer that employs a gas displacement technique to determine the volume of sample under test. The tests were performed using nitrogen as analysis gas at room temperature and the absolute density was the average value out of 10 measurements.

Attenuated Total Reflection Infrared Spectroscopy (ATR – IR) tests were used to confirm the presence of surface amine functionalities grafted to cellulose acetate and to reveal details about the molecular structure of the new materials. Since a chemical functional group tends to absorb infrared radiation in a specific wavelength range regardless of the structure of the rest of the molecule, this analytical technique was very useful to identify functional groups in the samples at different reaction stages. The infrared spectra were recorded on a Shimadzu IR Prestige-21 Fourier Transform Infrared Spectrophotometer (Shimadzu Scientific Instruments, Columbia, MD, USA). Each sample was analyzed using a scan time of 64 scans, scanner velocity of 10 kHz,

resolution of 4 cm^{-1} and an aperture setting of 6 mm. The spectra were recorded in absorbance units in the range of $4000 - 370\text{ cm}^{-1}$.

Thermogravimetric Analysis was also used to figure out the thermal stability, adsorbed moisture content and to confirm the change in molecular structure of modified cellulose acetate. The TGA instrument measured the changes in sample weight as a function of temperature. The measurements were performed using a dynamic temperature program at a rate of 10 K/min . A starting temperature of $20\text{ }^{\circ}\text{C}$ and a final temperature of $750\text{ }^{\circ}\text{C}$ were used in all measurements. Helium was used as purge and protective gas. The instrument used for the measurements was a Bruker TG – FTIR Interface (Bruker Corporation, Billerica, MA, USA).

In addition, Scanning Electron Microscopy analyses were carried out with the aim to image the samples surface and investigate their changes in morphology. The three-dimensional appearance of the images was a useful tool to understand the surface structure of the modified cellulose acetate. Each sample was sputter-coated with a 10-20 nm thick gold coating model P-S1 (International Scientific Instruments, Inc., Mountain View, CA, USA) and placed in a high resolution field emission scanning electron microscope Leo 1530 (Leo Electron Microscopy, Cambridge, UK).

4.3 Results

4.3.1 Sorbent Sorption Characterization

Several experiments were carried out in order to investigate the effect of the aminosilanes wet grafting reaction on cellulose acetate CO₂ sorption capacity. The main variation in the procedures was the amount and type of aminosilane species used. The rest of the conditions were held constant, for they were recognized as baseline values widely used in the literature for surface modification with aminosilanes of mesoporous silicas. The isotherms were recorded at 35 °C using the aforementioned pressure decay method.

Figure 3 presents the isotherms of samples *B*, *C*, and *D*, sorbents obtained by the wet grafting of C₉H₂₄N₂OSi with high-acetyl content cellulose acetate powder by varying the amount of aminosilane added to the grafting reaction.

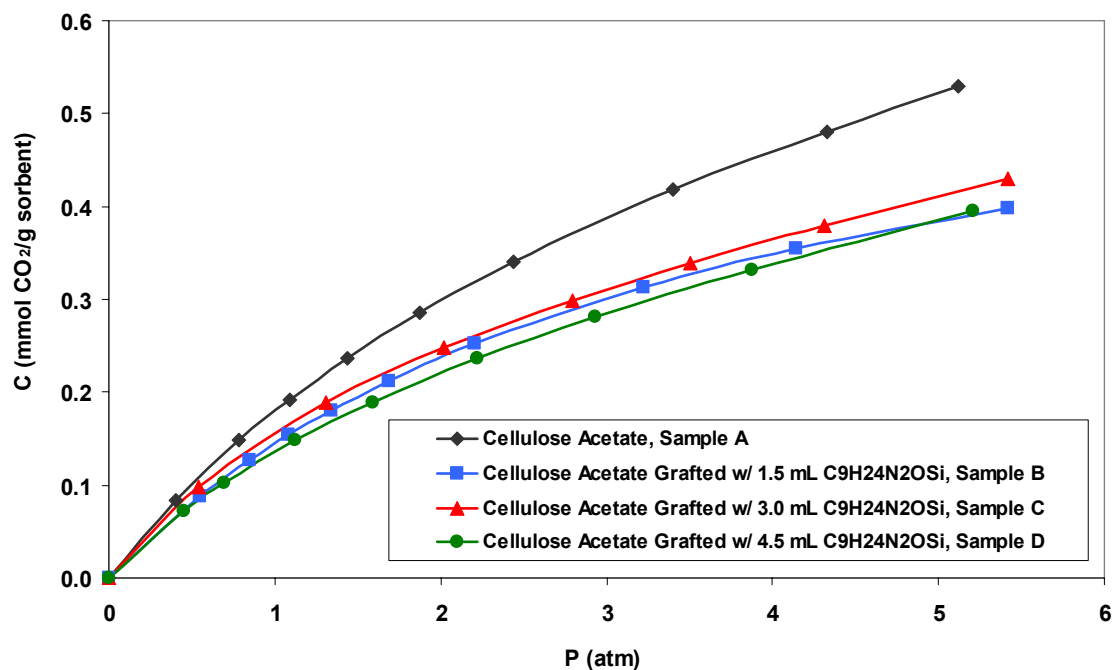


Figure 3. CO₂ sorption isotherms for cellulose acetate grafted samples *B*, *C*, and *D* with C₉H₂₄N₂OSi

Likewise, Figure 4 shows the isotherms of samples *E*, *F*, and *G*, corresponding to the wet grafting of aminosilanes with 1.5, 3.0, and 4.5 mL of C₇H₁₉NOSi, respectively.

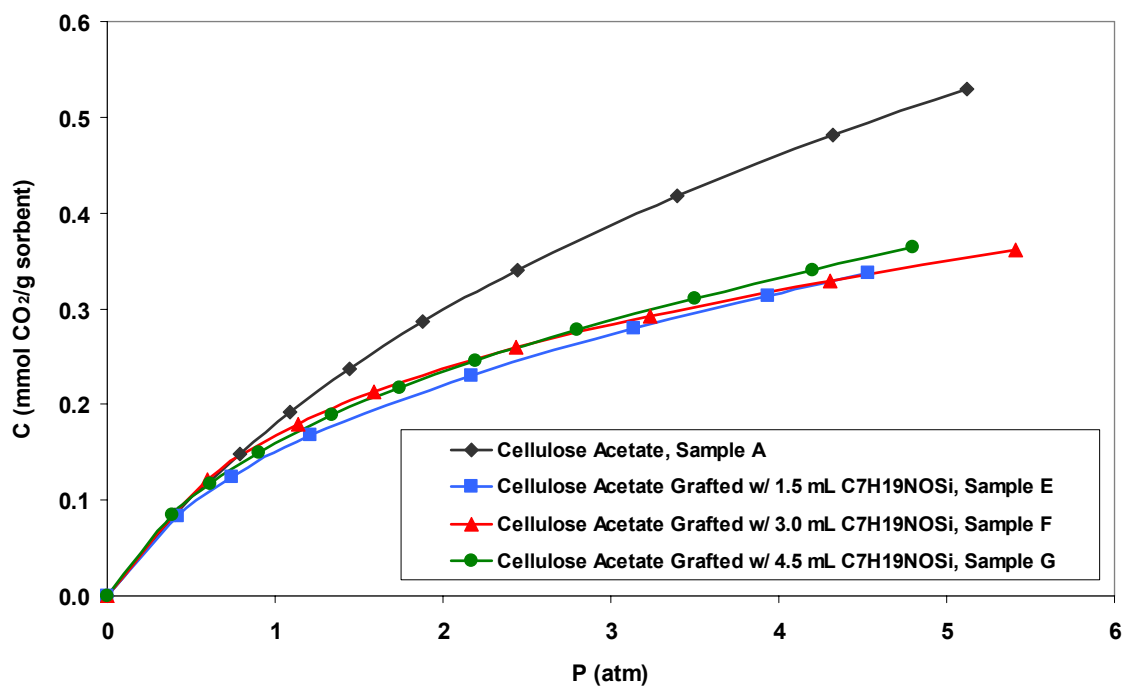


Figure 4. CO₂ sorption isotherms for cellulose acetate grafted samples *E*, *F*, and *G* with C₇H₁₉NOSi

The CO₂ sorption capacity of all amine-grafted cellulose acetate samples considerably decreased after the reaction with aminosilanes. For reactions using C₉H₂₄N₂OSi as grafting agent, the smallest decrease in sorption capacity was presented by sample *C*, cellulose acetate treated with 3.0 mL of aminosilane per gram of cellulose acetate. The highest sorption capacity achieved by this sample was 0.43 mmol CO₂/g sorbent at about 5 atm CO₂ partial pressure, well below the sorption capacity of pure cellulose acetate at a similar pressure (0.53 mmol CO₂/g sorbent). At the majority of the applied pressures, the lowest sorption capacity was showed by sample *D*, cellulose acetate grafted with 4.5 mL of C₉H₂₄N₂OSi per gram of cellulose acetate, with a value of 0.39 mmol CO₂/g sorbent at about 5 atm CO₂ partial pressure. Similarly, the wet grafting of cellulose acetate with different amounts of C₇H₁₉NOSi only led to a significant decrease in the CO₂ sorption capacity of the original sorbent. The highest sorption capacity registered employing this aminosilane species was 0.36 mmol CO₂/g sorbent at 5 atm CO₂ partial pressure, corresponding to the addition of 4.5 mL of C₇H₁₉NOSi per gram of cellulose acetate. Therefore, the sorption capacity of cellulose acetate decreased even further with the use of C₇H₁₉NOSi. It is clear that the experimental approach used only generate a decrease in cellulose acetate sorption capacity, instead of its improvement. This was definitely not our objective and alternative approaches will be considered to overcome this problem.

4.3.2 Elemental Analysis

Due to the unsuccessful results in terms of improvement of CO₂ sorption capacity of cellulose acetate and to the similarity of the isotherms obtained using different amounts of each aminosilane species, only those samples presenting the smallest decrease in sorption capacities were analyzed by Elemental Analysis. The results are shown in Table 5.

Table 5. EA of pure and selected samples of amine-grafted cellulose acetate by a wet grafting procedure

Sample		Elemental Analysis				
		% C	% H	% O	% N	% Si
<i>A</i>	High-acetyl content cellulose acetate powder (CA)	48.21	5.93	45.60	0.00	0.00
<i>C</i>	CA grafted with 3.0 mL of C ₉ H ₂₄ N ₂ OSi	43.91	6.30	49.53	0.22	<0.01
<i>F</i>	CA grafted with 3.0 mL of C ₇ H ₁₉ NOSi	48.26	5.47	46.15	0.09	<0.01

The estimation of the expected weight percent content of nitrogen in a successfully modified cellulose acetate glucoside unit with one molecule of C₉H₂₄N₂OSi per reactive hydroxyl group is around 6.70 wt%. Likewise, the estimation of expected nitrogen content on a successful grafting reaction using C₇H₁₉NOSi is 3.88 wt%. Therefore, Elemental Analysis showed the presence of very small amounts of amine functionalities on wet-grafted cellulose acetate samples and confirmed the low grafting efficiency achieved by the selected method under the applied reaction conditions.

4.3.3 Density Analysis

Likewise, only samples *C* and *F* were analyzed by Micromeritics Analytical Services for absolute density analysis. The results are presented in Table 6.

Table 6. Densities of pure and selected samples of amine-grafted cellulose acetate by wet grafting

Sample		Density (g/mL)
<i>A</i>	Acetone-soluble cellulose acetate powder (CA)	1.4205
<i>C</i>	CA grafted with 3.0 mL of C ₉ H ₂₄ N ₂ OSi	1.4150
<i>F</i>	CA grafted with 3.0 mL of C ₇ H ₁₉ NOSi	1.4187

The grafting of aminosilanes into the polymer chains of cellulose acetate is expected to decrease the absolute density of the material. The bulky aminosilane molecules grafted to the polymer backbone in substitution of hydroxyl groups should decrease the packing of the polymer chains and the total weight per unit volume of the sample. Therefore, the higher the amount of grafted aminosilane functionalities, the largest the expected decrease in absolute density of a sample. Results from density analyses show only a small decrease in the grafted samples densities, suggesting a low amount of grafted aminosilane functionalities.

4.3.4 Attenuated Total Reflection Infrared Spectroscopy

The infrared spectrum can be divided into two regions, the functional group region and the fingerprint region. The functional group region is generally considered to range from 4000 cm⁻¹ to 1500 cm⁻¹ frequencies. It includes generally stretching vibrations that are localized and characteristic of typical functional groups found in organic molecules. The frequencies of these bands are reliable and their presence or absence can be used confidently to determine the nature of the components that make up an unknown organic molecule. On the other hand, the fingerprint region, ranging about 1500 to 400 cm⁻¹, usually involves bending molecular vibrations that are characteristics of a whole molecule or large fragments of a molecule. When dealing with unknown structures, the

complexity of the infrared spectra in this region makes it difficult to assign all the absorption bands. Therefore, it is recommended to focus on identifying the characteristic features on the functional group region [76].

On the other hand, peak intensities reflect IR sensitivity to dipole moments of the molecular bonds analyzed. The most intense vibrations are seen in polar bonds where a change in dipole moment during the vibration is greatest, and therefore these are reflected in the biggest peaks in the spectrum. For rigorous analysis of peak intensities, knowledge of the refractive index, absolute density and packing density of powdered samples as they are compressed in the ATR cell is needed [77]. Such data has not been obtained during this study and, therefore, accurate peak intensities analyses are out of the scope of this report. Rather, analysis of the peaks location and relative intensity to the rest of the spectrum has been done to identify the presence of key functional components in the aminosilane-grated sorbents.

Infrared spectra were obtained for commercial high-acetyl content cellulose acetate powder and for aminosilane-grafted cellulose acetate powder samples *C* and *F*. The analyses were useful to investigate the main structural changes in the modified cellulose acetate molecules with respect to the pure polymer. Infrared analysis of cellulose acetate, presented in Figure 5, has been widely studied and a complete interpretation of the spectrum has already been published [78]. The weak absorption band at 900 cm^{-1} corresponds to amorphous regions in the polymer, while the strong doublet peaks at 1040 cm^{-1} and 1230 cm^{-1} are characteristics vibrations of acetate groups. At

1370 cm^{-1} a $-\text{CH}_3$ deformation accounts for a peak of medium intensity, and at 1740 cm^{-1} the carbonyl $\text{C}=\text{O}$ region shows an intense absorption band. The hydroxyl region (3400-3645 cm^{-1}) displays a broad and weak absorbance band, corresponding to the free hydroxyl groups dangling from the polymer backbone of high-acetyl content cellulose acetate, as well as those involved in intra- and intermolecular hydrogen bonding.

Grafting reactions are designed to introduce new functionalities into a macromolecule while conserving the basic molecular structure. The infrared spectrum of sample *C*, also displayed in Figure 5, shows that the molecular structure of cellulose acetate backbone was well conserved after the wet-grafting reaction. The most interesting feature to note is the shift in the hydroxyl and hydrogen bond stretching vibrations at 3400–3645 cm^{-1} to the N-H stretching frequency observed at 3200–3500 cm^{-1} . There is a larger dipole moment associated with the N-H bond leading to a stronger intensity in the absorption band. In addition, the presence of N-H bonds in a molecule, usually involved in hydrogen bonding, causes a shift toward lower frequency and broadens the peaks of all functional groups also involved in hydrogen bonding. The inspection of the spectrum reveals the presence of primary amines by the broad band at 3300-3340 cm^{-1} and by the presence of an additional weak peak at frequencies lower than 3300 cm^{-1} , suggested to indicate the presence of hydrogen bonding [76]. The broad band ranging from 3340-3550 cm^{-1} is widely recognized as an indication of intermolecular hydrogen bonds [79].

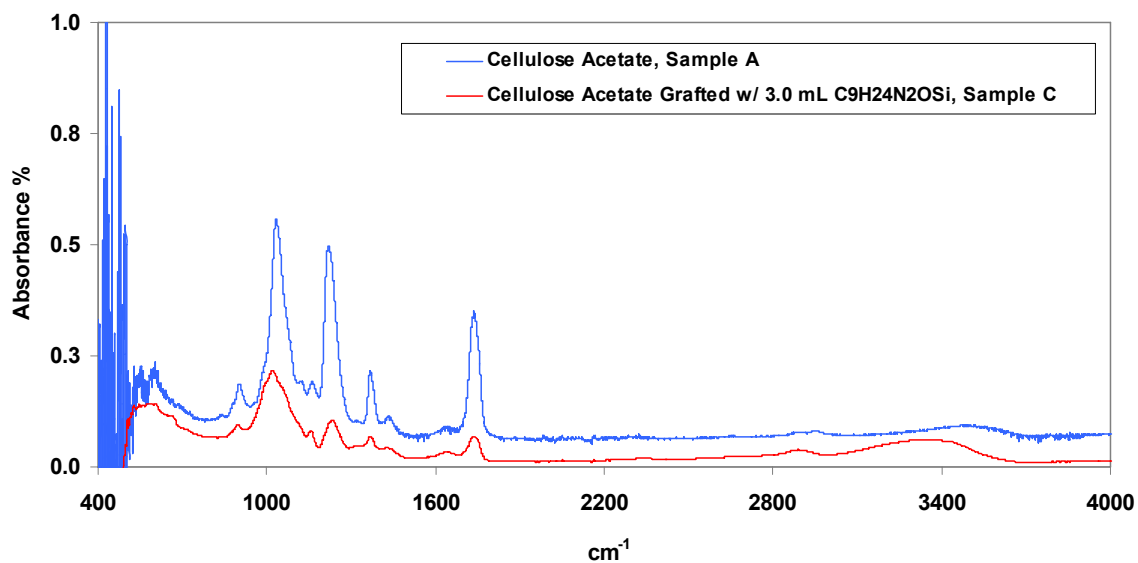


Figure 5. ATR spectrum for high-acetyl content cellulose acetate and wet-grafted cellulose acetate with $\text{C}_9\text{H}_{24}\text{N}_2\text{OSi}$, sample C

On the other hand, sample *F* presents a very similar IR spectrum, as shown in Figure 6; however, the N-H stretching displays a weaker intensity, suggesting the presence of fewer amounts of N-H bonds changing their dipole moment at that frequency.

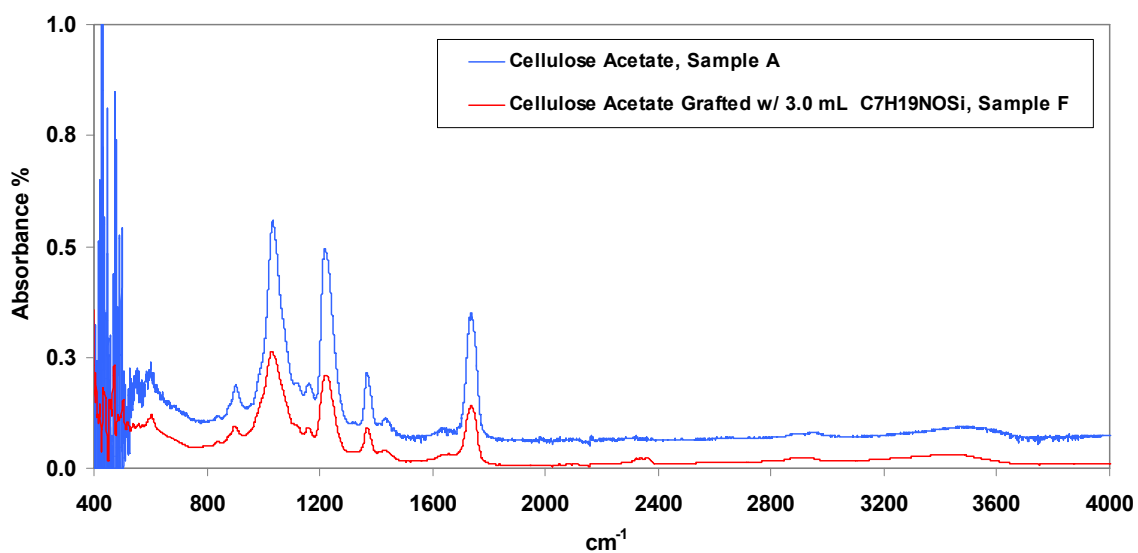


Figure 6. ATR spectrum for high-acetyl content cellulose acetate and wet-grafted cellulose acetate with $\text{C}_7\text{H}_{19}\text{NOSi}$, sample *F*

4.3.5 Thermogravimetric Analysis

The thermal stability of the pure and modified cellulose acetate sorbents was also investigated by thermogravimetry. TGA was performed for samples *A*, *C*, and *F* to determine the change in weight with respect to changes in temperature. A two-step dynamic temperature program was run in order to analyze the thermal stability and adsorbed moisture content of the samples. The measurements were performed using a heating rate of 10 K/min. The first step consisted in raising the temperature to 100 °C for about 1 h. Then the furnace temperature was elevated to 750 °C, holding it for about 30 min. Helium was used as purge and protective gas at a rate of 30 mL/min.

A sample of as received high-acetyl content cellulose acetate powder was tested in the TGA instrument under the conditions described above. The sample was thermally stable up to a temperature of 310 °C, at which a weight loss of about 90% was registered. After a temperature of 420 °C the sample degradation rate decreased considerably. The amount of residue after decomposition was about 7%. Both aminosilane-grafted cellulose acetate samples *C* and *F* presented a decrease in thermal stability with respect to the original polymer. A similar thermal behavior showed a degradation step at about 260 °C where 84% of the original sample mass was lost. Their TG curves are presented in Figures 7 and 8.

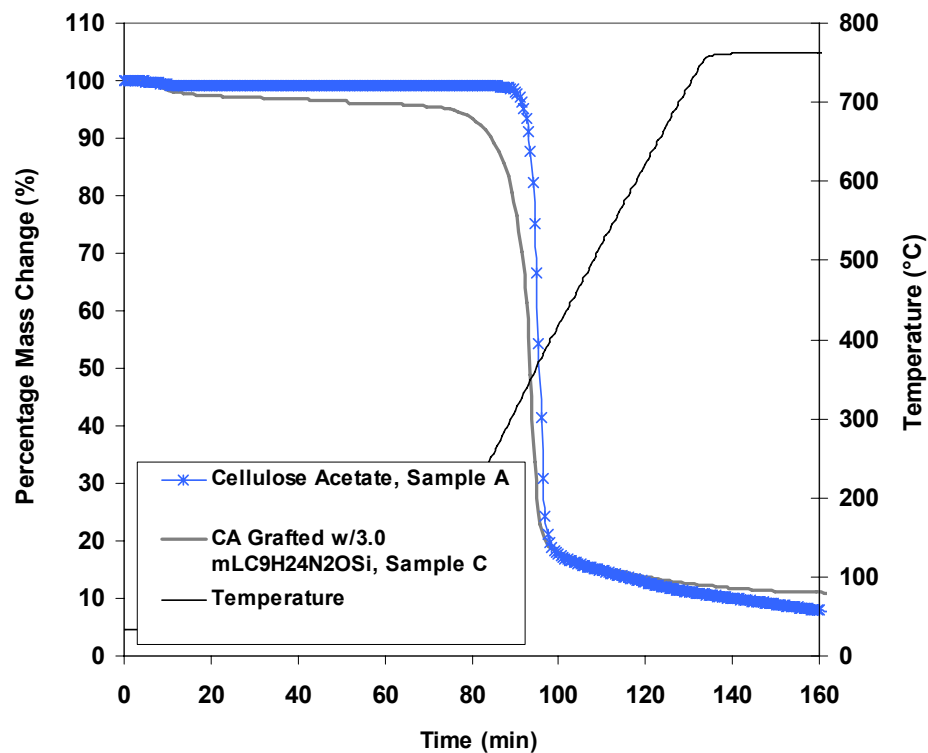


Figure 7. TG curve for cellulose acetate and wet-grafted cellulose acetate with $C_9H_{24}N_2OSi$, sample *C*

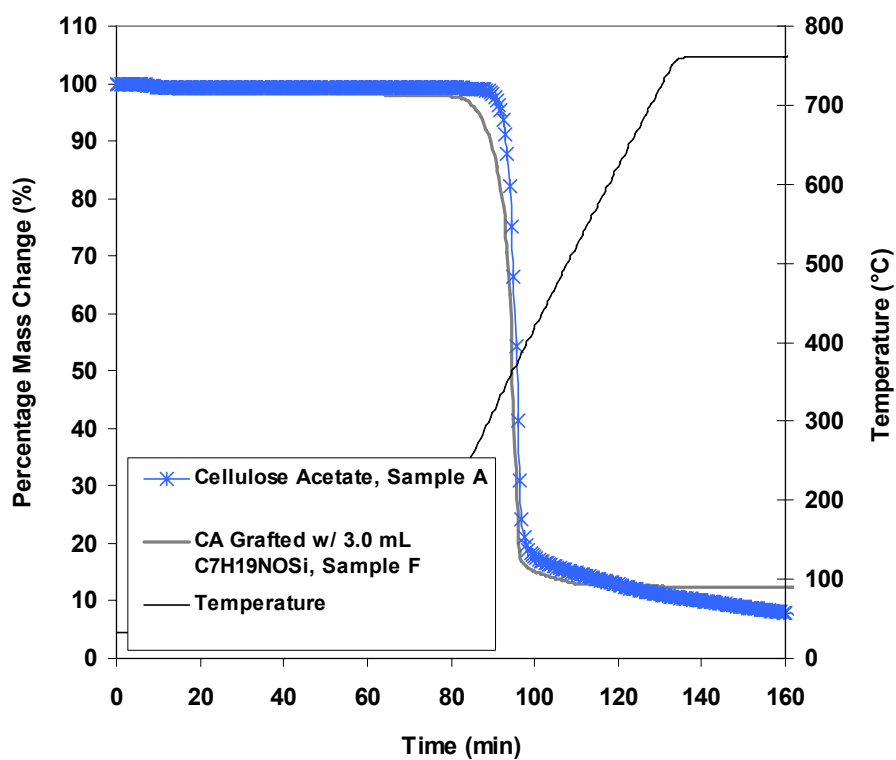


Figure 8. TG curve for cellulose acetate and wet-grafted cellulose acetate with $C_7H_{19}NOSi$, sample *F*

4.3.6 Scanning Electron Microscopy

Scanning electron micrographs of the aminosilane grafted samples were performed in order to observe possible changes in their morphology. A wide particle size distribution and heterogeneity is observed in the grafted sample powders. The images are not particularly revealing, but were included for consistency and uniformity with the rest of the study. Figure 9 presents the SEM images of samples *C* and *F*.

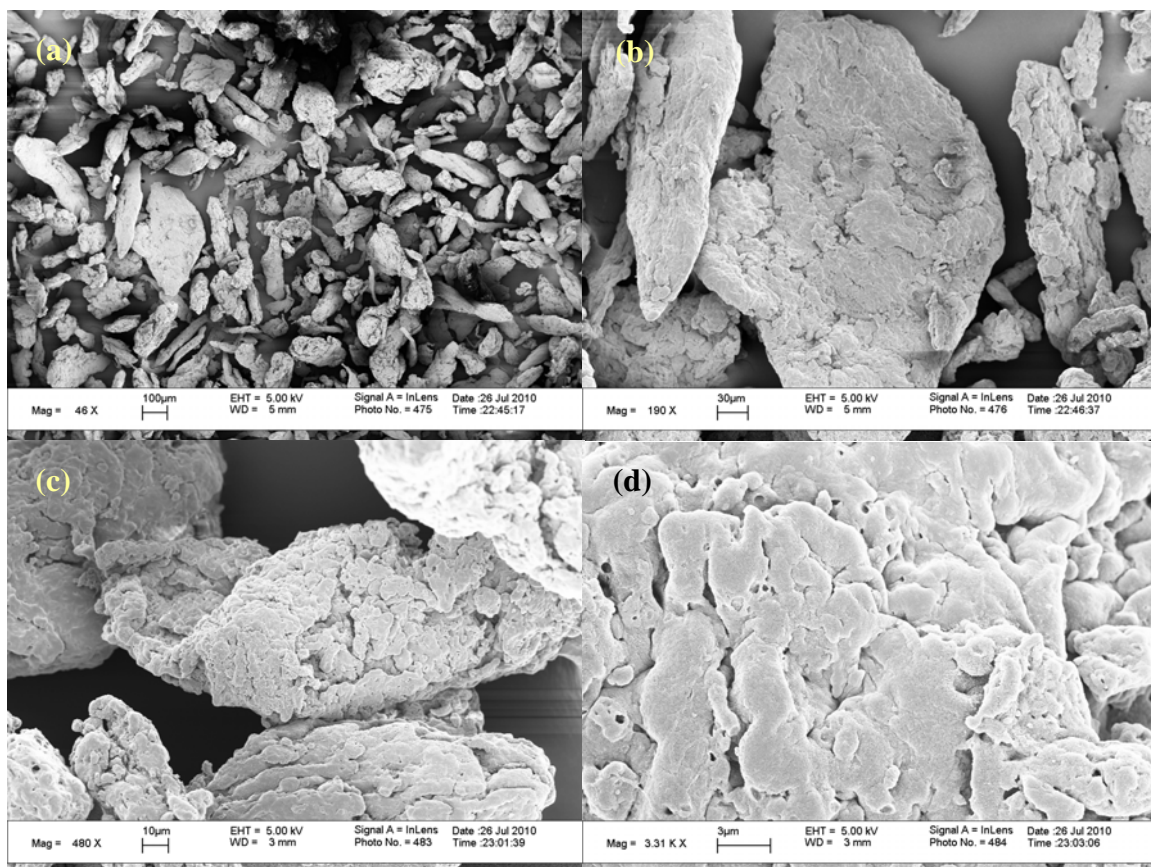


Figure 9. SEM images of (a) and (b): wet-grafted cellulose acetate with $C_9H_{24}N_2OSi$, sample *C*; (c) and (d): wet-grafted cellulose acetate with $C_7H_{19}NOSi$, sample *F*

4.4 Discussion

A wet grafting reaction of aminosilanes on high-acetyl content cellulose acetate powder was carried out using a set of baseline reaction conditions and two different species of aminosilanes. The proposed grafting reaction mechanism in the presence of water is proposed in Figure 10. It presents a three step mechanism. At the beginning, the hydrolysis of the alkoxy group and subsequent formation of silanol-containing species (Si–OH) takes place. Afterwards, the hydrogen bond of the silanol species with OH groups pending from cellulose acetate chains occurs. Finally, during the drying step a covalent bond is formed with the polymer while remaining water molecules are lost.

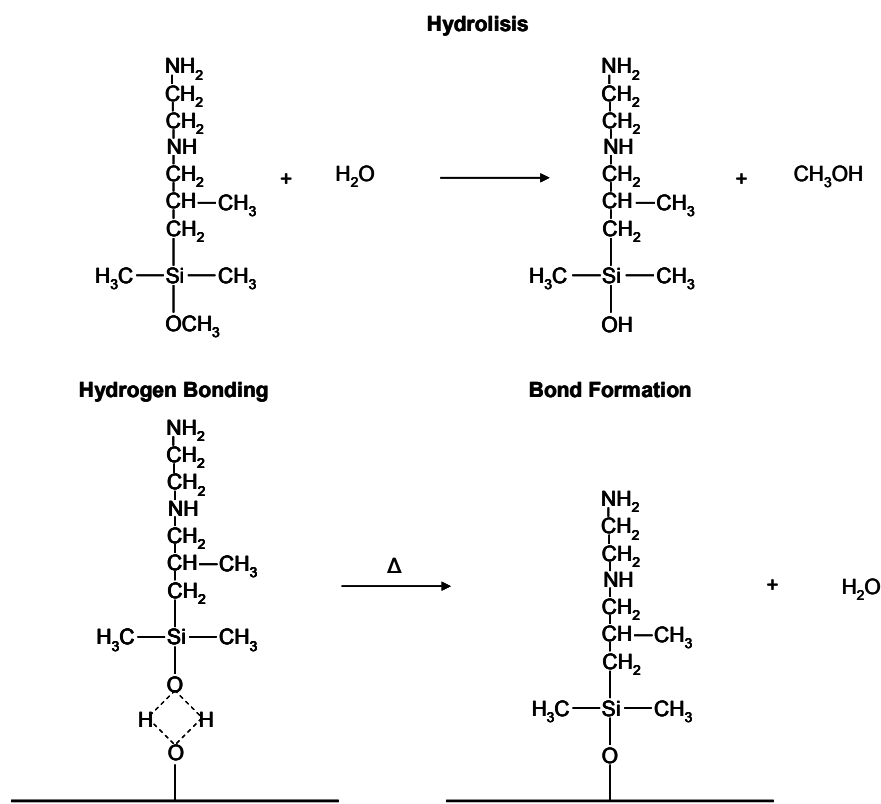


Figure 10. Humid grafting reaction of aminosilanes with hydroxylated species.

Another possible grafting mechanism starts with the interaction between the amino group and the hydroxyl functionality from cellulose acetate, where the protonated amine catalyzes the formation the siloxyl covalent bond and the release of the alkoxy functionality to form the corresponding alcohol. The sorption characterization results showed a decrease in CO₂ sorption capacity for the grafted sorbents with both types of aminosilanes. This can be due to a number of reasons. The chemistry of the adsorbent and aminosilanes used, as well as the reaction and post-treatment conditions employed could all have affected the unsuccessful sorption results.

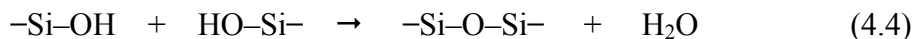
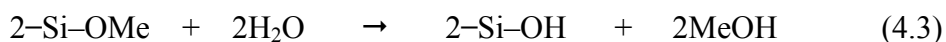
First of all, the concentration and type of hydroxyl groups present on cellulose acetate polymer chains have a deep influence in the success of the grafting reactions. Cellulose acetate used has a hydroxyl content of 3.5 wt%, that is, about one hydroxyl group per couple of glucoside units. This concentration of hydroxyl groups may be too low for adequate aminosilane attachment under the reaction conditions used. However, perhaps more important is the type of hydroxyl groups present. It has been suggested that isolated free hydroxyl groups react more reluctantly to aminosilane grafting agents than hydrogen bonded vicinal hydroxyl functionalities [66]. Finally, it is not clear why an actual decrease in sorption would result, since any grafting would be expected to increase CO₂ sorption capacity.

The aminosilanes used were carefully selected based on the number of amino and alkoxy functionalities per silane molecule. C₉H₂₄N₂OSi has two amino moieties and a

single methoxy group, while $C_7H_{19}NOSi$ has one amine functionality and a single ethoxy group. The existence of a single alkoxy group in both molecules facilitates the controlled formation of a surface monolayer over cellulose acetate polymer chains and helps to prevent silane polymerization in solution prior to the grafting reaction. It has been reported that only organosilanes containing methoxy functionalities are effectively reacted without catalysis, while less reactive ethoxy functionalities might need a catalyst for suitable reactivity. As mentioned before, the amine functionality in aminosilanes catalyze inter or intra-molecularly the reaction between aminosilane molecules and cellulose acetate hydroxyl groups, leading to the formation of siloxyl bonds (Si–O–C). The influence of the amine functionality is such that the reactivity of hydroxylated species with organo-functional silanes decreases in the order $Si-NR_2 > Si-Cl > Si-NH-Si > Si-O_2CCH_3 > Si-OCH_3 > Si-OCH_2CH_3$ [66]. Therefore, on one hand, aminosilanes have the advantage to catalyze the grafting reactions by itself but, on the other, the amine-surface interactions determine the orientation of the grafted molecule over cellulose acetate chains. The amine functionalities can hydrogen bond with the hydroxyl groups from the polymer chain or with other amino groups, decreasing its availability for interaction with CO_2 . The formation of a stable five-membered ring intermediate is believed to be a mode of amine catalysis. Aminosilanes with long chains of alkyl linkers can favor the formation of this cyclic structure between ending NH_2 groups and hydrogen and oxygen centers [71]. When this type of cyclic structures occurs, the number of available amine groups for CO_2 sorption can decrease considerably. The hydrated polymer chains with additional hydroxyl groups from humid grafting conditions can

further promote significant levels of amine hydrogen bonding, as revealed by infrared spectroscopy.

The presence of water is one of the most important reaction conditions to discuss. Water has a profound effect on the aminosilane structure in solution. Under humid conditions, the alkoxy groups of the aminosilane are hydrolyzed to silanols (Si–OH) that can combine to form a siloxane bond (Si–O–Si) between two aminosilane molecules in solution, with the production of a water molecule [67]. This is illustrated in the reactions



Therefore, the presence of water can cause uncontrolled polymerization and/or oligomerization in the grafting reaction solution. Aminosilanes like $\text{C}_9\text{H}_{24}\text{N}_2\text{OSi}$ and $\text{C}_7\text{H}_{19}\text{NOSi}$, containing only one alkoxy functionality per molecule, lose all their reactivity toward cellulose acetate hydroxyl functionalities after polymerization, remaining in solution and being washed out at the end of the grafting reaction. Aminosilanes containing multiple alkoxy groups per molecule are more likely to polymerize in the presence of water, but its reactivity towards hydroxyl groups is conserved as long as one alkoxy functionality remains free. However, its use for improvement of CO_2 sorption capacity in cellulose acetate is not recommended, since the formation of aminosilane multilayers grafted to the polymer chains can lead to increased

amine hydrogen bonding, slow CO₂ diffusion through the aminosilane layers and unsuccessful sorption due to steric hindrance effects.

Water presence in the reaction and subsequent polymerization of aminosilanes in solution can cause the formation of a number of possible grafted structures, like single covalent bonds, hydrogen bonding, two-dimensional self assembly or horizontal polymerization, and multilayers or vertical polymerization. Covalently attached aminosilane molecules can be positioned in a vertical or horizontal direction with respect to the polymer. Aminosilane molecules grafted in a horizontal direction decrease the amine grafting density [71]. When the interaction between cellulose acetate hydroxyl groups and aminosilane molecules is due to hydrogen bonds only, the aminosilane molecule is weakly attached to the surface and can easily be lost. In addition, the already grafted amine functionalities can hydrogen bond to another hydroxyls or get attracted to oxygen atoms in the cellulose acetate surface by dipole intermolecular forces. Figure 11 shows some chemical structures that can result from the bonding and interaction between aminosilane molecules and cellulose acetate [71]. Although the aminosilanes used in the grafting reactions contain only one alkoxy functionality, for illustration purposes some examples of aminosilane polymerization when multiple alkoxy reactive sites interact with a dry and hydrated surface are also presented. These types of intricate networks can hinder CO₂ diffusion and sorption onto free amine functionalities.

Likewise, Shinoda et al. have suggested that the lack of protonation from water molecules in the grafting reaction causes the amine groups of grafted aminosilanes on silica supports to hydrogen bond to surface silanol groups and/or other amino groups. However, the study indicated that protonation by hydrochloric acid (HCl) enhanced the reorientational mobility of the amine functionalities. Through the addition of HCl to a deuterium oxide and grafted silica suspension, the authors found an enhancement of the reorientational mobility of the former hydrogen-bonded amines and the subsequent formation of Brønsted complexes with the surface [80]. However, on this regard Caravajal et al. found that HCl protonation of grafted silicas resulted in both hydrogen bond and Brønsted complexes transformations. The study concluded that the highest level of aminosilane grafted to a silica surface occurred when samples were dried at 25 °C and 10^{-2} Torr prior to grafting and silylation conditions involved dry toluene at 25 °C.

Therefore, the literature reports on aminosilanes grafting on silica supports suggest that complete removal of water from silica surfaces can lead to hydrogen bonded amines with surface hydroxyl groups and unreacted alkoxy moieties. White et al. performed a dry gas-phase grafting reaction with a monoaminealkoxysilane over a silica surface. The results indicated that avoiding exposure to water, the aminosilane anchored to the surface through Si–O–Si bonds, but the amino groups did not freely dangle from the silica surface. Instead, the NH₂ groups hydrogen-bonded to a second surface silanol, so that each aminosilane molecule ended up occupying two silanol sites [81]. On the other hand, excess water can interfere in the grafting reaction by causing prior hydrolysis and polymerization of the aminosilane molecules. It can also lead to protonation of the

NH₂ groups and subsequent formation of hydrated complexes. Caravajal et al. carried out grafting reactions over silica supports in excess aqueous medium and obtained smaller aminosilane loadings. They suggested the existence of an optimum amount of water in the reaction [69]. Harlick et al. also investigated the effect of adding water to the grafting of a triaminoalkoxysilane to a silica-based support. It was found that the amount of water had a profound impact on the amount of aminosilane grafted, since it increased significantly when the amount of water reached an optimum amount [21]. This trade-off between dry and humid grafting conditions suggests the existence of an optimal amount of surface water under which the highest amount of aminosilane molecules is grafted to a hydroxylated species. Finding this optimum amount of water may not be an easy task. Smith et al. have reported unsuccessful attempts to prepare hydrolytically stable aminosilane layers over silica supports by the controlled addition of water to the reaction and use of preformed aminosilane oligomers/polymers in reaction solution [71]. Evidence has been found that different thickness of grafted aminosilane species in silica supports can be achieved by working with only the trace amounts of water present in anhydrous solvent and on glassware [71].

Finally, the post-treatment conditions after the grafting reaction can have a significant impact on the chemical stability of the final sorbent. The aminosilane-grafted cellulose acetate was subjected to a solvent rinsing procedure with equal amounts of toluene, methanol and deionized water. The final rinsing with water may have washed away some aminosilane molecules weakly hydrogen-bonded to the polymer or to other covalently grafted molecules. In this regard, an interesting investigation has been

reported by Smith et al., who studied the hydrolytic stability of silane-derived layers grafted to silica supports [71]. The loss of aminosilane layers was registered after exposure to water at 40°C for 24 h. Silica supports reacted in toluene at 20 °C resulted in complete removal of the aminosilane molecules after 24 h of water exposure, while supports reacted in toluene at 70 °C and those reacted using vapor phase silanization registered a 50% silane removal after 48 h of water exposure. The complete loss of the silane layers was attributed to hydrolysis of the siloxane bonds (Si-O-Si). The partial loss of the grafted layers was suggested to come from aminosilane molecules attached only through hydrogen bonds between surface silanols and alkoxy or amino groups from the aminosilane molecule. The hydrolytic degradation was catalyzed by the amine functionality, which coordinates with the silicon center and catalyzes the hydrolysis via formation of a stable five-membered ring. It was also found that the amount of aminosilane loss was proportional to the thickness of the grafted layer. The highest loss of aminosilane was registered on silica supports with low grafting densities, which allow more space for the amine moieties to coordinate with the siloxane bonds. The authors conducted a series of grafting experiments with alkylalkoxysilanes under the same reaction conditions. The results showed negligible losses of alkylalkoxysilane grafted layers after 48 h of water immersion at 40 °C. However, the rate of silanization of the silica surface was significantly slower than with aminosilanes. These findings confirmed the catalytic role of the amine functionality in aminosilane attachment to silica supports, as well as its catalysis function in the detachment mechanism under the presence of water [71].

In summary, it can be concluded that the decrease in CO₂ sorption capacity of the modified cellulose acetate is the result of the grafting conditions employed. The use of 1 mL of water per gram of cellulose acetate during the grafting reactions may have been an excess amount of water that led to uncontrolled dimerization of the aminosilane species in the reaction solution prior to its attachment to the polymer backbone. Dimerized aminosilane molecules would have lost its reactivity with respect to the hydroxylated polymer, remaining in solution and being washed away at the end of the reaction. On the other hand, some aminosilane molecules that actually reacted with a hydroxyl group from cellulose acetate may have formed different surface structures that hinder the availability of free amine groups for CO₂ sorption. These undesired complex structures would include hydrogen bonding of the amine functionality to adjacent hydroxyl groups or to surface sorbed water molecules; complexation of the amines with an oxygen atom from another aminosilane grafted to the polymer or from a water molecule, among other intricate structures. The presence of such complex structures may also represent a diffusion challenge for CO₂ molecules to find the small amount of available free amine groups dangling from the polymer chains. In addition, the applied solvent rinsing procedures including water may have contributed to the loss of some weakly attached aminosilanes by hydrogen bonding. With the information at hand, it can not be assured if rinsing water may have also affected the stability of the covalent siloxyl bonds (Si–O–C). Therefore, the reaction of hydroxyl groups in cellulose acetate with aminosilane molecules under the reaction conditions employed primarily led to their substitution with aminosilane structures with unfavorable orientations for CO₂ sorption. The diminishing of available sorption sites was reflected in a decreased of the overall sorption capacity.

CHAPTER 5

ANHYDROUS GRAFTING OF AMINOSILANES ON LOW-ACETYL CONTENT CELLULOSE ACETATE

By the time that a second reaction pathway was envisioned as an alternative way to increase CO₂ sorption capacity of cellulose acetate, it was believed that the lack of reactivity of the polymer chains towards aminosilanes was the main cause preventing the success of the grafting reactions. The low hydroxyl content in commercial cellulose acetate (3.5 wt%) seemed to be the immediate cause of the low yields of amine loadings obtained from our first grafting trials. The complex molecular interactions among aminosilanes, hydroxylated polymer and water that drive the course of the grafting reactions under the conditions previously applied were not evident at first sight and, therefore, the subsequent steps followed in the research were not focused on its optimization. This way, a second reaction framework was outlined with the aim to increase the amount of hydroxyl groups in the polymer backbone that could lead to a higher yield of effectively grafted amine functionalities. For this purpose, a de-acetylation procedure was applied to high-acetyl content cellulose acetate prior to the grafting reaction. Hydroxyl groups are the main reactive centers in cellulose acetate polymer chains for chemical bonding with aminosilanes. A de-acetylation reaction removes acetyl groups on cellulose acetate chains and substitutes them with reactive hydroxyl functionalities through a hydrolysis reaction in acid solution.

The following background theory and experimental sections present only relevant materials, methods, and processes not already addressed and explained in the previous chapter.

5.1 Background Theory

5.1.1 Cellulose Acetate De-acetylation

The conventional method to obtain cellulose acetate in the range of 14–19 wt% acetyl content is the homogeneous and controlled hydrolysis of highly acetylated cellulose acetate with 39–40 wt% acetyl content. The resulting hydroxylated cellulose acetate is water-soluble and is prepared starting from commercial high-acetyl content cellulose acetate and hydrolyzing it in an aqueous solution of acetic acid and a mineral acid as catalyst.

The reaction system consists of glacial acetic acid, water and hydrochloric acid as catalyst. Commercial, acetone-soluble cellulose acetate in the range of 39–40 wt% acetyl content is slowly dissolved in the solution and the reaction is allowed to proceed for 48–55 h. Gradual additions of water during the reaction assures a constant water content in the system and maintains all species in solution. When the water-soluble range is attained, the product is precipitated and washed in copious amounts of acetone.

During the de-acetylation reaction, both hydrolysis and re-esterification reactions take place. The amount of water in the system is the main factor defining the course of the reactions. If the water content in the hydrolysis bath is low, re-esterification is favored and products of low primary hydroxyl content are obtained. Malm et al. confirmed that an increment in the water content of the reaction medium produces an increase in the rate of hydrolysis and the amount of primary hydroxyl groups [82]. It was found that when the content of water in the reaction solution exceeds 2 wt%, hydrolysis starts to dominate over esterification, and the products contain increasing percentages of primary hydroxyl as the water content is increased. The rate of hydrolysis is known to be controlled by the temperature and time of the reaction, as well as by the amount of catalyst and water used [59]. However, the reaction medium also influences the distribution of the hydroxyl groups among the three reactive positions available and the degree of polymerization [83].

5.1.2 CO₂ Sorption in De-acetylated Cellulose Acetate

The CO₂ sorption in de-acetylated cellulose acetate, a hydroxylated polymer, is mainly based on acid-base attractions between the acidic gas molecules and the basic hydroxyl sites. The majority of the literature found describes the co-adsorption of CO₂ on hydroxyl sites and another reactive chemical species also present on the surface of a solid material. Knöfel et al. reports the co-adsorption of CO₂ onto hydroxyl sites pending from silica and titania supported functionalized materials. It was suggested that the basicity of the hydroxyl groups depends on the chemical character of the substrate. Hydroxyl groups

from titania surfaces are more basic in comparison to those from a silica surface, and therefore develop a stronger interaction with CO₂ molecules. It was determined that the weak basicity of the hydroxyl groups from silica contributed to CO₂ physisorption by attracting the molecule gas only by electrostatic attractions. On the other hand, it is suggested that the stronger interaction between CO₂ and hydroxyl groups from the titania surface leads to a bidentate carbonate structure formation and, therefore, chemisorption [20]. Baltrusaitis et al. have investigated surface reactions of CO₂ on a hydroxylated Fe₂O₃ and γ -Al₂O₃ solid surface. They proposed that in the absence of co-adsorbed water, the reaction of CO₂ with surface hydroxyl groups form adsorbed bicarbonate. In the presence of water, CO₂ reacts with the water molecule to yield adsorbed carbonate and protonated surface hydroxyl groups [84]. Wang et al. have reported on the acid-base properties of cellulose beads. Using IGC surface characterization, they concluded that cellulose beads behaved as Lewis base polymers [85]. Based on the similarity of the molecular structure of cellulose and de-acetylated cellulose acetate, it can be suggested that the latter may also behave as a Lewis base polymer. If so, the hydroxyl groups on low-acetyl content cellulose acetate may only weakly attract CO₂ molecules and physisorption may occur.

5.2 Experimental

5.2.1 Materials

All materials were used as received from the different suppliers. Cellulose acetate, acetic acid, hydrochloric acid, acetone, and anhydrous toluene were supplied by Sigma-Aldrich (St. Louis, MO, USA). $C_9H_{24}N_2OSi$ and $C_7H_{19}NOSi$ were purchased from Gelest, Inc. (Morrisville, PA, USA). Typical physical and chemical properties of cellulose acetate, $C_9H_{24}N_2OSi$ and $C_7H_{19}NOSi$ have been previously described.

5.2.2 Hydrolysis of High-acetyl Content Cellulose Acetate

The experimental method used for the de-acetylation of high-acetyl content cellulose acetate was proposed by Tanghe et al. [59]. The uniform hydrolysis of acetone-soluble cellulose acetate with acetyl content in the range of 39–40 wt% considerably modifies its properties, yielding products soluble in water with acetyl content in the range of 14–19 wt%.

54 g of deionized water were introduced into a 500 mL three-neck flask and 150 g of glacial acetic acid were added afterwards while mixing at room temperature. The solution was then immersed in a 40 °C oil bath and 30 g of high-acetyl content cellulose acetate were incorporated very slowly with stirring. When the solution was complete and well mixed, 4.5 mL of concentrated hydrochloric acid were slowly pipetted into the

system and the reaction was allowed to proceed at 40 °C with continuous stirring. As the cellulose acetate hydrolyzes, water was added to the reaction in order to keep it in solution. After the first 8 h of hydrolysis, 20 mL of deionized water were pipetted to the system very slowly in order to avoid local precipitation of the sample. Another 40 mL of water were slowly incorporated after 24 h of reaction. The water-soluble range, characteristic of cellulose acetate with acetyl content of 14-19 wt%, was reached after 50 h of hydrolysis at constant mixing and temperature. The acidic solution was then precipitated by gradual addition to 2 L of acetone in a blender at high speed stirring. A white, flaky powder was obtained and filtrated under vacuum using a Büchner funnel. It was washed five times with 1 L of acetone per wash. The product was dried in a vacuum oven at 50 °C overnight. Finally, the dried cellulose acetate was ground in a mortar until a fine white powder was obtained, which was stored in capped vials until further use.

5.2.3 Cast of Low-acetyl Content Cellulose Acetate Films

A standard procedure was used to prepare dense films by solution casting in a controlled environment. Low-acetyl content cellulose acetate powder obtained from the hydrolysis previously described was used to cast the films. About 1.0 g of sample was dissolved in 20.3 mL of deionized water to make a 5.0 wt% solution. The solution was filtered for elimination of bubbles and foam formed during the stirring. Afterwards, it was placed in a glove bag, purged with nitrogen, and sealed. Using a syringe, the solution was then slowly injected over a Teflon plate that allowed the easy removal of the films. The environment inside the glove bag allowed for slow and controlled drying of the films

and prevented direct exposure to atmospheric moisture. Water evaporation was complete within 3–4 days. After this time, the films were removed and dried in a vacuum oven at 35 °C until further use. Before its use on a certain reaction, the temperature of the vacuum oven was raised to 70 °C for 24 h to ensure complete solvent removal.

5.2.4. Anhydrous Grafting of Aminosilanes on Low-acetyl Content Cellulose Acetate Films

The low-acetyl content cellulose acetate films were subjected to anhydrous grafting of aminosilanes following a similar procedure to the one used for high-acetyl content cellulose acetate powder. The dry grafting method was chosen due to the water-solubility of low-acetyl cellulose acetate samples. A dense film of about 1 g of sample was dried at 70 °C under vacuum for 24 h. All glassware used was dried overnight in a convection oven at 130 °C and torched before its use. The film was cut into one in pieces and placed in a 500 mL three-neck flask with a magnetic stirrer and connected to a condenser. The system was closed afterwards and a stream of nitrogen was run through it for 1 h. After this time, 150 mL of anhydrous toluene were injected into the system through a syringe. The films and the solvent were allowed to mix for 30 min at room temperature under a nitrogen atmosphere. Then, the temperature of the reaction system was increased to 110 °C by placing it into a hot oil bath. 3 mL of the corresponding aminosilane were injected. The reaction was allowed to proceed during 16 h under a nitrogen atmosphere and constant temperature. After reaction was completed, the films were separated from the solvent and washed with 400 mL of anhydrous toluene. The modified films were put into a vacuum oven at 70 °C overnight and stored afterwards in

capped vials until further use. Table 7 identifies the samples obtained by the anhydrous grafting of aminosilanes on low-acetyl content cellulose acetate dense films.

Table 7. Reaction conditions for dry aminosilanes grafting of low-acetyl content cellulose acetate films

Sample	Cellulose Acetate (g)	Toluene (mL)	Aminosilane Species	Aminosilane (mL)	H ₂ O (mL)	Amination Time (h)	Amination Temperature (°C)
<i>J</i>	1	150	C ₉ H ₂₄ N ₂ OSi	3	0	16	110
<i>K</i>	1	150	C ₇ H ₁₉ NOSi	3	0	16	110

5.2.5 Sorbent Sorption Characterization

The characterization of the CO₂ sorption capacities of the aminosilane-grafted cellulose acetate films was carried out using a pressure decay method [55]. Detailed description of the method is provided in the previous chapter.

5.2.6 Instrumental Characterization of Sorbents

The composition and properties of the aminosilane-grafted cellulose acetate films were tested using Elemental Analysis (EA), density analysis, Fourier Transformed Infrared Spectroscopy (FT-IR), Thermogravimetric Analysis (TGA) and Scanning Electron Microscopy (SEM). A detailed description of these instrumental analyses was provided in the previous chapter.

Fourier Transformed Infrared Spectroscopy (FT-IR) analysis was used to confirm the presence of amine functionalities grafted to low-acetyl content cellulose acetate films

and to reveal details about the molecular structure of the new materials. The infrared spectra were recorded on the same spectroscopy instrument used for ATR-IR tests; however, a film sample holder was used instead. The instrument was a Shimadzu IR Prestige-21 Fourier Transform Infrared Spectrophotometer (Shimadzu Scientific Instruments, Columbia, MD, USA). Each sample was analyzed using a scan time of 64 scans, scanner velocity of 10 kHz, resolution of 4 cm^{-1} and an aperture setting of 6 mm. The spectra were recorded in absorbance units in the range of $4000 - 370\text{ cm}^{-1}$.

5.3 Results

5.3.1 Sorbent Sorption Characterization

Anhydrous grafting experiments with each type of aminosilane were carried out using low-acetyl content cellulose acetate dense films. The reaction conditions were held constant for both type of experiments and the only variation was the aminosilane species used. Isotherms were recorded at $35\text{ }^{\circ}\text{C}$ using the aforementioned pressure decay method.

Figure 13 presents the isotherms of samples *J* and *K*, aminosilane-grafted cellulose acetate film sorbents obtained by the dry grafting of $\text{C}_9\text{H}_{24}\text{N}_2\text{OSi}$ and

$C_7H_{19}NOSi$, respectively. In addition, the isotherm of sample *I*, non-silanated low-acetyl content cellulose acetate dense film, is also presented.

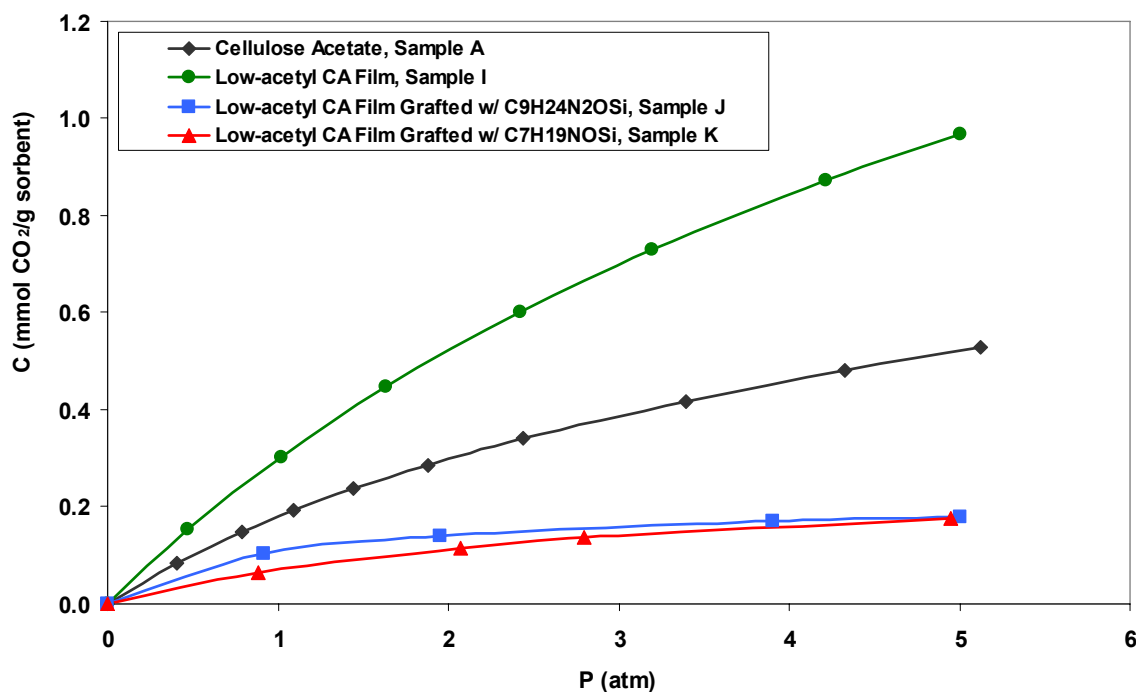


Figure 13. CO₂ sorption isotherms for low-acetyl content cellulose acetate dense film sample *I* and aminosilane-grafted samples *J* and *K*

De-acetylation of high-acetyl content cellulose acetate to a range of acetyl composition of 14–19 wt% considerably modifies the chemical properties of the polymer. Low-acetyl content cellulose acetate is the product of an aggressive acid hydrolysis during long reaction times where many of the initial acetyl functionalities were substituted with hydroxyl groups and the amorphousness of the polymer chains may have further increased. Therefore, the transport of CO₂ may have been benefited by an increment in the random order of the chains and sorption occurring both at the hydroxyl and acetyl functionalities may have been facilitated. This way, the sorption capacity of

Sample *I*, non-silanated low acetyl content cellulose acetate film, reached 0.97 mmol CO₂/g sorbent at 5 atm and 308 K.

On the other hand, an unexpected decrease in the CO₂ sorption capacity of the original polymer was registered for films subjected to anhydrous grafting of aminosilanes. The capacity of both aminosilane-treated sorbents decreased to about 0.18 mmol CO₂/g sorbent at 5 atm and 308 K. Although it is still not clear the reason for the decrease in sorption capacity, it is suggested that the various degrees of inter- and intra-molecular hydrogen bonding promoted by the increase in hydroxyl functionalities may have prevented the grafting reaction rather than trigger it. In any case, however, even a small amount of grafted aminosilanes should positively contribute to increase the CO₂ sorption capacity of the polymer. As the opposite occurred, it is suggested that the exposure of the low-acetyl content cellulose acetate films to an additional reaction step would have contributed to an unexpected change in morphology that hindered CO₂ sorption.

5.3.2 Elemental Analysis

Elemental analysis was carried out for low-acetyl content cellulose acetate obtained after 50 h of hydrolysis and for aminosilane-grafted cellulose acetate films under anhydrous conditions. The results are presented in Table 8.

Table 8. EA of high-acetyl content CA, low-acetyl content CA and aminated low-acetyl content CA films

Sample		Elemental Analysis				
		% C	% H	% O	% N	% Si
<i>A</i>	High-acetyl content cellulose acetate (CA)	48.21	5.93	45.60	0.00	0.00
<i>H</i>	Low-acetyl cellulose acetate powder (LACA)	47.84	6.66	48.66	0.00	0.00
<i>J</i>	LACA film anhydrous grafting with C ₉ H ₂₄ N ₂ OSi	42.14	6.33	50.96*	< 0.5	0.07
<i>K</i>	LACA film anhydrous grafting with C ₇ H ₁₉ NOSi	41.29	6.52	49.01	< 0.5	< 0.05

* Oxygen content could not be accurately determined by the instrument. Estimation by difference.

The increment in oxygen and hydrogen content of sample *H*, low-acetyl content cellulose acetate obtained by a de-acetylation method, is an evidence of the increase of hydroxyl groups linked to the polymer backbone. The percent increment in oxygen content was about 6.7%, while the percent increase in hydrogen content was around 12.3%. Estimation of the theoretical weight composition of a completely de-acetylated cellulose acetate glucoside unit leads to a carbon content of about 44.4 wt%, oxygen content of around 49.4 wt%, and hydrogen content of 6.2 wt%. The amounts obtained by EA are very near to the expected theoretical values and it can be suggested that the hydrolysis procedure worked rather well. Water-solubility of de-acetylated sample *H* and *I* are additional confirmations of their decrease in acetyl content.

Solution-cast low-acetyl content dense films of about 2–6 mils thickness were reacted with both aminosilanes species in order to introduce amine functionalities on the place of hydroxyl groups. EA results show that the anhydrous grafting method applied to low-acetyl content cellulose acetate films has not been effective under the reaction conditions used. The amounts of amine loaded using both aminosilanes was below the detection limit of the testing instrument and could not be measured accurately. The low grafting amine density in the films may be due to a number of reasons. 16 h long reaction time may not be enough for the bulky aminosilane molecules to reach the hydroxyl

reactive sites within the network of polymer chains under strong hydrogen bonding interactions. In addition, these intermolecular interactions in the highly hydroxylated polymer chains may be strong enough to not allow hydroxyls to successfully interact with aminosilanes molecules.

5.3.3 Density Analysis

The densities of the low-acetyl content cellulose acetate powder and films, as well as that of the two aminosilane-grafted films were obtained by gas pycnometry. For comparison purposes, the density of high-acetyl content cellulose acetate (LACA) is also presented. The results are presented in Table 9.

Table 9. Densities of high-acetyl content CA, low-acetyl content CA and aminated LACA films

	Sample	Density (g/mL)
<i>A</i>	High-acetyl content cellulose acetate powder (CA)	1.4205
<i>H</i>	Low-acetyl content cellulose acetate powder (LACA)	1.3953
<i>I</i>	Low-acetyl content cellulose acetate film (LACA)	1.4469
<i>J</i>	LACA film anhydrous grafting with C ₉ H ₂₄ N ₂ OSi	1.4791
<i>K</i>	LACA film anhydrous grafting with C ₇ H ₁₉ NOSi	1.4687

The absolute density of cellulose acetate powder slightly decreases after de-acetylation. This may be the result of replacing acetyl groups with hydroxyl functionalities with less molecular weight. However, the change in density is small due to the increment in molecular packing on the polymer chains after the attachment of smaller functional groups. Another important factor to consider is the significant increment in inter- and intramolecular hydrogen bonding interactions after de-acetylation that strongly pull together the polymer macromolecules. On the other hand, the density of the low-acetyl content cellulose acetate film increased with respect to its precursor powdered

sample and to the original powdered high-acetyl content cellulose acetate. After complete hydration, inter-and intra-molecular hydrogen bonding interactions may have increased due to chains rearrangement and orientation in the presence of the solvent. Additional hydroxylation from the dissociation of water molecules on the polymer surface can also contribute with additional intermolecular hydrogen bonding forces. Any of these factors can contribute to increment the packing of the polymer chains and, therefore, the material's absolute density. When the water-soluble cellulose acetate films were subjected to the grafting reaction with both aminosilane species, the increment in density was likely due to the incorporation of some aminosilane molecules with much higher molecular weights in some of the free hydroxyl groups. The change in density was small due to the low grafting density achieved by this approach.

5.3.4 Fourier-Transformed Infrared Spectroscopy

The infrared spectra of the high-acetyl and low-acetyl content cellulose acetate powder and film samples were also obtained. These spectra are presented in Figures 14 and 15. The films subjected to the anhydrous grafting reaction with aminosilanes were also tested with FT-IR spectroscopy and their spectra are shown in Figures 16 and 17. The matching of the most prominent peaks of the IR spectrum with their corresponding functional group provided a valuable tool to confirm the effectiveness of the reactions. A brief note has to be done regarding the difference in magnitude of the intensity scales between high/low acetyl content cellulose acetate powder and film samples spectra. On any IR instrument, the beam loses energy as it goes from its source to the detector due to

collisions with mirrors, lenses, and the atmosphere. On the IR instrument used in this study, the registered beam intensity without sample and ATR device is about 75% the intensity at its origin. When the ATR attachment is connected in order to test powdered samples, the intensity of the beam without sample is just around 4% its initial intensity. Therefore, the drop in magnitude for the intensity scales displayed by the cellulose acetate powder spectra is expected and normal. In addition, films are much denser than powder samples, and therefore the spectra obtained for films are expected to register higher intensities. It is difficult to draw conclusions about the absolute intensities of the absorbance bands with the information at hand. In order to perform a complete quantitative IR analysis, samples should have been prepared with exactly the same procedure in order to avoid that factors like powder packing density, film thickness or IR background negatively affecting the measurements. In addition, information about the refractive index, absolute and packing density of the samples has to be known in order to obtain required parameters like molar absorptivity, concentration of the sample, beam path length, etc. Therefore, quantitative IR analysis will be avoided. However, an analysis of the relative intensities of the absorption bands within a sample can be useful to confirm some general molecular structure changes after chemical reactions and the introduction of new functional groups.

Figure 14 shows a broadening and increase in the relative intensity of the hydroxyl region ($3200\text{--}3645\text{ cm}^{-1}$) for low-acetyl content cellulose acetate powder sample. The shift and increase of relative intensity of the hydroxyl absorption bands with respect to the rest of the spectrum become more evident for de-acetylated film sample *I*

(Figure 15). The increase in relative intensity of the absorption bands reflects an increment in the number of hydroxyl bond stretching vibrations after the hydrolysis of cellulose acetate. A shift to the left of the spectrum of about 135 cm^{-1} locates the majority of the hydroxyl absorption bands of the de-acetylated sample more in the region of inter- ($3200\text{-}3550\text{ cm}^{-1}$) and intra-molecular hydrogen bonds ($3450\text{-}3600\text{ cm}^{-1}$) than in the region of free hydroxyl groups ($3610\text{-}3645\text{ cm}^{-1}$). Although absorption bands in the region of free hydroxyls can be seen in the spectrum, they are rather weak in comparison to the intensity of hydrogen bonding bands. A comparison of the spectra of pure and de-acetylated cellulose acetates evidences that free hydroxyl absorption bands were stronger in the original polymer with respect to the other type of hydrogen bonding bands. Therefore, it can be suggested that various degrees of intermolecular and intramolecular hydrogen bonding on the de-acetylated polymer become more dominant over free hydroxyl species after the hydrolysis reaction.

On the other hand, a clear decrease in the acetate groups ($\sim 1040\text{ cm}^{-1}$, 1240 cm^{-1}) and the carbonyl ($1700\text{-}1800\text{ cm}^{-1}$) absorption bands with respect to the rest the spectrum peaks is seen after de-acetylation of the polymer. A broadening of the absorption bands at $990\text{-}1060\text{ cm}^{-1}$ indicates the presence of additional C-OH stretching vibrations in the hydroxylated polymer. Finally, an interesting feature to note is the appearance of a wide region of intense absorption bands at the core of the fingerprint region for the spectrum of de-acetylated cellulose acetate film after dissolution in water and solution-casting. This may be due to an increase in the amorphous regions in the polymer that causes an increment of the bending vibrations within the macromolecule.

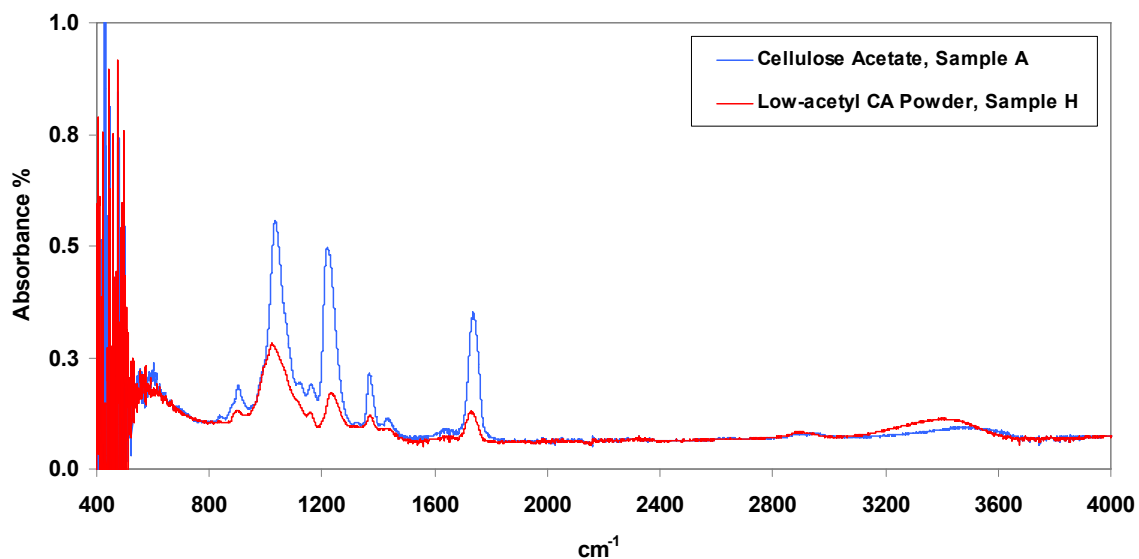


Figure 14. ATR-IR spectra of high-acetyl content and low-acetyl content cellulose acetate powders

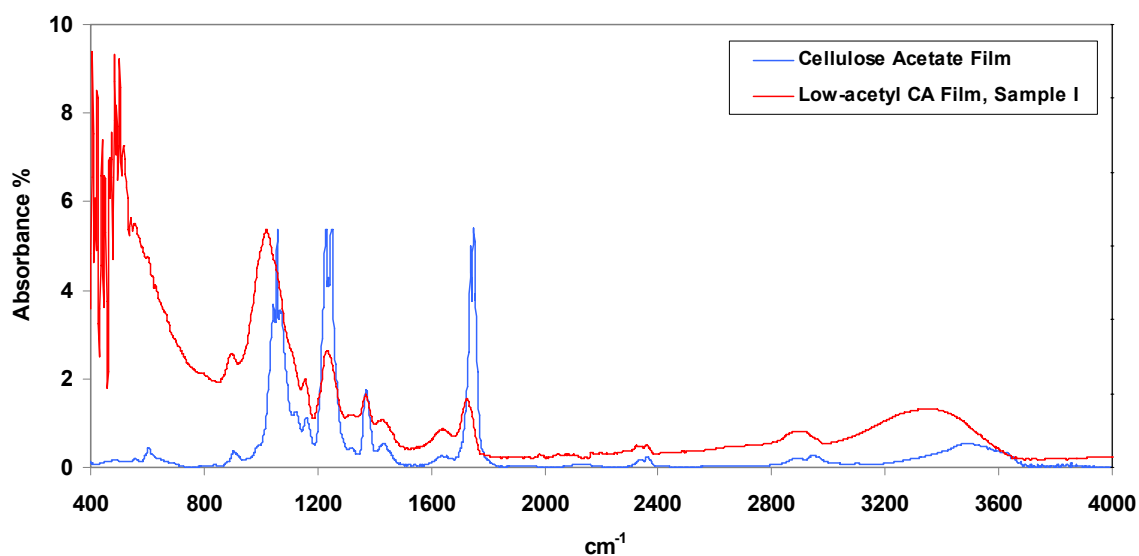


Figure 15. FT-IR spectra of high-acetyl content and low-acetyl content cellulose acetate films

The spectrum of low-acetyl content cellulose acetate film grafted with $C_9H_{24}N_2OSi$ is presented in Figure 16. The first evident feature is a significant increment in the absorbance band around 1020 cm^{-1} . This frequency corresponds both to the very strong, distinct band of dimethylsiloxane $(CH_3)_2SiO-$ bonds [86] and to one of the bands of the acetyl groups ($1010\text{-}1040\text{ cm}^{-1}$). The presence of both functional groups on the

polymer chains have resulted in a very strong peak dominating the spectrum. The absorption band of medium intensity around 1260 cm^{-1} has also been identified in the literature as characteristic of the $-\text{Si}(\text{CH}_3)_2\text{-O-}$ structure, present in $\text{C}_9\text{H}_{24}\text{N}_2\text{OSi}$ [86]. The broadening of both peaks comes from absorption bands related to the presence of $\text{Si-CH}_2(\text{CH}_2)_x\text{CH}_3$ at frequencies $945\text{-}975$, $1000\text{-}1020$, and $1220\text{-}1250\text{ cm}^{-1}$ [86]. An unexpected increase in the bands at 1370 and $1700\text{-}1760\text{ cm}^{-1}$ is registered, corresponding to acetyl groups attached to a silicon atom in the form Si-COOCH_3 [86]. A free amine functionalities produces bands either at 1622 [87], $1580\text{-}1650$ [88], or $3300\text{-}3500$ [79] cm^{-1} , while N-H bonds have absorption bands at $3070\text{-}3350$ [79], 1594 [87], or $1550\text{-}1650\text{ cm}^{-1}$ [88]. A small increment in the absorbance of the hydroxyl region at about $3300\text{-}3500\text{ cm}^{-1}$ may correspond to the presence of a small amount of amine groups grafted to the polymer, but the change in the spectrum is so small that one should not rely on this evidence for definitive conclusions. In general, the spectrum does not present any significant changes correlated with the presence of amine groups, so it can be concluded that, although silane groups absorbance bands are detected, there is no evidence of amines attachment to the polymer backbone.

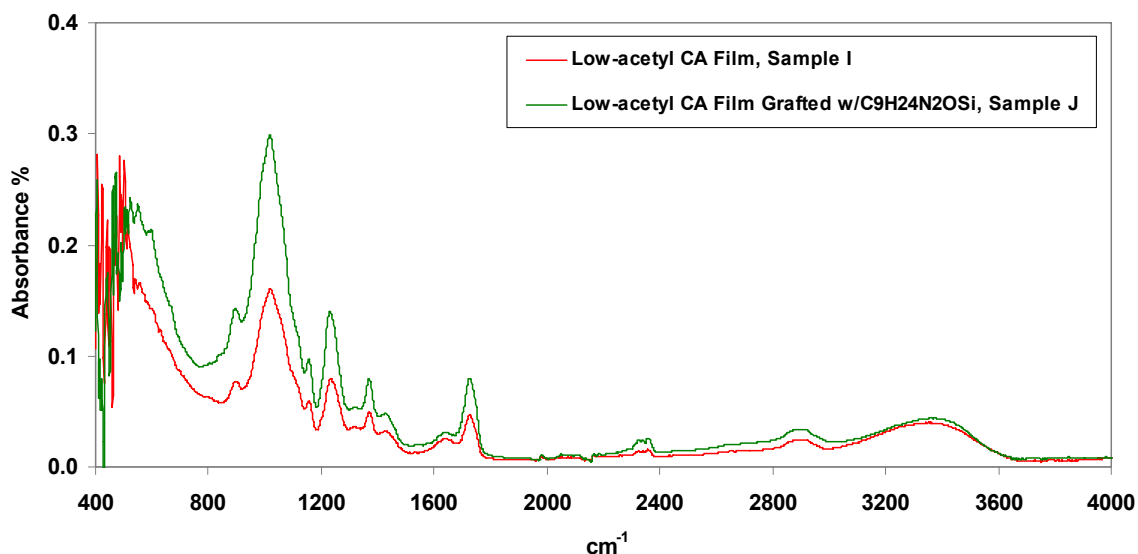


Figure 16. FT-IR spectra of low-acetyl content cellulose acetate film and anhydrous grafted film with $C_9H_{24}N_2OSi$

The infrared spectrum of low-acetyl content cellulose acetate film grafted with $C_7H_{19}NOSi$ is presented in Figure 17. Its high similarity with the spectrum obtained for sample *J* is evident, except for the presence of a stronger absorption band in the hydroxyl region. One may think about the presence of either free or bonded amine functionalities detected by the infrared beam at this frequency range; however, results from Elemental Analysis and decrease of the CO_2 sorption capacity for sample *K* suggest the absence of grafted amine groups. Therefore, a higher degree of inter- and intra-molecular hydrogen bonding interactions within the polymer structure of this particular sample is a reason to be considered. The presence of $Si-OCH_2CH_3$ bonds from $C_7H_{19}NOSi$ is detected on the broadening of the $\sim 1020\text{ cm}^{-1}$ peak ($970\text{-}940$, 1100 , and 1075 cm^{-1}) [86].

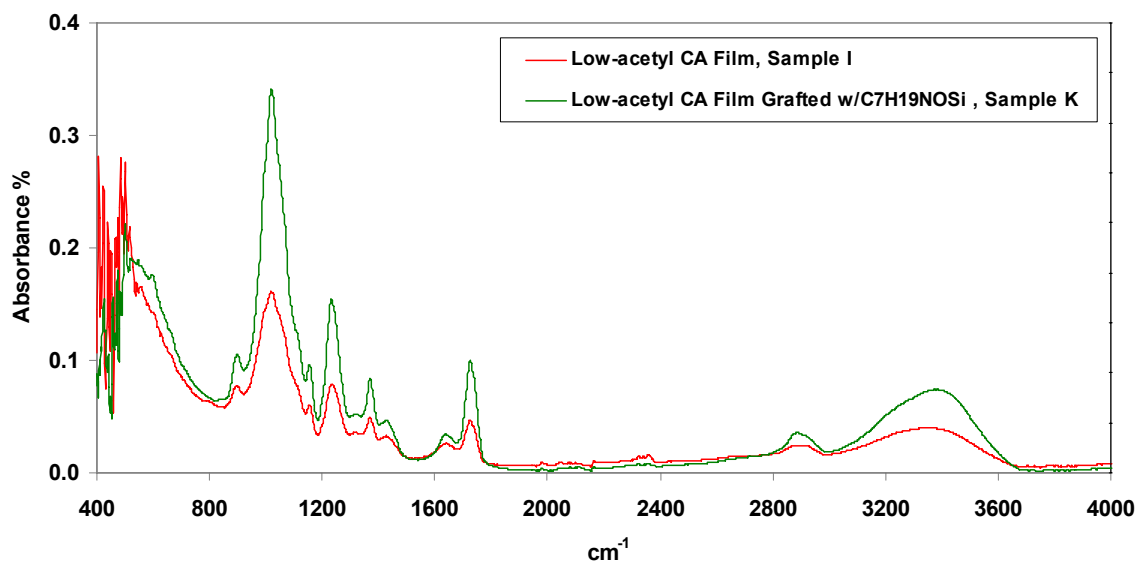


Figure 17. FT-IR spectra of low-acetyl content cellulose acetate film and grafted film with C₇H₁₉NOSi

5.3.5 Thermogravimetric Analysis

The TG curves of high-acetyl content, low-acetyl content cellulose acetate, as well as those of samples *J* and *K* are showed in Figures 18 to 20. The TG curve of low-acetyl content cellulose acetate powder is presented in Figure 18. It shows a small weight loss at a temperature of about 80 °C. The sample remained stable up to a temperature of about 280 °C, where its decomposition started to take place. The amount of sample lost in this step was around 82%, leaving a residue of about 9%. Compared to high-acetyl content cellulose acetate, which degradation takes place at about 310 °C, de-acetylated sample *H* presented a decrease in thermal stability of circa 10%.

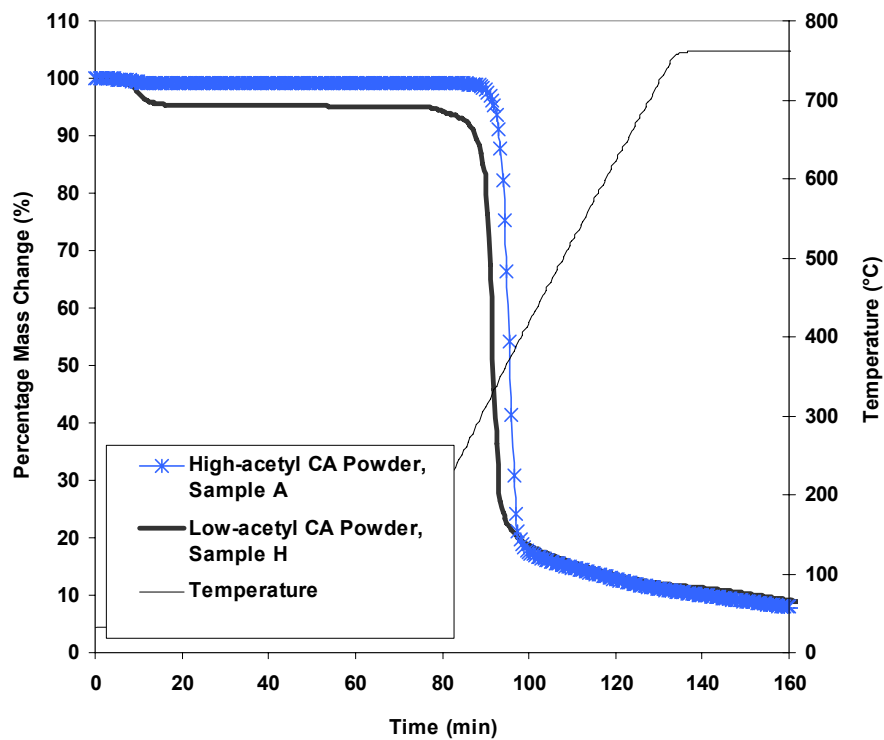


Figure 18. TG curves of high-acetyl and low-acetyl content cellulose acetate powder

On the other hand, the low-acetyl content cellulose acetate film reacted with $C_9H_{24}N_2OSi$ decreased its degradation temperature a little further to about 240 °C, as shown in Figure 19. The mass sample loss was about 80% of the original sample weight.

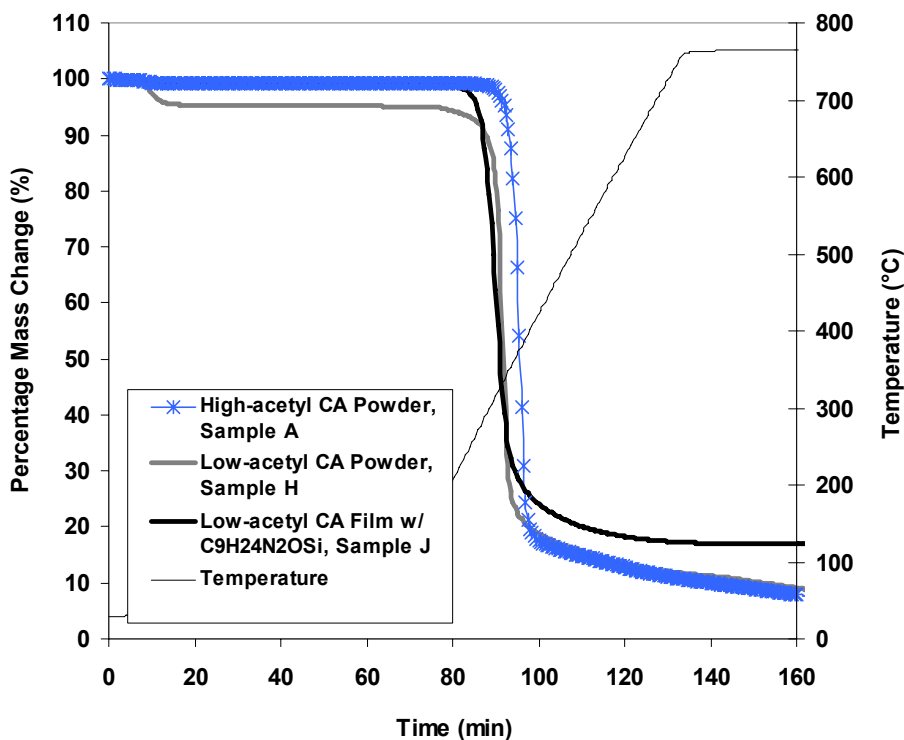


Figure 19. TG curves of high-acetyl, low-acetyl content cellulose acetate powder, and low-acetyl content cellulose acetate film grafted with C₉H₂₄N₂OSi

The TG profile of sample *K* is provided in Figure 20. It is observed that the profile remained almost constant after the grafting of C₇H₁₉NOSi with respect to its precursor low-acetyl cellulose acetate film. Its thermal stability decreased only slightly to a value of 260 °C and the amount of decomposed sample accounted for 78%. The decrease in thermal stability registered by cellulose acetate samples after de-acetylation is a reflection of the new intermolecular forces among the polymer chains. The high degree of hydroxylation has become the polymer structure more instable to thermal treatments. On the other hand, the low loading of amines on grafted samples produced almost no change in the thermal stability of the hydroxylated material.

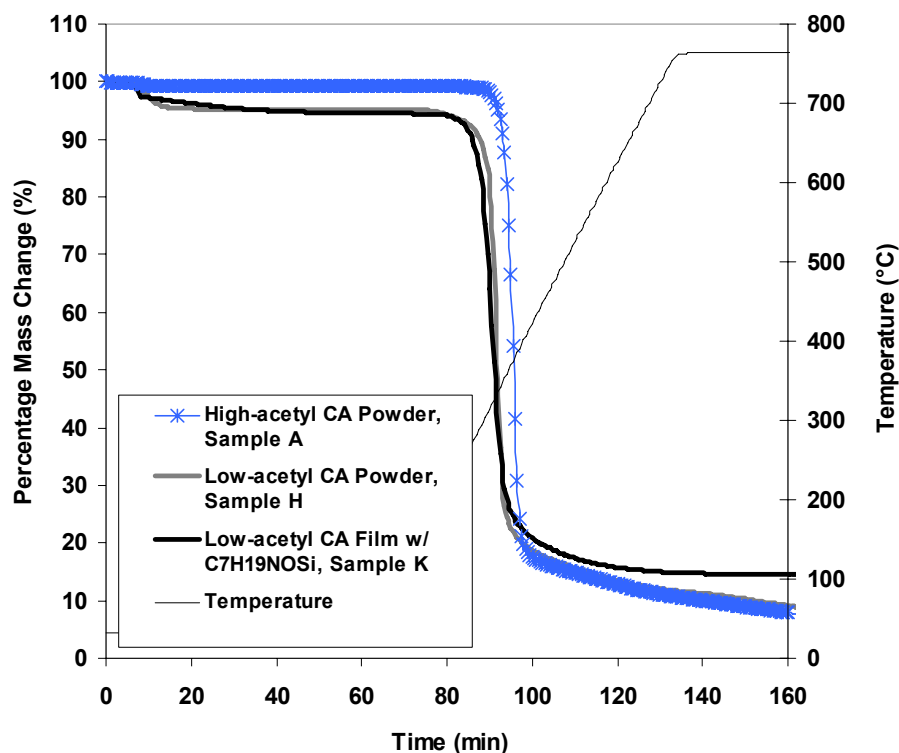


Figure 20. TG curves of high-acetyl, low-acetyl content cellulose acetate powder, and low-acetyl content cellulose acetate film grafted with $C_7H_{19}NOSi$

5.3.6 Scanning Electron Microscopy

Figure 21 presents the SEM images of low-acetyl content cellulose acetate film, sample *I*, and the morphology of the aminosilane-grafted films, samples *J* and *K*. SEM micrographs show the change in surface morphology of low-acetyl content cellulose acetate films after aminosilane grafting reactions. It is interesting to note that despite the absence of significant amounts of amine functionalities as suggested from previous characterization analyses, the films surface present a rough surface with some whitish spots that contrasts with the smooth surface of non-silanated low-acetyl content cellulose acetate film showed in Figure 21 (a). Due to the lack of success on the grafting of amine

functionalities in these films, further analysis to investigate the nature of these surface morphology changes was out of our scope.

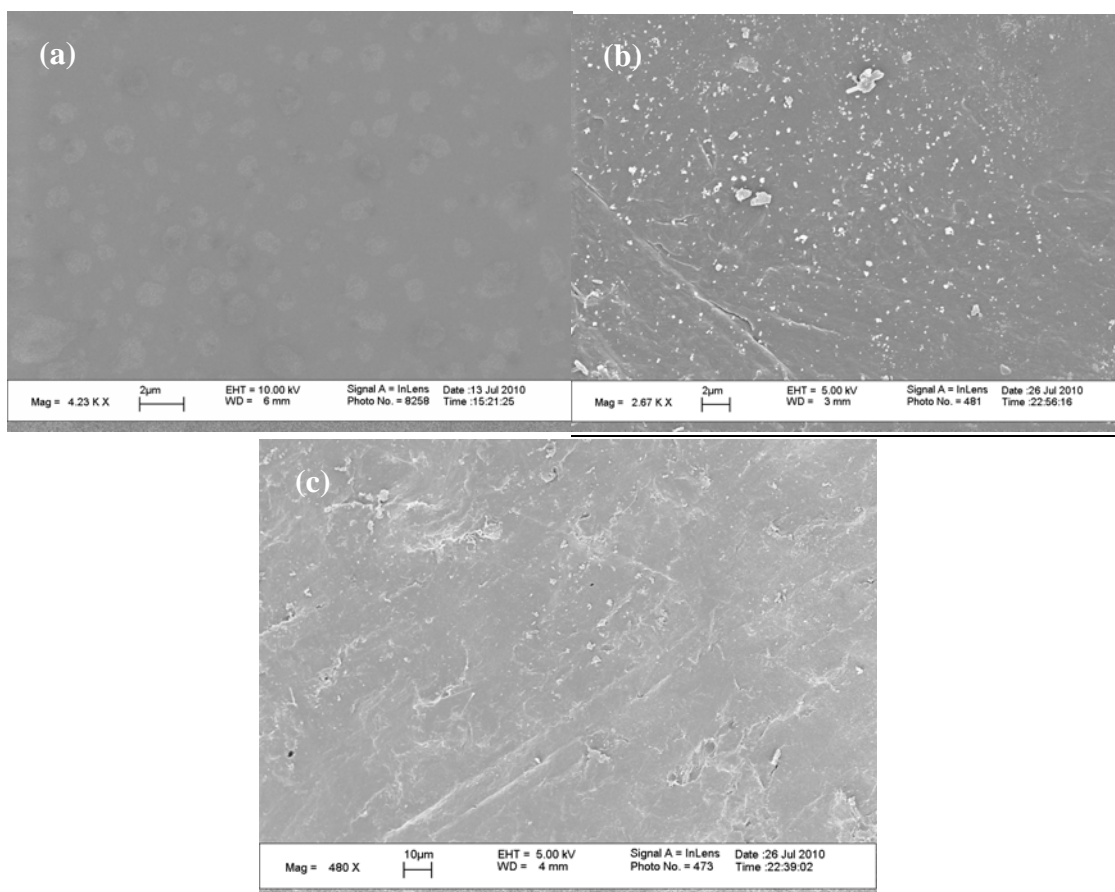


Figure 21. SEM images of (a): sample *I*; (b): sample *J*; (c): sample *K*.

5.4 Discussion

With the objective to increase the reactivity of cellulose acetate toward aminosilane grafting reactions, a de-acetylation procedure was carried out to yield products soluble in water of acetyl content in the range of 14–19 wt%. The resulting hydroxylated polymer was envisioned to be a highly reactive material toward

aminosilanes, with the ability to be transformed into dense films due to its water-solubility property.

The hydroxylated cellulose acetate films were subjected to anhydrous grafting with both aminosilanes species used in the first grafting approach. Only the dry grafting procedure was applied to the low-acetyl content polymers since the addition of water to the reaction would have caused solubilization of the films. The ideal reaction of anhydrous grafting of aminosilanes over a cellulose acetate hydroxylated polymer is schematically represented in Figure 22.

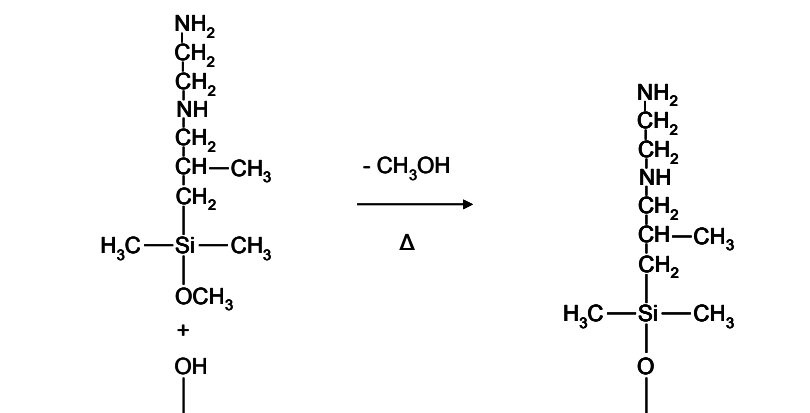


Figure 22. Ideal anhydrous grafting of aminosilanes on low-acetyl content cellulose acetate films

Ideally, the dry grafting reaction should occur in the ratio of one hydroxyl per aminosilane molecule grafted, forming a uniform coverage of amine functionalities dangling from the polymer backbone and producing the corresponding alcohol. It was envisioned that the large density of hydroxyl groups in the polymer chains would facilitate aminosilane grafting, and that the crosslinking properties of the aminosilanes would avoid water solubility of the polymer after the reaction.

However, the results obtained from sorption characterization, elemental analysis and infrared spectroscopy indicated that low-acetyl content cellulose acetate films barely reacted with aminosilanes during the anhydrous grafting reactions. The sorption capacity decreased after the reaction with aminosilanes. Although infrared spectroscopy detected the presence of different silane bonds, it failed to detect amine functionalities. The amount of nitrogen in grafted samples was below the detection limit of the instrument and the silicon content was rather low.

A number of factors may have affected the efficiency of the reaction. The reactivity of the hydroxylated polymer may have been compromised by the elevated amount of hydroxyl groups involved in strong inter- and intra-molecular hydrogen bonding interactions, and the original idea of a macromolecular structure full of free and reactive hydroxyl functionalities may not apply to our material. If so, the strong molecular interactions among a fraction of hydroxyl groups may have hinder the reactivity of the polymer toward the aminosilanes species, instead of enhance it. In addition, the grafting reaction times may not have been sufficient to allow complete diffusion of the reactants through the polymer matrix and the type of solvent used may not have helped to swell the films and facilitate the transport of species.

Elemental analysis and infrared spectroscopy results confirmed that the acidic hydrolysis of cellulose acetate to the water-soluble range yielded a polymer with very low degree of substitution (DS). It has been reported that the DS for water-soluble

cellulose acetates ranges from 0.5 to 1.1 [89]. On this type of cellulosic polymers, the presence of considerable amounts of hydroxyl groups is essential for their water-solubility. Among the three types of intermolecular interactions that can occur in cellulose acetate polymers (hydroxyl-hydroxyl or hydrogen bonding, hydroxyl-acetyl, and acetyl-acetyl interactions), hydroxyl-hydroxyl are among the strongest ones [54] and the dominant in water-soluble cellulose acetate. They determine the mobility, reactivity and packing of the polymer chains. Interestingly, the ease of hydrogen bond formation and its strength is different among the three types of hydroxyl groups that can exist in cellulose acetate. The strength of hydrogen bonding by the hydroxyl groups in the C₂ and C₃ positions of the glucoside unit of is much stronger than that of hydroxyl groups in the C₆ position. Therefore, the reactivity of hydroxyl groups in water-soluble cellulose acetate in the C₆ positions is very high compared to that of hydroxyl groups in the C₂ and C₃ positions [89]. This way, the reactivity of the polymer may have been reduced in many of its glucoside units to 1 out of 3 hydroxyl groups. In principle, this degree of reactivity would be similar to that of the original polymer containing one hydroxyl group and two acetyl groups per repeating unit. However, it has been reported that water-soluble cellulose acetates are essentially non-crystalline polymers [89], with a non-uniform distribution of reactive C₆ hydroxyl groups along the polymer chains that can further increase the degree of chain packing and decrease the reactivity of the material overall. These findings are in accordance with the infrared spectroscopy results showing strong absorption bands in the hydrogen bonding region and very weak absorption bands in the free hydroxyl frequencies.

On the other hand, some of the grafting reaction conditions applied may have also had a significant impact on the low amine loadings. The reaction time employed was 16 h; however, it may have been an insufficient period of time for the aminosilane molecules to diffuse through the highly packed and entangled polymer chains and find those particular reactive and free hydroxyl groups in a “sea” of less reactive hydrogen bonded hydroxyl functionalities. Longer reaction times may be needed in order for the aminosilane molecules to reach the reactive hydroxyl sites in the polymer.

The total anhydrous conditions at which the grafting reaction was run could have affected the final amine content as well. As previously discussed, some research groups have found the existence of an optimum amount of water that increase the reactivity of aminosilane used and of the substrate employed [21, 34, 52]. However, other researches affirm that uncontrolled polymerization caused by the presence of water can promote the loss of reactivity of the silane dimers toward the hydroxyl functionalities, remaining in solution and being washed out at the end of the grafting reaction. Therefore, further investigation is needed in order to find the optimum grafting conditions if a de-acetylated, water-soluble cellulose acetate is employed.

On the other hand, a discussion about the improvement in CO₂ sorption capacity of the low-acetyl content cellulose acetate films and the decrease in sorption capacity of the aminosilane-reacted films is needed. Pressure decay sorption experiments registered an increase in the CO₂ sorption capacity of water-soluble cellulose acetate with respect to the original polymer. The low-acetyl content cellulose acetate films offer a vast array of hydrogen-bonded hydroxyl functionalities that may behave as a weak Lewis base

polymer [85]. The basic polymeric matrix may attract the polar, acidic CO₂ molecules and enter into weak interactions with them, leading to physical adsorption. The strong hydrogen bonding interactions in the polymer may prevent any further reaction with the attracted CO₂ molecules and therefore, chemisorption is not likely to occur. The physisorption mechanism may involve free hydroxyl groups or hydrogen bonded ones. In the case of physisorption on free hydroxyl groups, the interactions may be via hydrogen bonding, as showed in Figure 23 [90]. Physisorption of CO₂ on bridging hydroxyl groups may involve a charge transfer mechanism between the carbon atom in CO₂ and the oxygen atom from the hydroxyl group, which acts as an electron donor [91]. The amorphous polymer chains may favor the transport and sorption properties of CO₂ into the low-acetyl content cellulose acetate. Although a significant increment in the CO₂ sorption capacity was achieved through de-acetylation and solution-casting of the low-acetyl content cellulose acetate, its water-solubility property made the sorbent impractical for industrial applications.

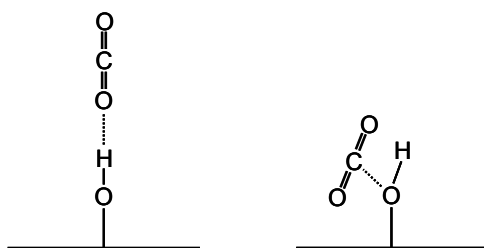


Figure 23. Possible physisorption mechanisms of CO₂ in low-acetyl content cellulose acetate films

Finally, a decrease in the sorption capacity of the aminosilane-grafted low-acetyl content cellulose acetate films was observed. Elemental analysis results revealed the

presence of minimal amounts of amines and silane functionalities after the grafting reactions, while infrared spectroscopy did not detect the presence of amine groups, but suggested the presence of some silane functionalities. The grafting of silane functionalities without their amine moieties would explain a decrease in the sorption capacity of the polymer, through blockage of the only available sorption sites, the hydroxyl functionalities, with silane species. However, with the information at hand it is not possible to draw a conclusion about the complete loss of amines functionalities and only the partial loss of their organosilane counterparts.

CHAPTER 6

PREPARATION OF CELLULOSE ACETATE/TITANIUM(IV) OXIDE HYBRID POLYMER

Previous experimental approaches have attempted to increase the CO₂ sorption capacity of cellulose acetate by 1) introducing amine functionalities into the neat polymer backbone applying literature-based reaction conditions and by 2) modifying the polymer's chain molecular structure to increase its reactivity towards the grafting of aminosilanes under similar reaction conditions. While the reaction conditions applied in the first experimental approach may have hindered the grafting of amines, the polymer's new chemical structure obtained in the second approach may have adversely affected the amine grafting reactions. The lack of success through these previous approaches for the creation of a novel amine-functionalized cellulose acetate sorbent with enhanced CO₂ sorption capacity and appropriate physical-chemical properties for industrial use led the present study to attempt a significantly different approach. Based on literature reports of successful improvement of cellulose reactivity to form cellulose/titanium(IV) hydroxide hybrid materials suitable for further modification with organosilanes [56], a third experimental pathway was chosen. It consisted in the anhydrous reaction of low-acetyl content cellulose acetate films with titanium tetrachloride to form a cellulose acetate/titanium(IV) hydroxide hybrid material and further modification through aminosilanes grafting. At that stage of the research work, the reaction was envisioned as a method to break down the high degree of inter- and intra-molecular hydrogen bonding generated by plenty hydroxyl groups in the low-acetyl content cellulose acetate chains

and that hindered the aminosilane grafting attempted before. Therefore, the formation of cellulose acetate/titanium(IV) hydroxide material was expected to enhance the reactivity of the hydroxylated polymer by breaking down some of the hydrogen bonds in the polymer chains and adding instead metal hydroxide functionalities capable to react with aminosilanes through a grafting reaction.

However, this chapter will describe how the water-solubility property of the low-acetyl content cellulose acetate obtained from the previous experimental approach became an unexpected obstacle for the successful preparation of cellulose acetate/titanium(IV) hydroxide hybrid materials suitable for aminosilane grafting. In place, the preparation of cellulose acetate/titanium(IV) oxide hybrid materials was achieved and the assessment of its sorption properties showed the potential of this hybrid material as a promising CO₂ sorbent.

The background theory and experimental sections presented in this chapter are only relevant materials, methods, and processes not already addressed and explained in previous chapters.

6.1 Background Theory

6.1.1 Preparation of Cellulose/Metal Hydroxide and Cellulose/Metal Oxide Hybrid

Materials

Reports have been found about scientific research aimed to improve the reactivity of cellulose by the breaking of its elevated degree of inter- and intra-molecular hydrogen bonding interactions. The properties and application scope of cellulose has been improved by changes in its macromolecular structure containing high hydroxyl content per glucoside unit. Meng et al. have reported on the preparation, characterization and sorption properties of cellulose/titanium(IV) hydroxide modified with an aminosilane, suitable for sorption of heavy metal ions and transition metal ions in aqueous solutions [56]. With similar applications, Alfaya and Gushikem have investigated the sorption properties of cellulose/aluminum oxide modified with organosilicones [92]. The breaking of cellulose hydrogen bonds through the preparation of cellulose/metal oxide hybrid materials has been reported by Silva et al. [57]. They coated cellulose with a layer of titanium(IV) oxide, resulting in a material with improved sorption properties towards metal ions.

The preparation of cellulose/metal hydroxide hybrid materials is better understood when looking in detail to its reaction mechanism. In the presence of an aprotic solvent, titanium tetrachloride (TiCl_4) behaves as a strong Lewis acid, accepting a pair of

electrons. It reacts with the hydroxyl groups in cellulose (strong Lewis bases donating a lone pair of electrons) producing gaseous hydrochloric acid (HCl) and forming oxygen metal bonds (O–Ti). An intermediate chemically modified cellulose material is formed in which the metal is bonded to the carbon backbone through the oxygen atom, C–O–Ti–Cl₃. When this intermediate is further immersed in dry ethanol, the titanium center liberates the remaining chlorine atoms and interacts with the ethoxy functionalities resulting from the alcohol dissociation. An instable intermediate with the structure C–O–Ti–(OEt)₃ is formed, while the hydrochlorides in solution are neutralized in the presence of ammonia gas. A final immersion in copious amounts of a mixture of water/ethanol (50 vol%) and pure water allows the intermediate to stabilize in its final form as hydrated metal oxide C–O–Ti–(OH)₃ [56]. The total absence of water during this reaction or the use of aggressive drying procedures at its end leads to the formation of cellulose/metal oxide hybrids.

When the research work on this approach started, it was envisioned that a similar experimental method would allow the successful preparation of cellulose acetate/titanium(IV) hydroxide hybrid materials with lower degree of hydrogen bonding and higher reactivity towards aminosilanes molecules. The similarity in molecular structures between the cellulosic materials successfully treated in the literature and the low-acetyl content cellulose acetate obtained from previous approaches was believed to be a good reason to try this experimental pathway. It was expected that the initial water-solubility of the low-acetyl content cellulose acetate would be hindered by reaction with TiCl₄ and the attachment of metal-derived functionalities to the polymer backbone. The

reacted cellulose acetate/metal hybrid material would be then insoluble in water and suitable to exposure to aggressive hydration steps like the ones proposed in the selected method for preparation of metal hydroxides.

6.1.2 Modification of Cellulose/Metal Oxide Hybrid Materials with Aminosilanes

Meng et al. have reported the preparation, characterization, and adsorption properties of cellulose/titanium(IV) hydroxide modified with 4-aza-6-aminoethyl triethoxysilane (CTSN), which has high sorption capacity for heavy metal ions and transition-metal ions in aqueous solutions. The modification of the cellulose/metal hydroxide hybrid material with the organosilane was achieved by a conventional wet grafting reaction. The modified cellulose hybrid was equilibrated with toluene at room temperature and then treated with the organosilane and a small amount of water at high temperature and inert conditions. The alkoxy functionality in the aminosilane molecule reacts with the hydroxyl group from the cellulose/titanium(IV) hydroxide and forms a covalent Ti – O – Si bond. The final structure of cellulose/titanium(IV) hydroxide modified with 4-aza-6-aminoethyl triethoxysilane (CTSN) is presented in Figure 27.

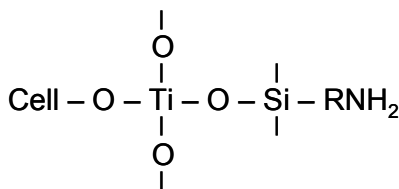


Figure 24. Structure of cellulose/titanium(IV) hydroxide modified with CTSN

6.1.3 CO₂ Sorption in Cellulose Acetate/Titanium(IV) Oxide Hybrid Materials

The actual cellulose acetate/metal oxide hybrid material obtained through this experimental approach is a polymer resulting of a series of chemical procedures: acidic hydrolysis, solution-casting, and reaction with a metal halide. Some of the hybrid materials have also been reacted with aminosilanes. Therefore, it is expected that several functionalities could be attached to the polymer backbone and to the outer surface of the polymer chains after completing the series of reactions. It is also expected that some functional groups originally attached to the polymer chain remain unreacted at the end of the whole treatment due to diffusion and transport limitations inside the intricate network of polymer chains. Therefore, the different type of CO₂ sorption mechanisms that could be occurring on the cellulose acetate/titanium(IV) oxide hybrid material will be discussed on the results section.

6.2 Experimental

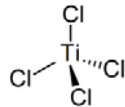
6.2.1 Materials

All materials were used as received from the different suppliers. Cellulose acetate, titanium tetrachloride, carbon tetrachloride, ethanol, anhydrous toluene, and xylenes were

supplied by Sigma-Aldrich (St. Louis, MO, USA). $C_9H_{24}N_2OSi$ and $C_7H_{19}NOSi$ were purchased from Gelest, Inc. (Morrisville, PA, USA).

The typical physical and chemical properties of cellulose acetate, $C_9H_{24}N_2OSi$ and $C_7H_{19}NOSi$ have been previously described. The main physical and chemical properties of titanium tetrachloride supplied are described in Table 10.

Table 10. Titanium tetrachloride typical properties as provided by Sigma-Aldrich

TITANIUM TETRACHLORIDE <i>(Product Code: 697079)</i>	
Typical Properties	Typical Values
Molecular weight	189.68 g/mol
Vapor pressure	50 mmHg at 55 °C, 9.6 mmHg at 20 °C
Purity	≥ 99.995 % based on trace metals basis
Boiling point	135 – 136 °C
Melting point	–25 °C
Density	1.73 g/mL at 20 °C
Trace metal analysis	≤ 50.0 ppm
Appearance and color	Colorless to light yellow dense liquid
Molecular formula	$TiCl_4$
Molecular structure	

6.2.2 Hydrolysis of High-acetyl Content Cellulose Acetate

The experimental method used for the de-acetylation of high-acetyl content cellulose acetate was proposed by Tanghe et al. [59] and already described in previous chapters.

6.2.3 Cast of Low-acetyl Content Cellulose Acetate Films

A standard procedure was used to prepare dense films by solution casting in a controlled environment. Further details are provided in previous chapters.

6.2.4 Preparation of Cellulose Acetate/Titanium(IV) Oxide Hybrid Materials

The low-acetyl content cellulose acetate films were also treated with a metal halide in order to introduce hydrated metal oxide functionalities into the polymer backbone that allowed further grafting of aminosilanes in a polymeric matrix with lower degree of hydrogen bonding. The experimental method proposed by Meng et al. for preparation of cellulose/titanium(IV) hydroxide was adapted for the preparation of a cellulose acetate/titanium(IV) hydroxide hybrid materials [56]. Experiments were run using different amounts of TiCl_4 and different reaction times, in order to find out the conditions that yielded the highest loading of titanium hydrated oxides attached to the polymer backbone.

In preparation for the experiments, all glassware used was dried in a convection oven at 130 °C overnight and torched prior to its use. Samples were also dried overnight in a vacuum oven at 70°C. About 1 g of low-acetyl content cellulose acetate film was cut into 1 in. pieces and introduced into a three-neck flask with a magnetic stirrer and connected to a condenser. The reaction system was completely closed and a stream of dry nitrogen flowed through it for about 1 h. Next, 100 mL of carbon tetrachloride (CCl_4)

were injected to the flask and the solution was stirred at room temperature for about 30 min. After this time, the system was immersed in a hot oil bath at 70°C and a volume between 0.25 and 2.0 mL of TiCl_4 was injected to the flask. The reaction was allowed to proceed with constant stirring at 70 °C under a nitrogen atmosphere. Experiments were initially run for 5 h; however, the first results from the CO_2 sorption tests on low-acetyl content cellulose acetate films showed that diffusion through the films can be significantly slower than in the powdered polymer. Therefore, experiments were also run for 48 h. For these longer experiments, 100 mL of CCl_4 were added after 8 h and 30 h of reaction to keep reactants in solution. After cooling, the mixture was filtered inside a nitrogen-evacuated glove bag, using a Büchner funnel under vacuum. The films were washed with 400 mL of CCl_4 , filtrated and put into a clean, dried and torched three-neck flask with a magnetic stirrer. After the reaction system was closed, a nitrogen stream was run for 1 h. Afterwards, 250 mL of anhydrous ethanol were injected at room temperature and the solution was stirred under nitrogen for 12 h when the reaction with TiCl_4 lasted 5 h long. For 48 h long TiCl_4 reactions, the reacted films were immersed for 24 h in ethanol at room temperature. As before, the solution was placed inside a nitrogen-evacuated glove bag and filtrated under reduced pressure. At this point, a water-solubility test was carried out to determine the type of washing procedures that should be applied. All reacted films were still sensitive to water; therefore, an alternative post-treatment procedure was adapted. It consisted in a final, exhaustive wash with fresh anhydrous ethanol under a nitrogen atmosphere to avoid exposure to atmospheric moisture. By proceeding in this direction, it was expected to retain the metal alkoxide functionalities already attached to the titanium centers from the prolonged immersion in ethanol and

avoid its hydrolysis and further stabilization as metal oxides. However, as it will be addressed later, the ease of hydrolysis of metal alkoxide functionalities, particularly ethoxy functionalities, made it a difficult task to avoid the formation of metal oxides with the laboratory equipment at hand. The final product was dried in a vacuum oven at 70°C overnight and stored in capped vials for later analysis. An identical experimental procedure was also applied to as received high-acetyl content cellulose acetate powder in order to compare the CO₂ sorption capacities achieved by both polymers. Table 11 specifies the reaction conditions applied to each sample.

Table 11. Reaction conditions for low-acetyl content cellulose acetate films and high-acetyl content cellulose acetate powder during TiCl₄ reactions

Sample	Material	Sample (g)	TiCl ₄ (mL)	CCl ₄ (mL)	Ethanol (mL)	TiCl ₄ Reaction Time (h)	Ethanol Immersion Time (h)
<i>L</i>	LACA film	1	0.25	100	250	5	12
<i>M</i>	LACA film	1	0.25	300	250	48	24
<i>N</i>	LACA film	1	2.00	100	250	5	12
<i>O</i>	LACA film	1	2.00	300	250	48	24
<i>P</i>	LACA film	1	0.40	100	250	5	12
<i>Q</i>	High-acetyl CA powder	1	0.40	100	250	5	12

A compilation of the main experimental steps in the preparation of cellulose acetate/titanium(IV) oxide hybrid polymers is presented in Figure 25.

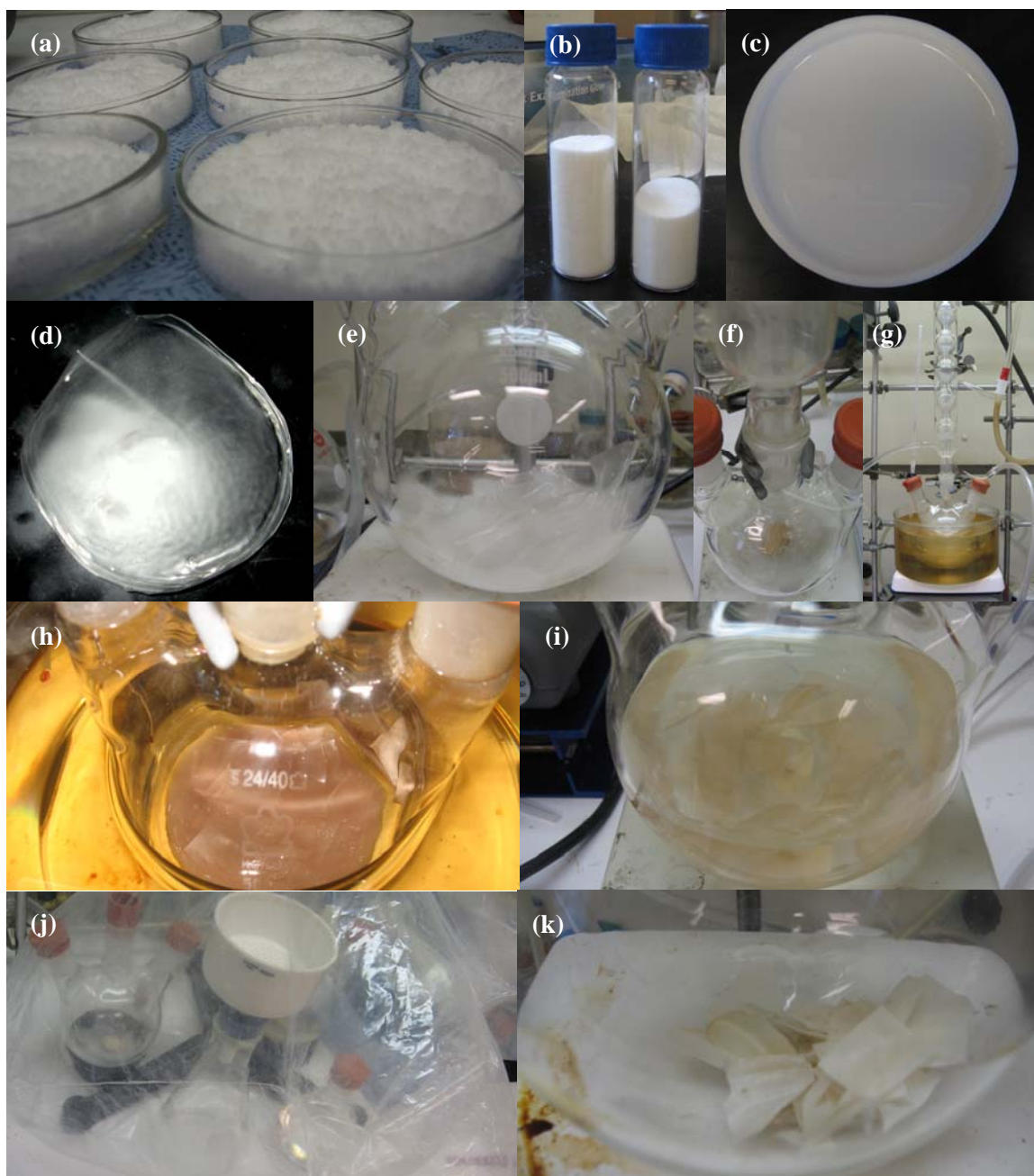


Figure 25. Main experimental steps in the preparation of cellulose acetate/titanium(IV) oxide hybrid polymers: (a) low-acetyl content cellulose acetate powder after hydrolysis reaction, (b) low-acetyl content cellulose acetate powder after grinding and drying, (c) low-acetyl content cellulose acetate after water dissolution, (d) dried dense film, (e) 1 in. film pieces before reaction, (f) N_2 drying and purging of reaction system, (g) reaction system after addition of $TiCl_4$ under a N_2 atmosphere at $70^\circ C$ (h) cellulose acetate/titanium(IV) oxide films after 5h of reaction (i) cellulose acetate/titanium(IV) oxide films in ethanol immersion under a N_2 atmosphere, (j) filtration and rinsing under a N_2 atmosphere, (k) dried cellulose acetate/titanium(IV) oxide hybrid polymers

6.2.5 Anhydrous Grafting of Aminosilanes on Cellulose Acetate/Titanium(IV) Oxide Hybrid Polymers

The persistent solubility in water of the obtained cellulose acetate/titanium(IV) oxide hybrid polymers was suspected to be due to unreacted hydroxyl functionalities from the polymer backbone. Therefore, some of the titanium-treated films were subjected to anhydrous grafting with $\text{C}_9\text{H}_{24}\text{N}_2\text{OSi}$ and $\text{C}_7\text{H}_{19}\text{NOSi}$ in order to test if the remaining hydroxyl groups in the polymer matrix could work as reactive sites for the aminosilane molecules and further increase the CO_2 sorption capacity of the material. It was believed that the unreacted hydroxyls from the polymer backbone could have decreased its degree of hydrogen bonding after the introduction of titanium-oxide functionalities and, therefore, become reactive centers toward aminosilanes. In addition, it was thought that the crosslinking nature of aminosilanes could be of help to hinder water solubility of the titanium-treated films. Not all the titanium-treated films were subjected to aminosilanes grafting. Considering that a higher CO_2 sorption capacity of the cellulose acetate/titanium oxide hybrid polymers could be a consequence of a higher amount of unreacted hydroxyl groups contributing with the titanium oxide functionalities as active sorption sites, only the films showing the best improvements in sorption capacity were subjected to the anhydrous grafting of aminosilanes.

For the anhydrous grafting reaction, about 1 g of cellulose acetate/titanium(IV) oxide hybrid polymer was placed into a dried and torched three-neck flask with magnetic stirrer and connected to a condenser. After the system was closed, nitrogen gas was flowed through it for about 1 hour. Next, 150 mL of anhydrous toluene were injected to

the flask at constant stirring for 30 min and at room temperature. Then, the temperature of the mixture was raised to 110 °C and 3 mL of the corresponding aminosilane were added. After 16 h at constant stirring and an inert atmosphere, the reaction was cooled down and filtrated under reduced pressure. The product was washed with 400 mL of toluene. The silanated films were dried into a vacuum oven at 70°C overnight and stored in capped vials for subsequent analysis. Table 12 presents the reaction conditions applied to the silanated cellulose acetate/titanium(IV) oxide materials.

Table 12. Reaction conditions for aminosilane grafting of cellulose acetate/titanium(IV) oxide films

Sample	CA/Ti(IV) Oxide Film (g)	Toluene (mL)	Aminosilane Species	Aminosilane (mL)	H ₂ O (mL)	Amination Time (h)	Amination Temperature (°C)
<i>R</i>	1	150	C ₆ H ₂₄ N ₂ OSi	3	0	16	110
<i>S</i>	1	150	C ₇ H ₁₉ NOSi	3	0	16	110

6.2.6 Sorbent Sorption Characterization

The characterization of the CO₂ sorption capacities of the cellulose acetate/titanium(IV) oxide hybrid materials and the silanated films after the TiCl₄ reaction was carried out using the aforementioned pressure decay method [55]. Detailed description of the method is provided in previous chapters.

6.2.7 Instrumental Characterization of Sorbents

The composition and properties of the cellulose acetate/titanium(IV) oxide hybrid polymers and the afterwards silanated films were tested using Elemental Analysis (EA),

density analysis, Fourier Transformed Infrared Spectroscopy (FT-IR), Thermogravimetric Analysis (TGA) and Scanning Electron Microscopy (SEM). A detailed description of EA, density analysis, TGA and SEM was provided in the previous chapter.

6.3 Results

6.3.1 Sorbent Sorption Characterization

Figure 26 presents the isotherms of samples *L*, *M*, *N*, *O* and *P*, cellulose acetate/titanium(IV) oxide hybrid films obtained under different reaction conditions. They are compared to previous showed isotherms of high-acetyl and low-acetyl content pure cellulose acetate samples. CO₂ sorption experiments performed at 35 °C for all films reacted with TiCl₄ show the relevance of the TiCl₄ reaction conditions in the improvement of the CO₂ sorption capacity of the sorbents. In terms of the amount of TiCl₄ added to the reaction, it was discovered the existence of an optimum dose that achieves the highest improvement in sorption capacity. This greater improvement in sorption capacity was achieved by sample *P*, cellulose acetate/titanium(IV) oxide film obtained after 5 h of reaction with 0.40 mL TiCl₄/g LACA. This sorbent showed an increase in the sorption capacity of 13.60 cc (STP) CO₂/ cc sorbent or 0.41 mmol CO₂/g sorbent at 1 atm of pressure and 49.27 cc (STP) CO₂/ cc sorbent (1.48 mmol CO₂/g

sorbent) at equilibrium pressures of 5 atm. This represents an additional capture of about 0.22 mmol CO₂/g sorbent at 1 atm and 0.97 mmol CO₂/g sorbent at 5 atm after the titanium modification of cellulose acetate. Films treated with 0.25 mL TiCl₄/g LACA resulted in only a small improvement of the original cellulose acetate CO₂ sorption capacity when reacted for 5 h (sample *L*), and a significant worsening of the original sorption capacity when the reaction lasted 48 h (sample *M*). On the other hand, the films reacted with the highest dose of TiCl₄, 2.00 mL TiCl₄/g LACA, registered an improvement in the sorption capacity at short reaction times (sample *N*), and a decrease at longer times of reaction (sample *O*).

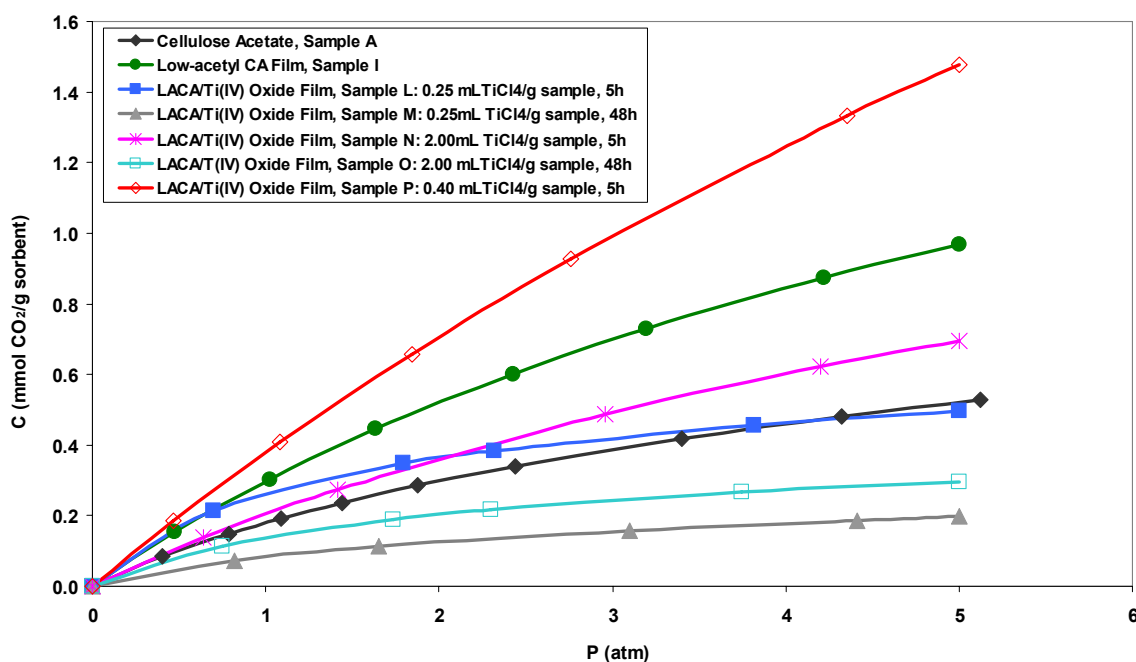


Figure 26. CO₂ sorption isotherms for high-acetyl and low-acetyl content cellulose acetate films, cellulose acetate/titanium(IV) oxide film samples *L–P*

Overall, it can be noted that short reaction times tend to favor the improvement of the CO₂ sorption capacity of the polymer, and its degree of enhancement depends on the

amount of TiCl_4 added to the reaction. It could be thought that higher doses of TiCl_4 infer a greater increment in the sorption capacity of the polymer, but it was discovered that high doses of metal halide does not necessarily improves the sorption capacity, rather decreases it. This may be due to the production of higher amounts of hydrochloric acid as byproduct of the TiCl_4 reaction, which may attack the acetyl functionalities in the polymer chains and scission them, causing an irreversible degradation of the material.

Preliminary sorption kinetics data from the pressure decay test indicates that sorption equilibration times for the cellulose acetate/titanium(IV) oxide films is rather long. Sample *P*, which achieved the highest improvement in CO_2 sorption capacity, reached sorption equilibration within an average of 28 h. Sample *N*, which also presented an improvement in the CO_2 sorption capacity, reached sorption equilibrium within an average of 42 h. Sample *L* with the smallest increase in sorption capacity showed a significantly smaller equilibration time at all applied pressures of about 15 h. On the other hand, sample *O* did not attain sorption equilibrium after 10 days, since the pressure in the sample cell continued to decrease very slowly with time. Sample *M*'s sorption equilibration time was about 70 h or 3 days.

On the other hand, the sorption characterization of sample *Q*, high-acetyl content cellulose acetate powder reacted with 0.40 mL TiCl_4 /g CA, showed an increase in the CO_2 sorption capacity of the polymer. At an equilibration pressure of 5.88 atm and 35 °C, the sorption capacity of sample *Q* was 0.75 mmol CO_2 /g sample, capturing about 0.19 mm CO_2 additional per gram of sample *Q*. It may be observed that, compared to the

increment in sorption capacity reached by sample P, the improvement achieved by sample Q was modest. However, it is important to note that sample Q has the great advantages of water insolubility and a more straightforward method of preparation. Isotherm of sample Q is presented in Figure 27.

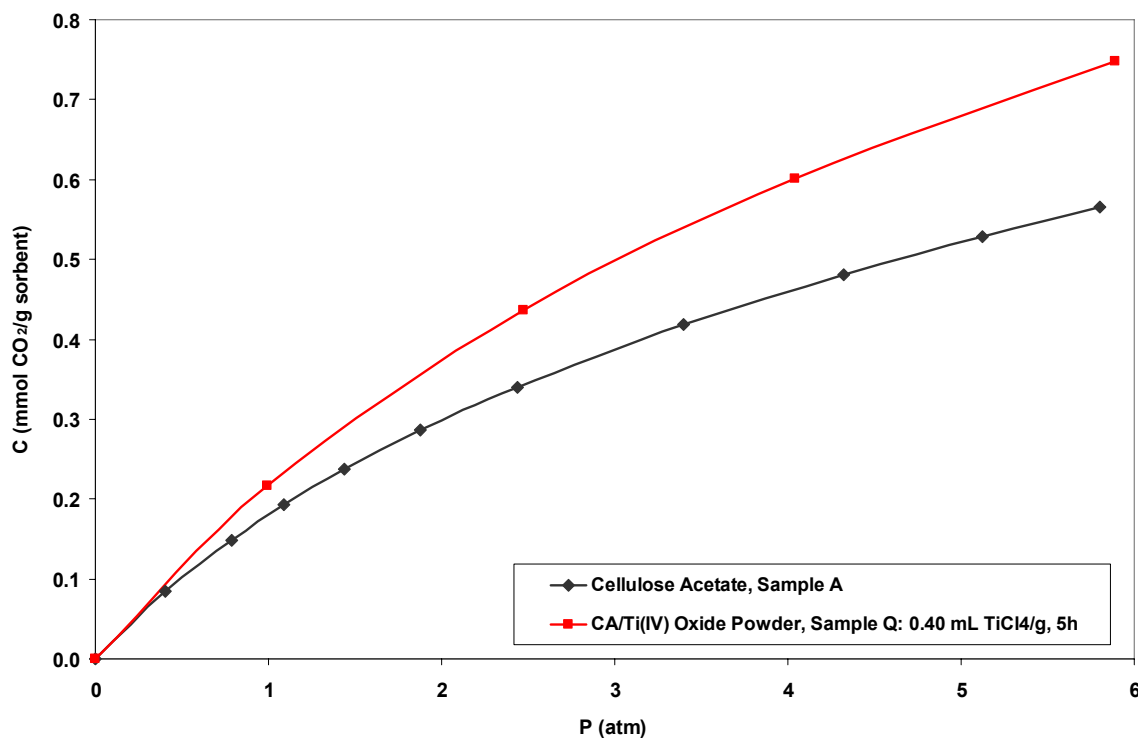


Figure 27. CO₂ sorption isotherms for cellulose acetate powder and cellulose acetate/titanium(IV) oxide powder, sample Q

Furthermore, when sample P, low-acetyl content cellulose acetate/titanium(IV) oxide film with best sorption capacity enhancement, was subjected to a grafting reaction with aminosilanes under anhydrous conditions, the products showed a decrease in its sorption capacity, as can be observed in Figure 28. Sample R, grafted with C₉H₂₄N₂OSi under anhydrous conditions decreased its sorption capacity from 1.48 mmol CO₂/g

sorbent to 1.39 mmol CO₂/g sorbent. A similar behavior was observed for the grafting of sample *P* with C₇H₁₉NOSi under dry conditions. This time, the sorption capacity presented a sharper decrease, from 1.48 mmol CO₂/g sorbent to only 0.78 mmol CO₂/g sorbent. Although the CO₂ sorption capacity of both films is still higher than that of pure high-acetyl content cellulose acetate, the objective of the grafting reaction was obviously to increase it further and this was not achieved.

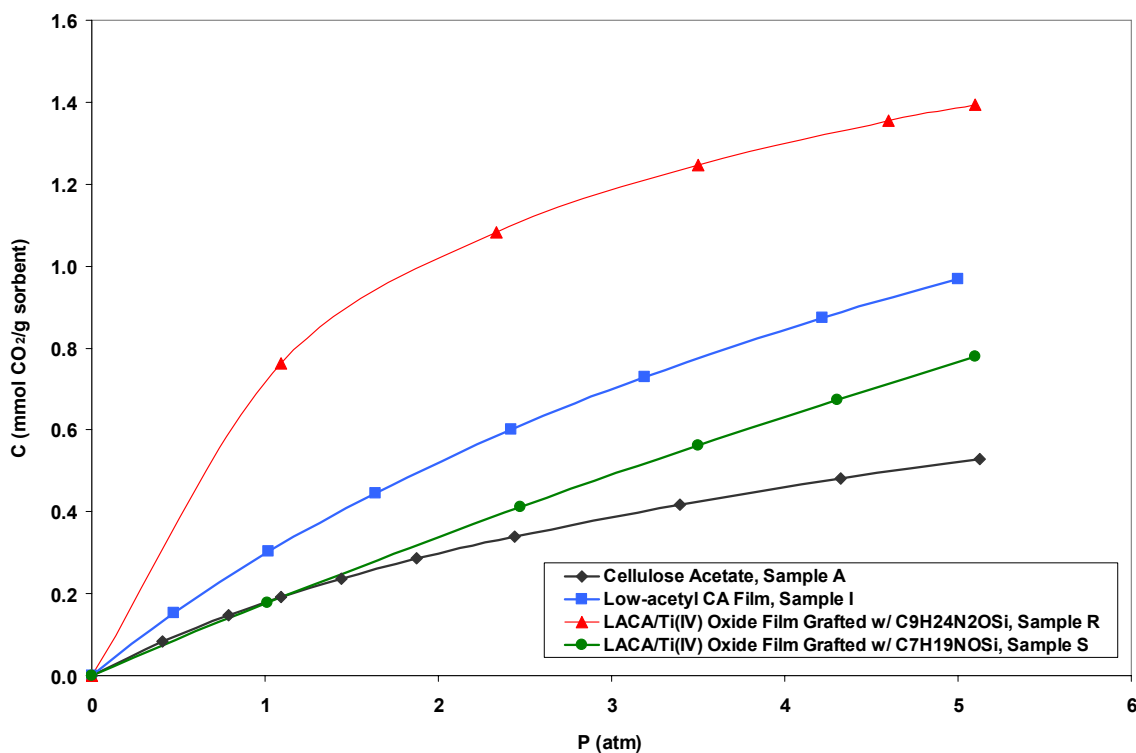


Figure 28. CO₂ sorption isotherms for silanated cellulose acetate/titanium(IV) oxide films, samples *R* and *S*

6.3.2 Elemental Analysis

Elemental Analysis was used to determine the percentage weights of the elements present in each cellulose acetate/titanium(IV) oxide sample. The analyses were carried

out by Galbraith Laboratories, Inc. (Knoxville, TN, USA). Carbon, hydrogen and nitrogen weight percentages were determined by a combustion technique. Silicon and titanium amounts were measure by the inductively coupled plasma–optical emission spectroscopy (ICP-OES). The amounts of chlorine were found using ion chromatography (IC) tests. Results are summarized in Table 13.

Table 13. Elemental Analysis of LACA/Ti(IV) oxide films and silanated LACA/Ti(IV) oxide films

Sample		Elemental Analysis						
		% C	% H	% O	% Ti	% Cl	% N	% Si
<i>A</i>	High-acetyl content cellulose acetate powder (CA)	48.21	5.93	45.60	0.00	0.00	0.00	0.00
<i>I</i>	Low-acetyl content cellulose acetate (LACA) film	47.84	6.66	48.66	0.00	0.00	0.00	0.00
<i>L</i>	LACA/Ti(IV) Oxide Film, 0.25 mL TiCl ₄ , 5h reaction	43.73	6.25	49.84	0.245	595 ppm	0.00	0.00
<i>M</i>	LACA/Ti(IV) Oxide Film, 0.25 mL TiCl ₄ , 48h reaction	43.16	6.32	49.65	0.257	0.177	0.00	0.00
<i>N</i>	LACA/Ti(IV) Oxide Film, 2.00 mL TiCl ₄ , 5h reaction	37.96	6.49	48.69	1.93	0.886	0.00	0.00
<i>O</i>	LACA/Ti(IV) Oxide Film, 2.00 mL TiCl ₄ , 48h reaction	44.74	6.13	48.81*	0.288	285 ppm	0.00	0.00
<i>P</i>	LACA/Ti(IV) Oxide Film, 0.40 mL TiCl ₄ , 5h reaction	48.74	7.52	41.41*	2.08	0.246	0.00	0.00
<i>Q</i>	CA/Ti(IV) Oxide Powder, 0.40 mL TiCl ₄ , 5h reaction	47.73	5.55	46.48	799 ppm	<100 ppm	0.00	0.00
<i>R</i>	LACA/Ti(IV) Oxide Film grafted w/ C ₉ H ₂₄ N ₂ OSi	40.68	6.15	50.07	0.649	0.15	<0.5	0.391
<i>S</i>	LACA/Ti(IV) Oxide Film grafted w/ C ₇ H ₁₉ NOSi	44.00	6.04	48.84	0.669	0.18	<0.5	0.183

* Oxygen content could not be accurately determined by the instrument. Estimation by difference.

Elemental Analysis results show that sample *P*, cellulose acetate/titanium(IV) oxide film obtained after 5 h of reaction with 0.40 mL TiCl₄/g LACA, presents the highest titanium loading of all reacted low-acetyl content films. This sample also exhibited the highest increase in CO₂ sorption capacity. However, it should be noted that the sample with the lowest amount of fixed titanium (sample *L*) does not corresponds to the one exhibiting the lowest sorption capacity (sample *M*). Therefore, it can be inferred that the amount of titanium loading is not the only factor affecting the equilibrium sorption capacity of the polymer. It is interesting to note that for a fixed reaction time the amount of titanium incorporated increases as the amount of TiCl₄ added is also increased (from sample *L* to sample *P*), but this does not appear to be a linear correlation. Results show that after an optimum amount of TiCl₄ is added to the reaction, the loading of

titanium in the final cellulose acetate/titanium(IV) oxide film starts to decrease (sample *P* to sample *N*). On the other hand, EA results show that for low doses of TiCl_4 (0.25 mL $\text{TiCl}_4/\text{g LACA}$), the amount of titanium fixed increases with time. However, the opposite effect is registered for high doses of TiCl_4 (2.00 mL $\text{TiCl}_4/\text{g LACA}$), since the amount of titanium incorporated into the polymer decreases significantly with longer reaction times (sample *N* to sample *O*). For all samples reacted over 48 h, the amount of titanium loaded is very similar and rather small, independently of the amount of TiCl_4 added to the reaction. Based on these results and the previously analyzed sorption isotherms, it can be suggested that long reaction times degrade the polymer chain to the extent of inhibit titanium fixation and CO_2 sorption into another reactive sites like remaining hydroxyl groups. Although the 5 h-reacted sample *L* has the lowest titanium load of all samples, its sorption behavior is much better than samples *O* and *M* with higher titanium loads but longer reaction times. For samples reacted only for 5 h, the existence of an optimum amount of TiCl_4 incorporated into the reaction seems to exists, since larger additions of TiCl_4 does not correlate with higher amounts of fixed titanium.

On the other hand, the amount of grafted amines on the cellulose acetate/titanium(IV) oxide films is rather low. Although there may be a number of reasons that contribute to hinder the grafting reaction mechanism in the titanium-treated polymer, it is suggested that the main one should be the lack of reactive hydroxyl sites on the polymer chains more near the surface of the sorbent, which may have already reacted with TiCl_4 , forming non-reactive oxides. Therefore, the bulky titanium functionalities dangling from the outer polymer chains may become a kind of surface barrier that

difficult the diffusion of the aminosilane molecules into the inner polymer chains, where unreacted hydroxyl groups still exist prolonging the polymer's water-solubility.

6.3.3 Density Analysis

Density measurements were also performed in order to determine the change in mass per unit volume of the cellulose acetate/titanium(IV) oxide films. Table 14 shows the results obtained for titanium and aminosilane treated samples.

Table 14. Densities of LACA/Ti(IV) oxide films and silanated LACA/Ti(IV) oxide films

	Sample	Density (g/mL)
<i>A</i>	High-acetyl content cellulose acetate powder (CA)	1.4205
<i>I</i>	Low-acetyl content cellulose acetate (LACA) film	1.4469
<i>L</i>	LACA/Ti(IV) Oxide Film, 0.25 mL TiCl ₄ , 5h reaction	1.4553
<i>M</i>	LACA/Ti(IV) Oxide Film, 0.25 mL TiCl ₄ , 48h reaction	1.4561
<i>N</i>	LACA/Ti(IV) Oxide Film, 2.00 mL TiCl ₄ , 5h reaction	1.5006
<i>O</i>	LACA/Ti(IV) Oxide Film, 2.00 mL TiCl ₄ , 48h reaction	1.4579
<i>P</i>	LACA/Ti(IV) Oxide Film, 0.40 mL TiCl ₄ , 5h reaction	1.4882
<i>Q</i>	CA/Ti(IV) Oxide Powder, 0.40 mL TiCl ₄ , 5h reaction	1.4554
<i>R</i>	LACA/Ti(IV) Oxide Film grafted w/ C ₉ H ₂₄ N ₂ OSi	1.4686
<i>S</i>	LACA/Ti(IV) Oxide Film grafted w/ C ₇ H ₁₉ NOSi	1.4458

The increment in absolute density of the cellulose acetate/titanium(IV) oxide films is due to the incorporation of titanium-derivative functional groups into the polymer matrix. Although these functional groups may decrease the packing density around reacted polymer chains, they have higher molecular weights than the original surface hydroxyls groups and can increase the film's density value proportionally. The largest increment in density came from sample film *N*, which was titanated using 2.00 mL TiCl₄/g LACA during 5 h and registered around 4% increment in density. Samples additionally reacted with aminosilanes under anhydrous conditions presented a decrease

in its absolute density with respect to their precursor sample *P*. This may be due to the grafting of small amounts of aminosilane molecules to the polymer matrix, as elemental analysis reveals. These bulky new functionalities may decrease even further the packing density of the polymer chains around them and therefore, produce a very small decrease in the overall density of the material. As silicon derivatives have lower molecular weights than titanium ones, the attachment of some silane groups to the polymer matrix does not generate a significant increment in the overall absolute density of the material.

6.3.4 Fourier-Transformed Infrared Spectroscopy

The infrared spectra of samples *L* through *S* are presented in Figures 29 through 36. Elemental analysis revealed that sample *L*, cellulose acetate/titanium(IV) oxide film obtained by the reaction of 0.25 mL TiCl₄/g LACA during 5 h, only fixed very small amounts of titanium, and the results were confirmed by the interpretation of its infrared spectrum. Figure 29 shows that the spectrum of sample *L* did not present any significant change with respect to that of low-acetyl content cellulose acetate film. Therefore, it may be suggested that the TiCl₄ dose used in this experiment was rather low to fix any significant amount of titanium in the polymer matrix.

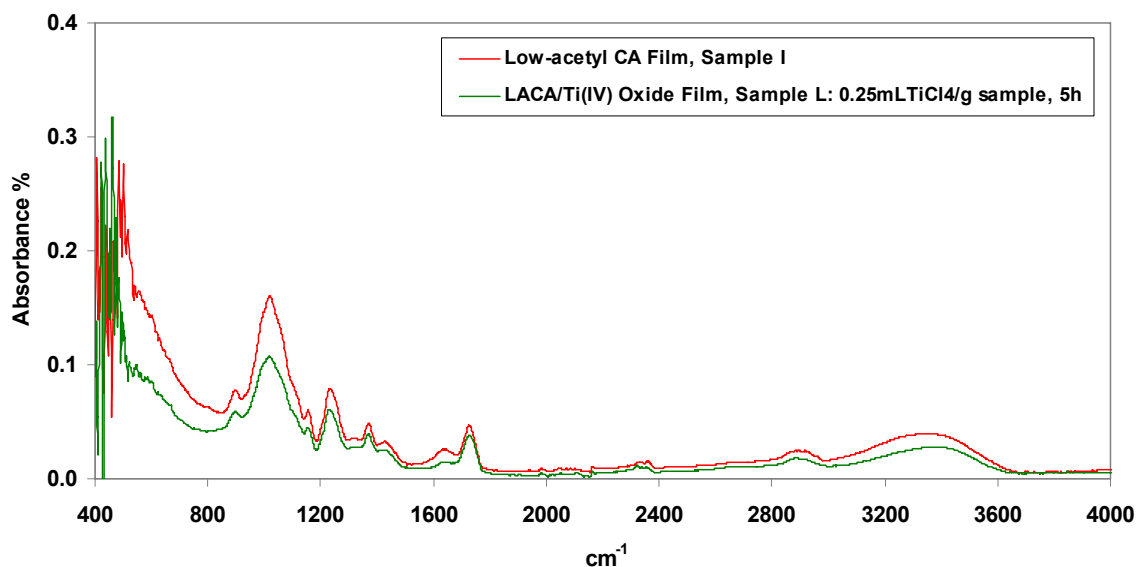


Figure 29. FT-IR spectra of LACA film and LACA/Ti(IV) oxide film, 0.25 mL TiCl₄ for 5h, sample *L*

Likewise, sample *M*, prepared using 0.25 mL TiCl₄/g LACA during 48 h, did not show major spectrum changes after the TiCl₄ reaction. Its spectrum appears in Figure 30. It should be noted, however, an increase in the absorbance bands below 800 cm⁻¹ and above 2800 cm⁻¹. The first may be due either to the formation of some Ti-O bonds, which are expected in the region of 200-800 cm⁻¹ [93], or by an increase in the amorphicity of the polymer after long reaction times. As mentioned before, the fingerprint region of the spectrum provides not reliable evidence of molecular structure and therefore, one may not draw conclusions based on its reading. On the other hand, the small increase in the absorbance bands in the region of 2850-2970 cm⁻¹ may be associated with the presence of titanium ethoxide functionalities [94, 95]. However, due to the high amount of hydroxyl groups in the chemical structure of low-acetyl content cellulose acetate, the increase and shift of absorption bands in this region may also be due to a re-ordering of the hydrogen-bonded hydroxyl functionalities.

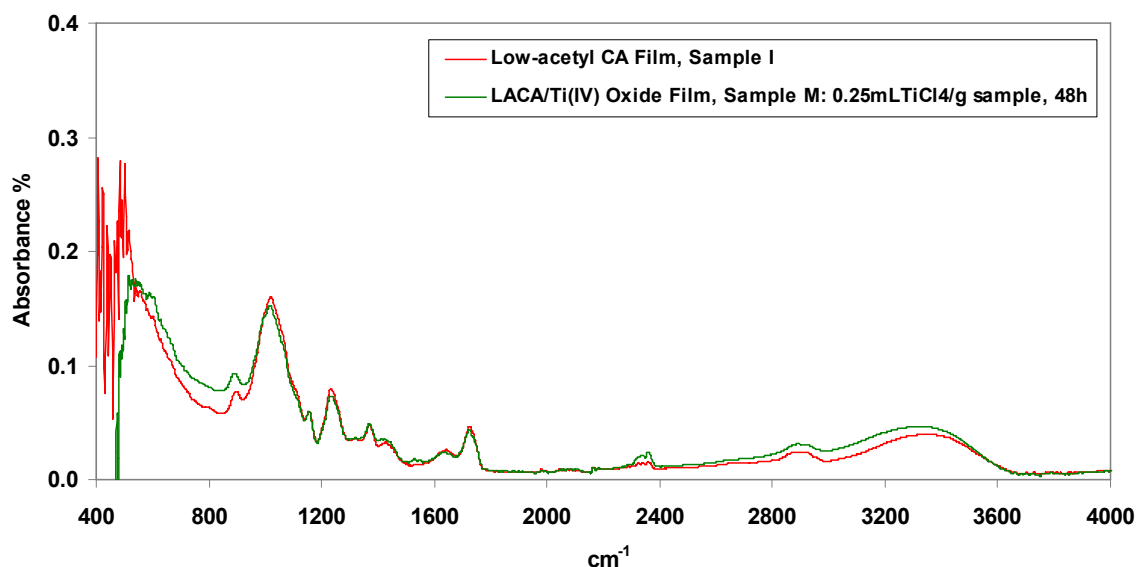


Figure 30. FT-IR spectra LACA film and LACA/Ti(IV) oxide film, 0.25 mL TiCl₄, 48h reaction, sample *M*

Sample *N*, with a titanium content of 1.93 wt%, presents significant changes in its infrared spectrum (Figure 31) due to the reaction of the polymer with 2.00 mL TiCl₄/g LACA for 5 h. On one hand, the appearance of broad absorption bands around 500-885 cm⁻¹ is an evidence of the formation of Ti-O bonds [93, 94, 96]. In addition, it has been reported that the bands around 520-530 cm⁻¹ and 760 cm⁻¹ are characteristics of amorphous titanium dioxides [97]. The absorption band around 1040 cm⁻¹ associated with acetyl groups in cellulose acetate disappeared after the reaction with TiCl₄, which may be due to reaction with hydrochloric acid produced during the fixation of titanium and associated with chemical degradation of the polymer. This effect is observed in the spectra obtained in this study as the dose of TiCl₄ is increased in the reaction. The strong absorption band around 1442 cm⁻¹, as well as those bands in the spectral range of 2600-2970 cm⁻¹ are reported in the literature as characteristic of titanium ethoxide functionalities [94]. The appearance of a band around 1617 cm⁻¹ is also characteristic of titanium dioxides [97]. Interestingly, the hydroxyl region ranging from 3000-3645 cm⁻¹

remains unchanged, suggesting that a significant amount of hydroxyl functionalities in the polymer did not react, even when using a high dose of TiCl_4 .

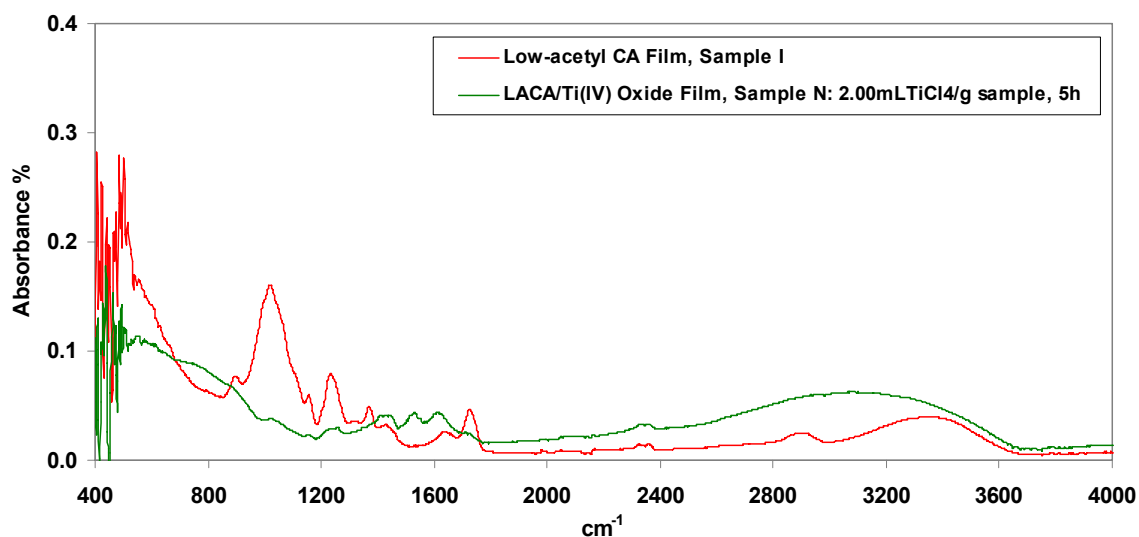


Figure 31. FT-IR spectra of LACA film and LACA/Ti(IV) oxide film, 2.00 mL TiCl_4 for 5h, sample *N*

Sample *O* was obtained by reacting 2.00 mL TiCl_4 /g LACA during 48h with low-acetyl content cellulose acetate. The high dose of TiCl_4 utilized and the long reaction time significantly affected the molecular structure of the polymer. Figure 32 shows the absence of acetyl, hydroxyl or any other titanium functionality absorbance bands in the spectrum of the material after its reaction with TiCl_4 . This suggests an extensive degradation of the molecular structure of the material, confirmed by its decrease in CO_2 sorption capacity and the extreme brittleness of the final material.

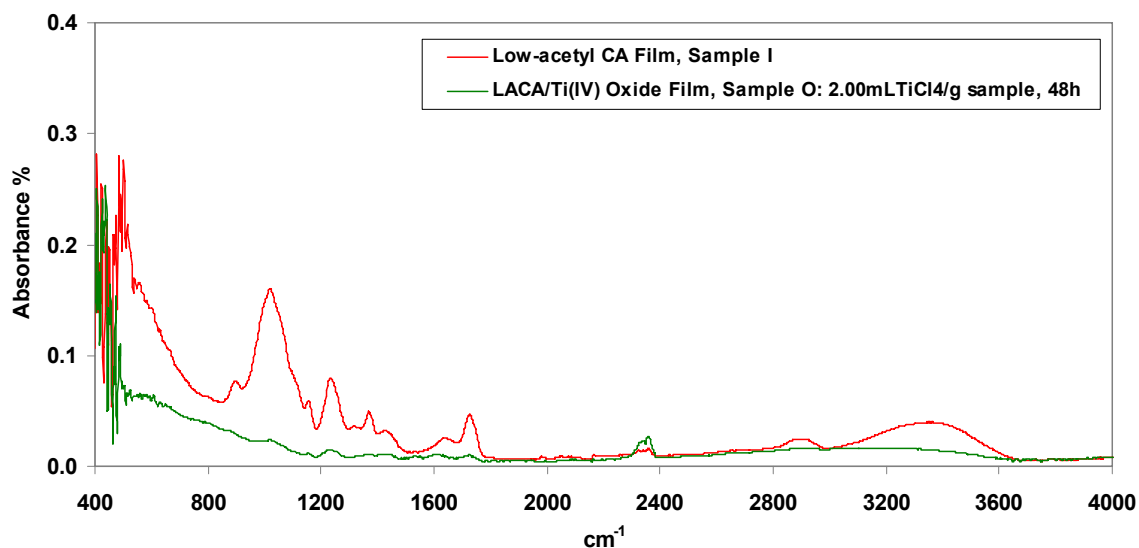


Figure 32. FT-IR spectra of LACA film and LACA/Ti(IV) oxide film, 2.00 mL TiCl₄ for 48h, sample *O*

The IR spectrum of sample *P*, cellulose acetate/titanium(IV) oxide film showing the best CO₂ sorption capacity, the highest titanium load and prepared by the addition of 0.40 mL TiCl₄/g LACA during a reaction time of 5 h, is presented in Figure 33. The spectrum shows the appearance of bands at about 520-530 cm⁻¹, characteristic of titanium-oxygen bonds in amorphous titanium dioxides [97], and additional weaker bands in the region of 600-800 cm⁻¹, reported for titanium ethoxides spectra [94]. The addition of a smaller amount of TiCl₄ did not shop away all the acetyl groups in the polymer, as it is suggested by the weak absorption bands around 1020-1040 cm⁻¹ and 1240 cm⁻¹, characteristic of the acetyl groups of cellulose acetate. The weak band at 1375 cm⁻¹ and those in the range of 2600-2970 cm⁻¹ reveal the presence of titanium ethoxide functionalities [94, 97]. In addition, a considerable decrease in the intensity of the absorption bands at the hydroxyl region (3000-3645 cm⁻¹) suggests a better diffusion throughout the polymer chains and a higher amount of reacted hydroxyl groups.

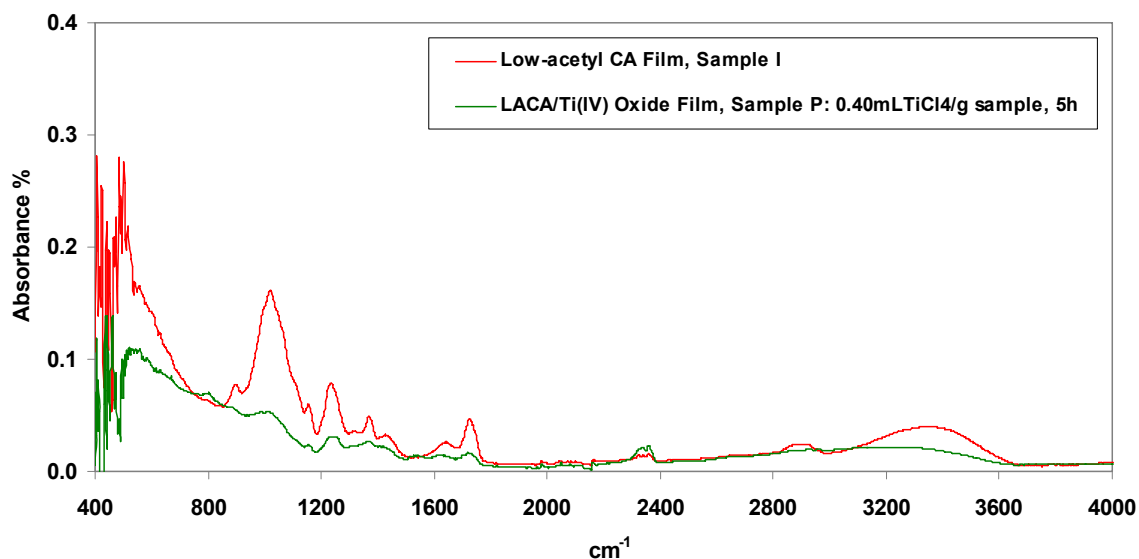


Figure 33. FT-IR spectra of LACA film and LACA/Ti(IV) oxide film, 0.40 mL TiCl_4 for 5h, sample *P*

On the other hand, Figure 34 illustrates the spectra of high-acetyl content cellulose acetate powder and sample *Q*, cellulose acetate powder reacted with 0.40 mL TiCl_4 /g LACA during a reaction time of 5 h. Although the structure of the polymer was well conserved, the appearance of absorbance bands at 540, 560 and 600 cm^{-1} reveals the formation of Ti-O bonds after the TiCl_4 reaction. The significant increase in the absorbance bands at 900, 1030 and 1370 cm^{-1} may suggest additional stretching vibration coming from titanium ethoxide functionalities [94]. In addition, the appearance of a couple of weak bands at 2890 and 2960 cm^{-1} is suggested to be characteristic of different titanium alkoxides. The weak band at 3480 cm^{-1} may be due to adsorbed and coordinated water molecules [97].

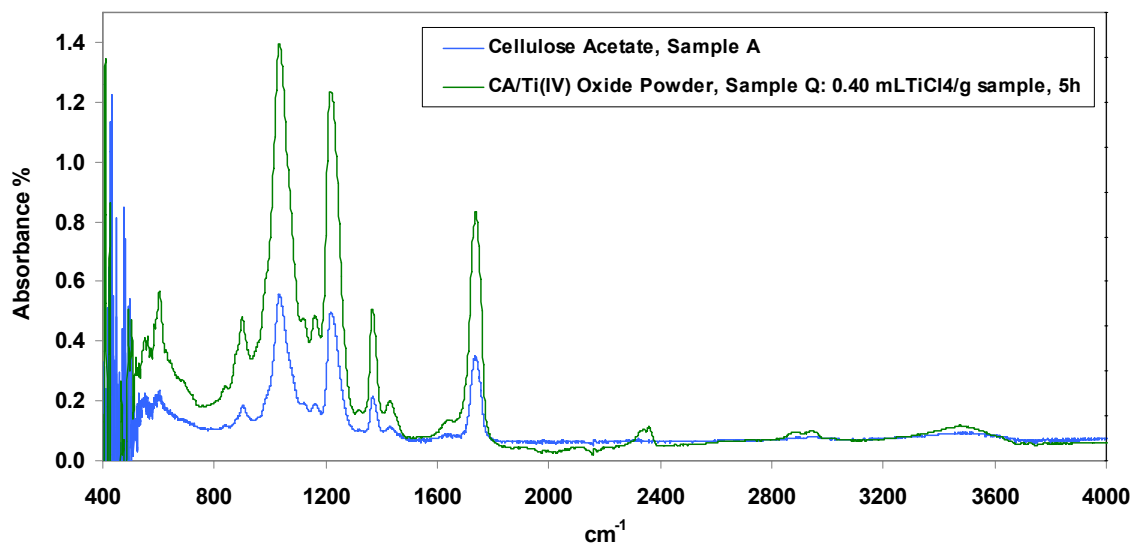


Figure 34. ATR spectra of CA powder and CA/Ti(IV) oxide powder, 0.40 mL TiCl_4 , 5h reaction, sample *Q*

The IR spectra of sample *R*, cellulose acetate/titanium(IV) oxide film grafted with $\text{C}_9\text{H}_{24}\text{N}_2\text{OSi}$, is shown in Figure 35. It shows strong absorption bands in the region of $500\text{--}900\text{ cm}^{-1}$, characteristics of the titanium-oxygen bonds. A peak at 1016 cm^{-1} may correspond to the strong and distinct band of dimethylsiloxane $(\text{CH}_3)_2\text{SiO-}$ bonds [86]. The band at 1620 cm^{-1} may be an evidence of amine functionalities in the polymer, but its intensity is rather low. The broad band ranging from 2890 and 2960 cm^{-1} belongs to stretching vibrations from titanium alkoxide functionalities, while the hydroxyl region after 3000 cm^{-1} evidences high amount of unreacted hydroxyl groups in the polymer.

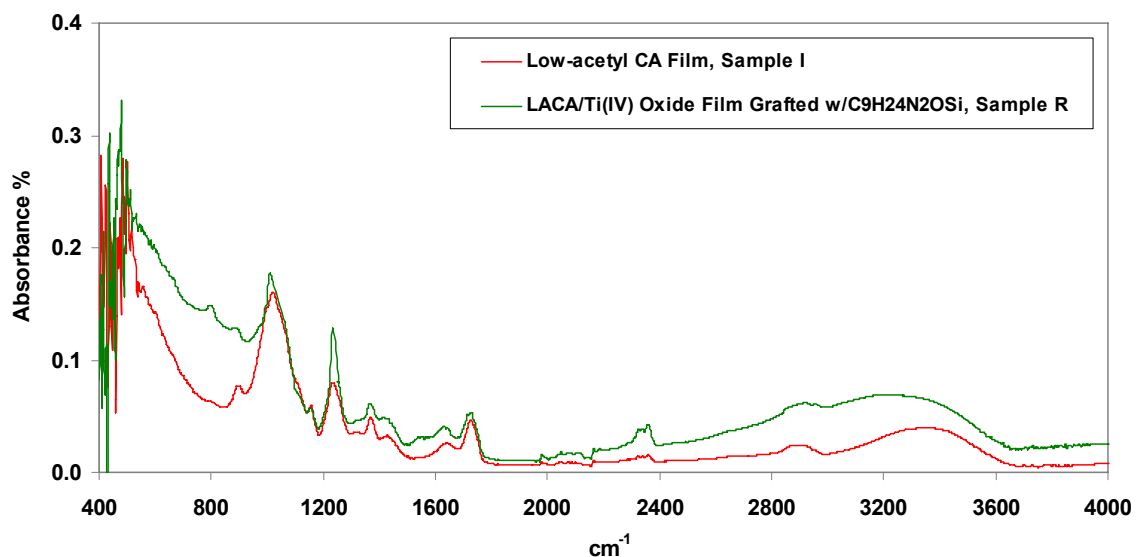


Figure 35. FT-IR spectra of LACA film and LACA/Ti(IV) oxide film grafted with $\text{C}_9\text{H}_{24}\text{N}_2\text{OSi}$, sample *R*

The spectrum of sample *S*, cellulose acetate/titanium(IV) oxide film grafted with $\text{C}_7\text{H}_{19}\text{NOSi}$, is very similar to the one of sample *R*, as can be observed in Figure 36; however, a weaker absorption band around 1020 cm^{-1} suggests a smaller amount of alkoxy silane bonds in the polymer.

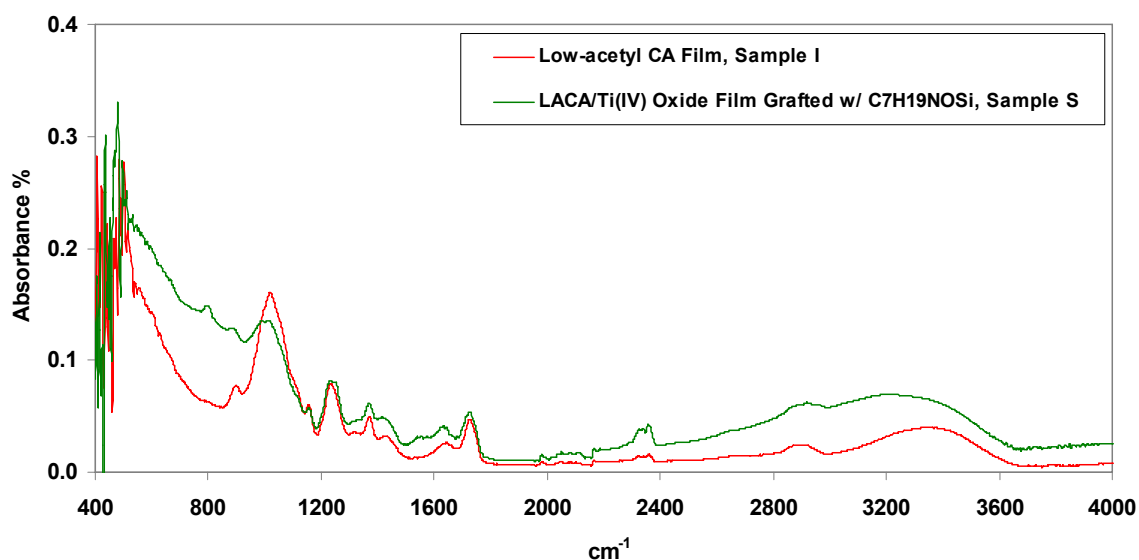


Figure 36. FT-IR spectra of LACA film and LACA/Ti(IV) oxide film grafted with $\text{C}_7\text{H}_{19}\text{NOSi}$, sample *S*

6.3.5 Thermogravimetric Analysis

The TG curves of cellulose acetate/titanium(IV) oxide materials and aminosilane-grafted cellulose acetate/titanium(IV) oxide films are showed in Figures 37 to nn. Sample *L*, low-acetyl content cellulose acetate film reacted with 0.25 mL TiCl_4/g sample during 5 h, presented a decrease in thermal stability with respect to pure high-acetyl content cellulose acetate, as shown in Figure 37. However, with respect to low-acetyl content cellulose acetate its thermal stability was slightly affected. A weight loss of about 98% was registered when the temperature reached 260 °C. After 140 min almost all the sample was completely decomposed.

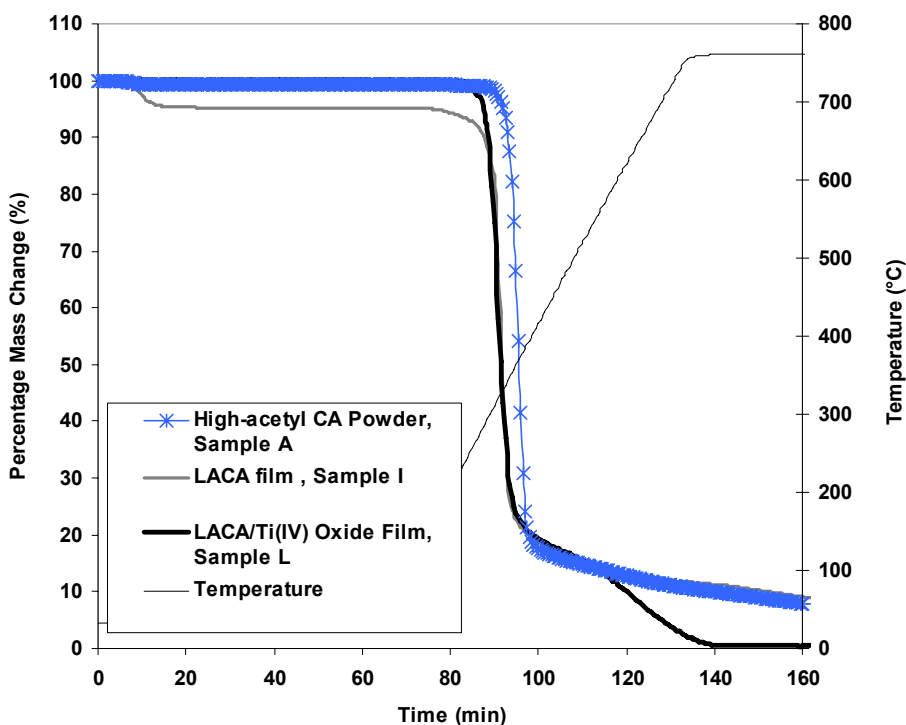


Figure 37. LACA/Titanium(IV) oxide film prepared with 0.25 mL TiCl_4/g LACA and 5 h reaction

The TG curve of sample *M* is presented in Figure 38. The low-acetyl content cellulose acetate film treated with a 0.25 mL TiCl_4/g LACA ratio for 48 h registered a weight loss of about 83% at about 220 °C, evidencing that longer reaction times adversely affect the thermal stability of titanium-treated cellulose acetate. In addition, the presence of a char residue of about 10% weight is observed at the end of the analysis.

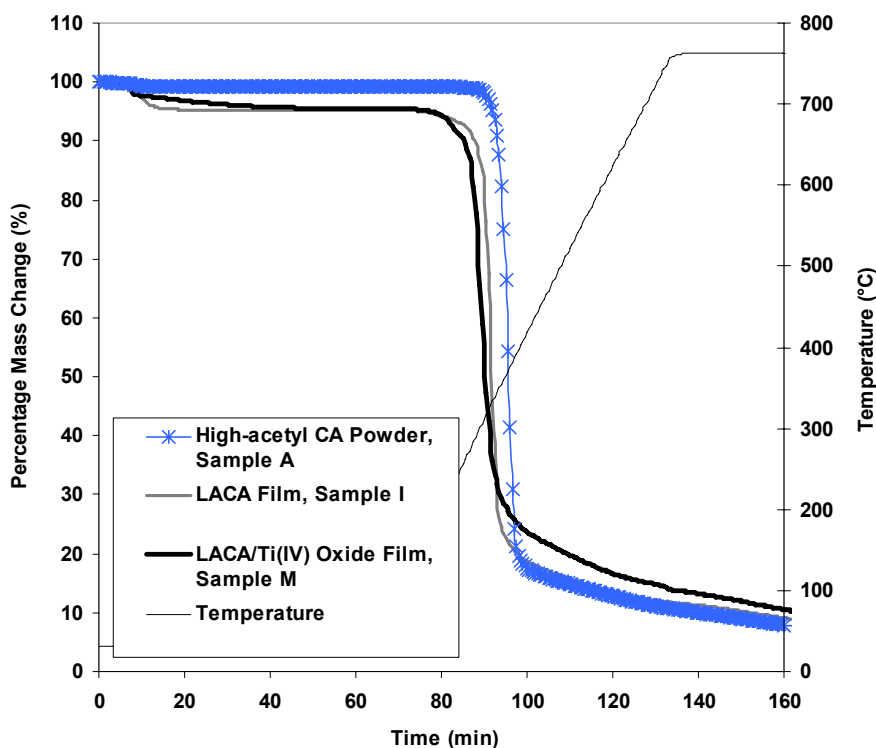


Figure 38. LACA/Titanium(IV) oxide film prepared with 0.25 mL TiCl_4/g LACA and 48 h reaction

The thermogravimetric analysis of sample *N* (low-acetyl content cellulose acetate film reacted with 2.00 mL TiCl_4/g sample during 5 h) is displayed in Figure 39, showing that a higher amount of TiCl_4 used in the reaction causes a greater impact on the thermal stability of the material than an increment in the reaction time. The cellulose acetate film

treated with a higher amount of TiCl_4 started its degradation at about 180 °C and the sample lost about 75% of its initial mass during this step. A residue of about 20% of the sample weight was observed at the end of the measurement.

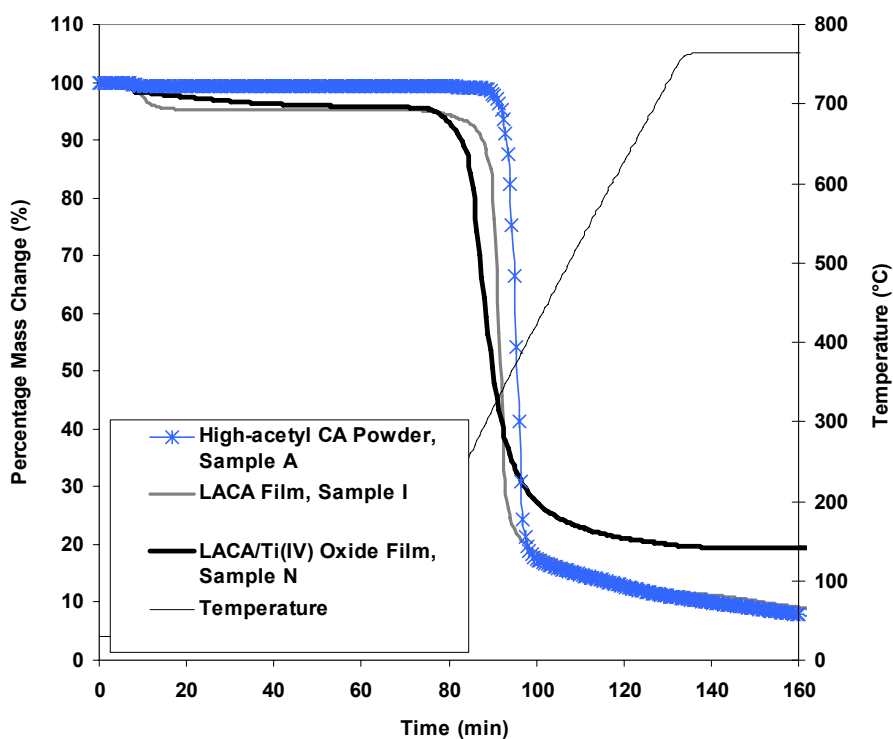


Figure 39. LACA/Titanium(IV) oxide film prepared with 2.00 mL TiCl_4 /g LACA and 5 h reaction

Similarly, the low-acetyl content cellulose acetate sample *O*, treated with 2.00 mL TiCl_4 /g sample during a longer reaction time of 48 h, was thermally stable up to a temperature of about 180 °C. A change in weight of 85 % was registered during the test and the amount of char residue decreased to 13%. Its TG profile is shown in Figure 40.

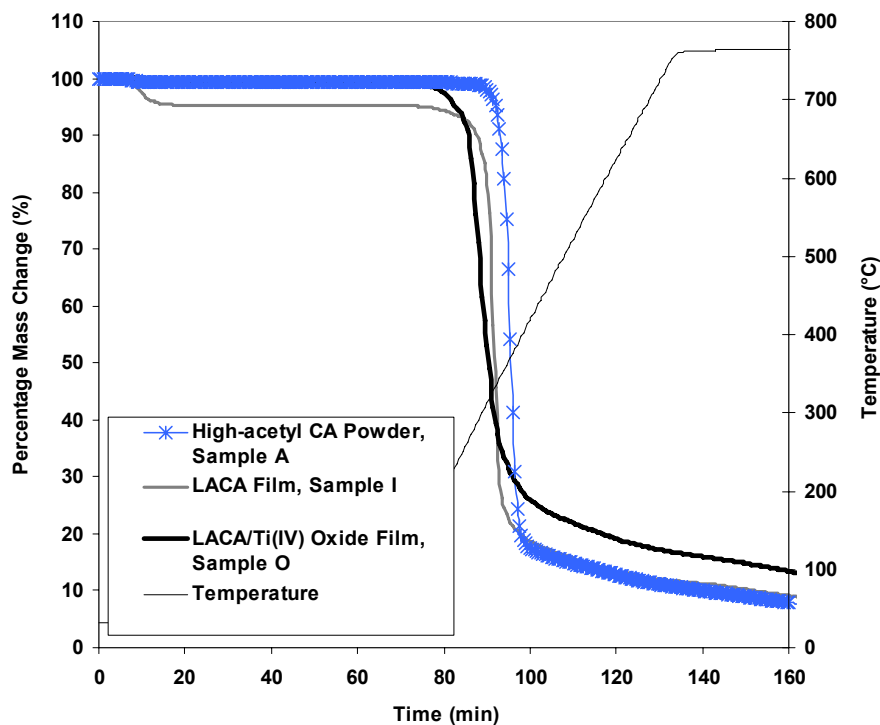


Figure 40. LACA/Titanium(IV) oxide film prepared with 2.00 mL TiCl_4/g LACA and 48 h reaction

Sample *P*, reacted with 0.4 mL TiCl_4/g sample by 5 h, also presented a decrease in its thermal stability with respect to the pure cellulose ester when subjected to the described temperature program, as observed in Figure 41. However, its decrease in thermal stability was rather small with respect to that of low-acetyl content cellulose acetate. The material was degraded at a temperature near 240 °C and presented a weight loss of about 80% of the original mass. After 120 min, the sample degradation was completed and a residue of about 14% the original weight was left.

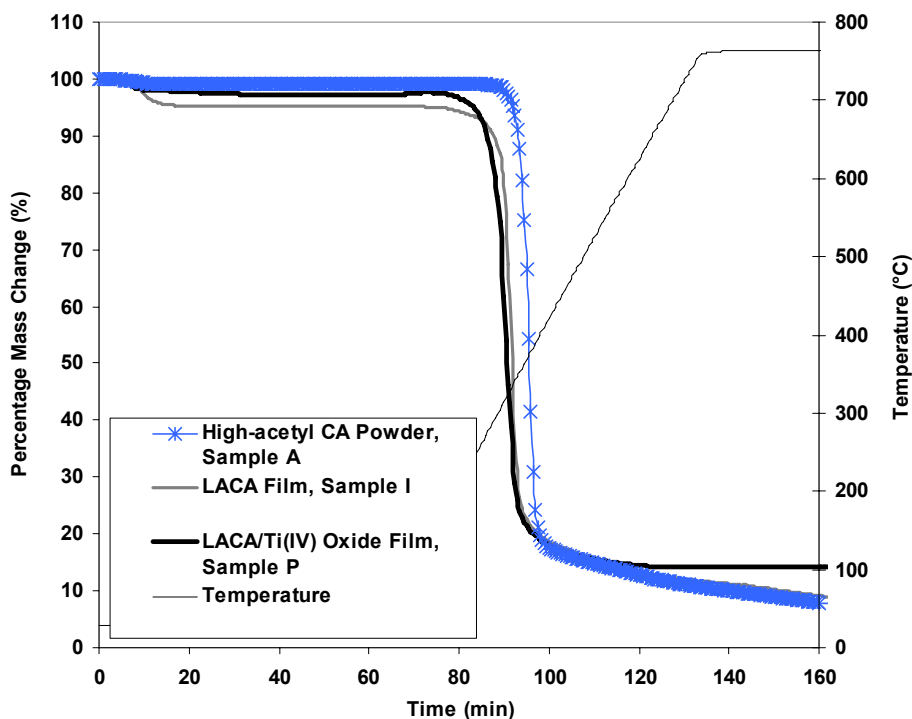


Figure 41. LACA/Titanium(IV) oxide film prepared with 0.40 mL TiCl_4 /g LACA and 5 h reaction

Sample *Q*, high-acetyl content cellulose acetate powder reacted with 0.4 mL TiCl_4 /g sample by 5 h displayed a different TG curve profile (Figure 42). The sample presented a pronounced drying step at the beginning of the temperature program where it lost about 36% of its initial weight, evidencing the high hydrophilicity of the polymer. The sample did not lose its thermal stability in comparison with the original cellulose acetate polymer, since both degrade at about 310 °C. At this temperature, the sample presented a similar weight loss of about 37%. A char residue of about 21% the original weight was left at the end of the test.

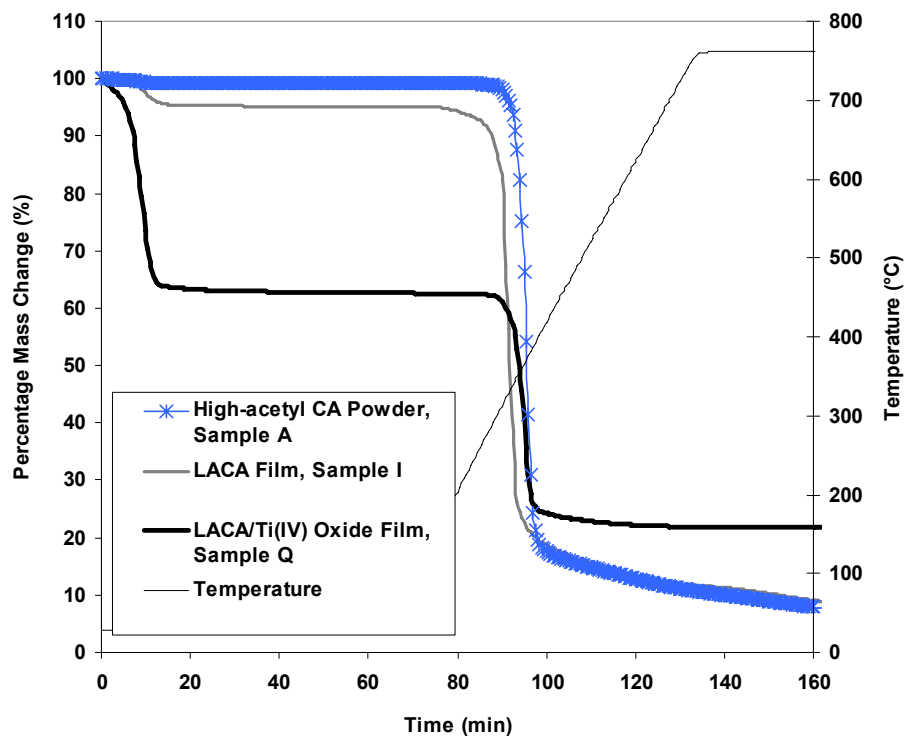


Figure 42. CA/Titanium(IV) oxide powder prepared with 0.40 mL TiCl_4 /g CA and 5 h reaction

The low-acetyl cellulose acetate/titanium(IV) oxide film that showed the best improvement in CO_2 sorption capacity was further reacted with $\text{C}_9\text{H}_{24}\text{N}_2\text{OSi}$ in order to compare both the performance of both sorbents. When sample *R* was tested in the TGA instrument, the sample started to degrade at 220 °C and presented a weight loss of about 97%, as displayed in Figure 43. It can be seen that additional reaction steps on cellulose acetate contribute to deteriorate the material stability.

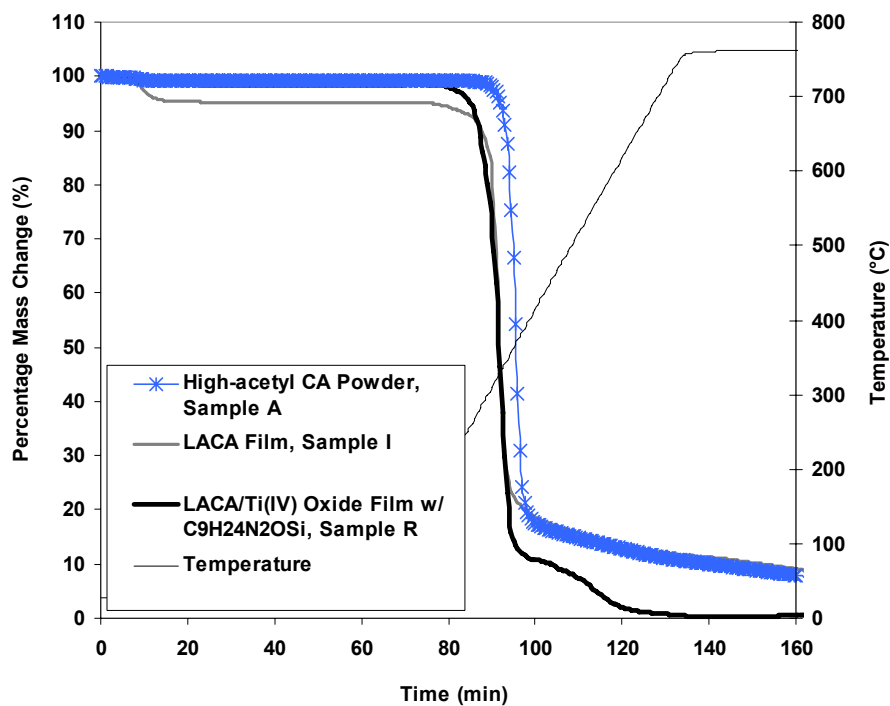


Figure 43. LACA/Ti(IV) oxide film prepared with 0.40 mL TiCl_4 /g LACA for 5h, grafted with $\text{C}_9\text{H}_{24}\text{N}_2\text{OSi}$

Finally, the grafting of $\text{C}_7\text{H}_{19}\text{NOSi}$ on low-acetyl cellulose acetate/titanium(IV) oxide film has a very similar thermal behavior than sample *R*. as seen in Figure 44. After the anhydrous grafting reaction, the sample is still degraded at about 220 °C and registers a weight loss of 92%. The char residue weight about 3% of the original sample mass.

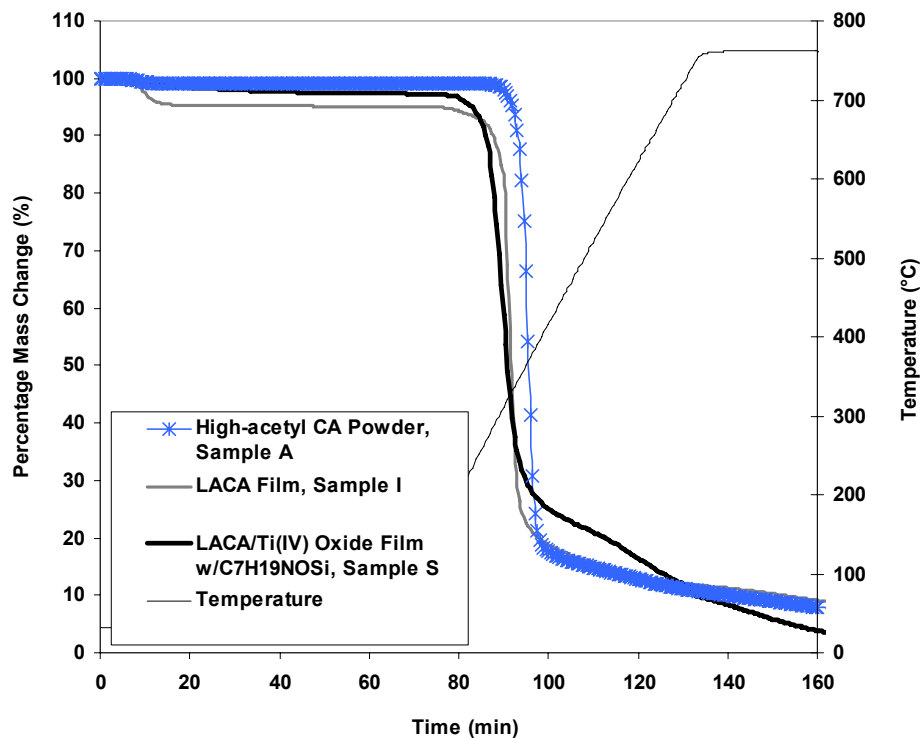


Figure 44. LACA/Ti(IV) oxide film prepared with 0.40 mL TiCl_4 /g LACA for 5h, grafted with $\text{C}_7\text{H}_{19}\text{NOSi}$

The thermogravimetric analyses demonstrated that the amount of TiCl_4 added to the titanation reaction has a greater impact on the thermal stability of the polymer than reaction times. As the amount of TiCl_4 added to the titanation reactions increased, the thermal degradation of cellulose acetate was consistently registered at a lower temperature. Longer reaction times adversely affected the thermal stability of the films at a lower degree. It can be concluded that cellulose acetate stability is degraded with each subsequent reaction step applied, so the milder the reaction conditions, the less affected the thermal behavior of the original polymer.

6.3.6 Scanning Electron Microscopy

Figure 45 presents the SEM images of low-acetyl cellulose acetate/titanium(IV) oxide films. SEM images are a useful tool to track and confirm morphology changes on the surface of the modified cellulose acetate samples. The SEM image of sample *L* is shown in Figure 45(a), low-acetyl cellulose acetate/titanium(IV) oxide film treated with 0.25 mL TiCl₄/g LACA for 5h, reveals the presence of some lighter color spots and fissures around the surface of the polymer. Fractures may be due to surface degradation after the TiCl₄ reaction. The sample presented only a small improvement in the CO₂ sorption capacity and very low titanium loading.

Figure 45 (b) presents the surface morphology of sample *M*, low-acetyl cellulose acetate/titanium(IV) oxide film treated with 0.25 mL TiCl₄/g LACA for 48h. It is interesting to find out that, although its titanium load is very similar to that of sample *L* (about 0.2 wt%), sample *M* does not exhibit any whitish spots or fissures over the surface of the polymer. Its IR spectrum shows a molecular structure barely modified after the reaction. However, the CO₂ sorption capacity of this sample decreased considerably with respect to the original polymer.

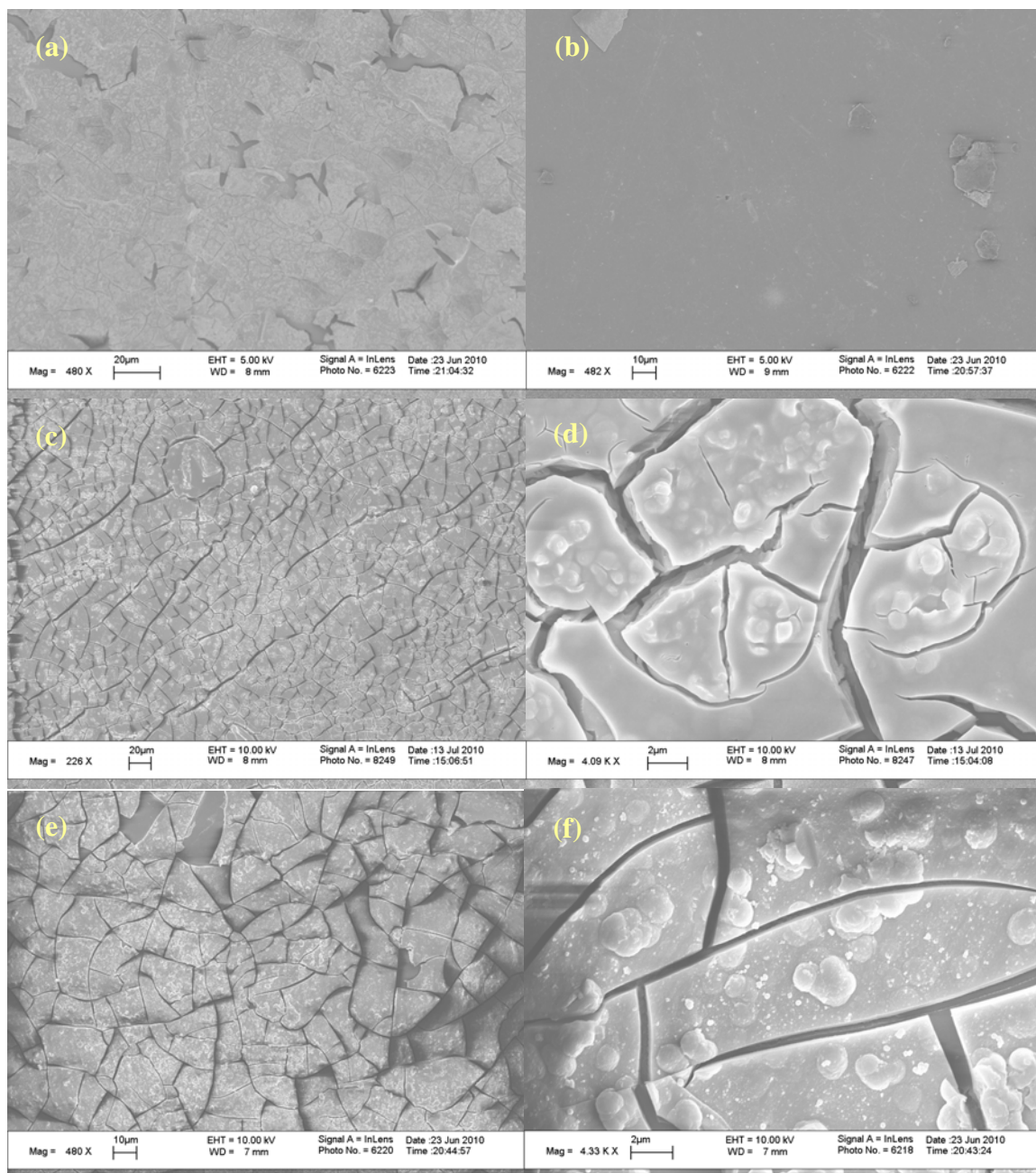
Sample *N* was reacted with 2.00 mL TiCl₄/g LACA under 5h of reaction, and its SEM images (Figure 45 (c) and (d)) show a significant change in its surface morphology. A greater extent of surface fracturing is observed. Magnified images show the presence of well-dispersed white spots over the surface of the polymer. The sorption capacity of

this sample was superior to that of the pure polymer and its titanium loading was about 1.9 wt%.

The SEM image of sample *O*, low-acetyl cellulose acetate/titanium(IV) oxide film treated with 2.00 mL $\text{TiCl}_4/\text{g LACA}$ for 48h, is displayed in Figure 45 (e) and (f). They show the magnitude of the polymer's surface changes suffered by the titanation reaction. A higher density of white spots is observed over the highly fractured surface of the polymer. The titanium loading was similar to that of samples *L* and *M* (~ 0.3 wt%), but its sorption capacity decreased with respect to the pure polymer.

On the other hand, sample *P*, which registered the highest titanium loading (~ 2 wt%) and the largest increase in CO_2 sorption capacity, presents the most uniform dispersion of white spots over all the fractured polymer's surface, as observed in Figure 45 (g) and (h). In order to verify if the surface white spots presented by several of the titanium-reacted films actually formed a coating over the surface of the polymer, cross-sectional profile SEM images were obtained for sample *P*. Unfortunately, Energy-Dispersive X-Ray Spectroscopy (EDX) was out of service at the moment of the analysis and the elemental composition of the cross-sectional profile observed in the images could not be obtained. However, Figures 45 (i) through (l) are useful to show the formation of a kind of layer at the surface and its vicinity that may be composed by titanium oxides. A non-uniform distribution of white regions can be observed across the thickness of the film, suggesting that the composition of the sample after the TiCl_4 reaction changed only in the regions near the polymer's surface. Although this evidence may not be definitive, it

strengthens the hypothesis of a TiCl_4 reaction occurring mainly at the polymer chains most near to the surface of the material. The slow diffusion of the reactants through the polymer matrix may not allow the reaction of hydroxyl groups in the most inner chains of the material. The significant amounts of unreacted hydroxyl groups in these regions promote the water-solubility of the films after the TiCl_4 reaction.



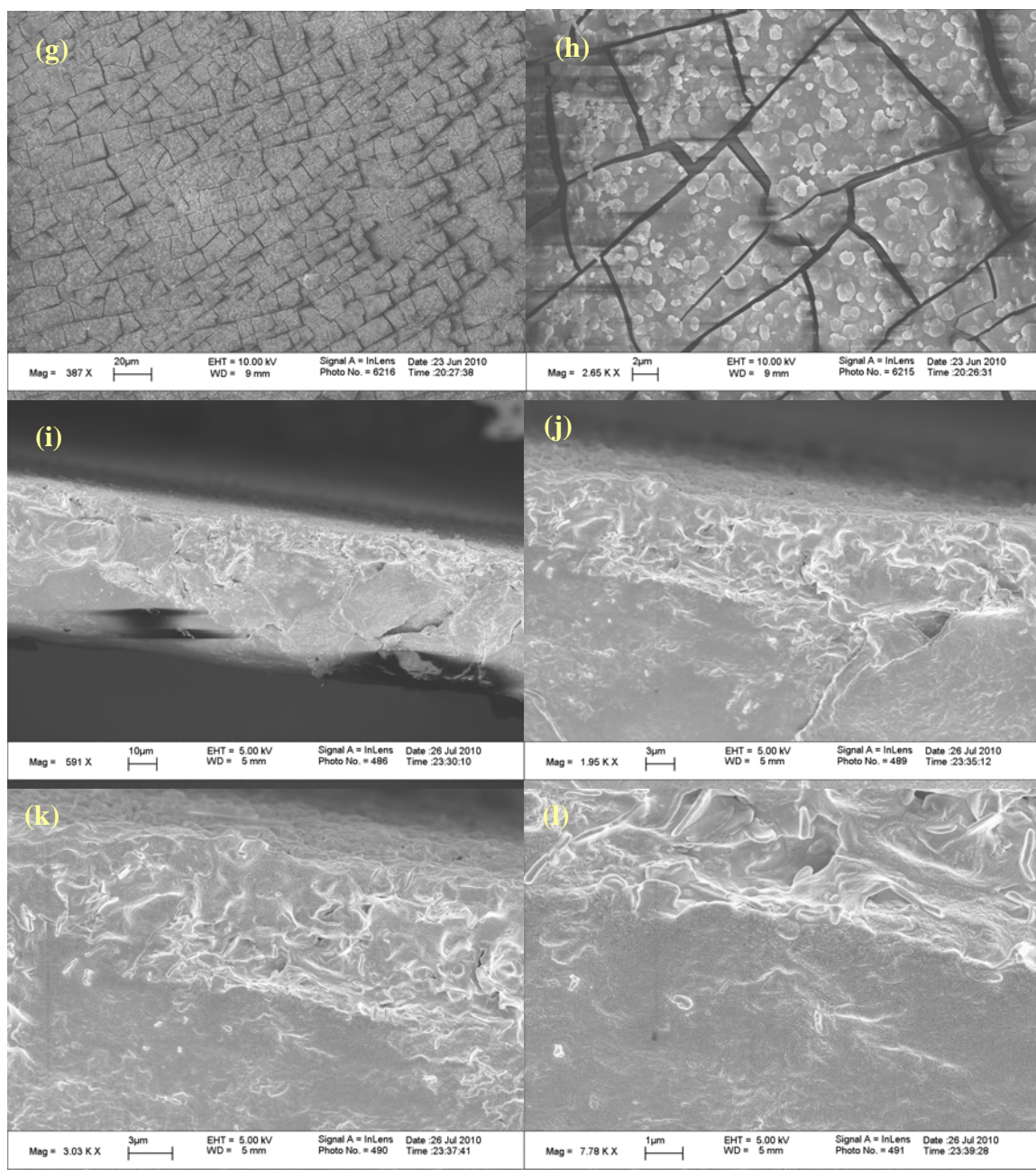


Figure 45. SEM images of (a): Sample *L*; (b): sample *M*; (c) and (d): sample *N*; (e) and (f): sample *O*; (g) and (h): sample *P*, (i), (j), (k) and (l): cross-sectional cut of sample *P*

Similarly, Figure 46 shows a gallery of SEM images from aminosilane grafted films after the TiCl_4 reaction. Samples *R* and *S*, cellulose acetate/titanium(IV) oxide film treated with 0.40 mL TiCl_4 /g LACA for 5h and aminosilane-grafted, displayed a complex

surface morphology. A scarce, non-uniform coating of particles with different morphology than the titanium oxides is observed as a result of the additional grafting treatment.

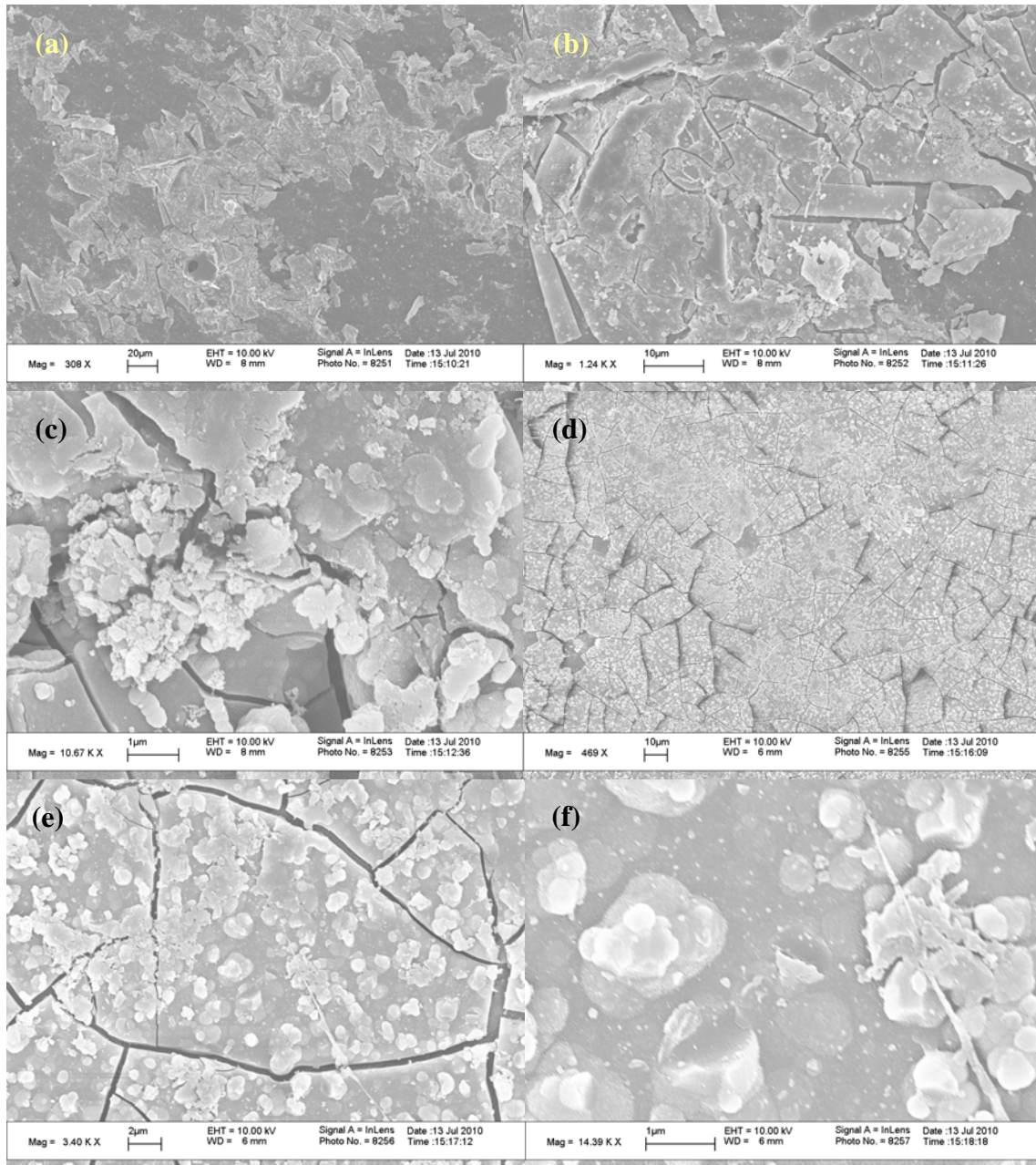


Figure 46. SEM images of (a), (b) and (c): sample *R*; (d), (e) and (f): sample *S*

6.4 Discussion

The initial motivation for the experimental approach described in this chapter has been to break down the high degree of inter- and intra-molecular hydrogen bonding present in the hydroxylated cellulose acetate polymer tailored in our second experimental approach. By this means, it was intended to increase the reactivity of the polymer towards the grafting of aminosilanes and improve the loading of amine functionalities. The use of a strong Lewis acid, like TiCl_4 , is recommended in order to successfully break down the strong hydrogen bond interactions in cellulosic polymers with very low degree of acetylation. Therefore, a reaction procedure based on the work of Meng et al. [56] and Silva et al. [57] with cellulose was adapted for low-acetyl content cellulose acetate. However, water-solubility of the highly hydroxylated cellulose acetate limited the application of the experimental method found in the literature and some modifications had to be applied in order to exclude the presence of water at the end of the reaction. In addition, unsuccessful attempts to dissolve the low-acetyl content cellulose acetate in a different solvent other than water did not allow carrying out a reaction in complete dissolution of the reactants. Water could not be used as the reaction solvent due to its polarity and the high hygroscopicity of TiCl_4 that makes it instantaneously react with water, forming titanium oxides and hydrochloric acid vapors.

The reaction of hydroxyl groups from low-acetyl content cellulose acetate films with TiCl_4 in the presence of CCl_4 and inert conditions leads to the formation of an

intermediate species in which the titanium center bounds to the cellulose acetate backbone through an oxygen atom. Hydrochloric acid is simultaneously formed in the reaction. The reaction scheme is presented in Figure 47.

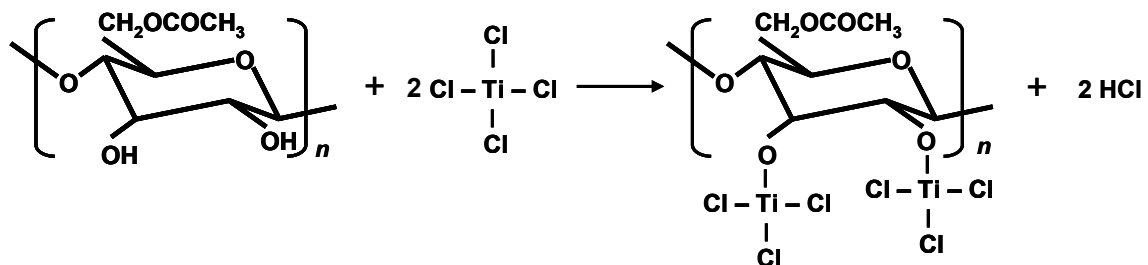


Figure 47. TiCl_4 reaction with cellulose acetate

If this intermediate species is further immersed in anhydrous ethanol, the titanium atom liberates the remaining chlorine atoms and bounds to the ethoxy groups resulting from alcohol dissociation. An instable intermediate species with the structure $\text{C}-\text{O}-\text{Ti}-(\text{OEt})_3$ is then formed, as shown in Figure 48.

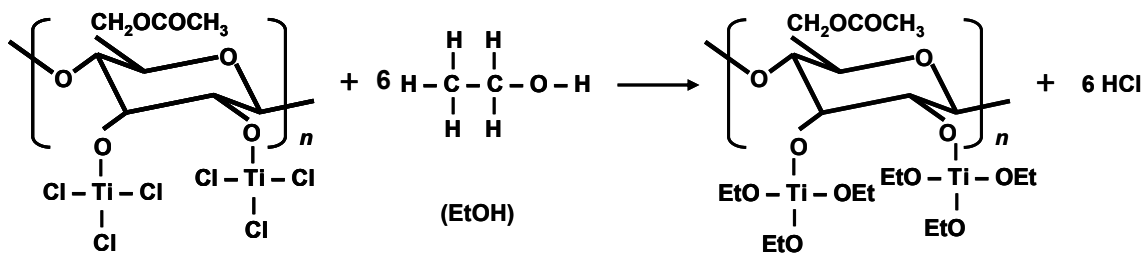


Figure 48. Formation of $\text{C}-\text{O}-\text{Ti}-(\text{OEt})_3$ intermediate species through immersion in ethanol.

The hydrochlorides in solution are subsequently washed away with additional fresh ethanol. The literature suggests a final immersion in a mixture of water/ethanol (50

vol%) and additional washes with pure water. This allow the hydrolysis of the titanium ethoxide functionalities and the formation of hydrated metal oxides of the form C–O–Ti–(OH)₃ [56]. These post-treatment steps were envisioned as part of the experimental approach at the beginning of the work, since it was expected that products from the TiCl₄ reaction would be already insoluble in water. Surprisingly, the titanium-reacted films conserved the water-solubility property of their precursor samples. This suggests the presence of a significant amount of unreactive hydroxyl groups in the polymer or the tendency of the ethoxy functionalities to hydrolyze and form Ti–OH functionalities, which may also promote water-solubility of the films.

At this point, it was envisioned that the intermediate species C–O–Ti–(OEt)₃ with dangling ethoxy functionalities from the polymer backbone could also be an attractive species for improvement of the CO₂ sorption capacity of cellulose acetate. Therefore, it was decided to modify the TiCl₄ reaction post-treatment steps in order to prevent further loss of the ethoxy functionalities.

Titanium ethoxide-derived functionalities have a strong reactivity due to the difference of polarizabilities between the metal and the ethoxy groups. This high reactivity makes them easily hydrolyzable even at room temperature. When hydrated to the maximum possible extent, titanium ethoxide functionalities are still highly reactive and dehydrate at low temperatures, often simultaneously to their hydrolysis step, producing stable titanium oxides. It has been report that titanium ethoxide functionalities hydrolyze about 150 times faster than titanium butoxide ones [98, 99]

In order to avoid the hydrolysis of titanium ethoxide functionalities attached to the polymer, all post-treatment procedures were performed under anhydrous conditions and the best effort was made to maintain constant inert conditions with the available equipment. Glassware was dry overnight in a convection oven at 130 °C and torched before its use. All closed reaction systems and species containers were evacuated with nitrogen during at least 1 hour before its use. All filtration and washing procedures were carried out in a nitrogen evacuated glove bag. However, the lack of enough space, visibility and maneuverability inside the glove bag difficult executions and occasional contact of the samples with the atmospheric moisture was allowed. It is believed that, despite the careful handling of the reacted films, the trace amounts of water in the atmosphere and the solvents used, as well as the high ease of hydrolization of the titanium ethoxide functionalities, allowed the formation of some titanium oxides. IR spectra of the reacted films suggest that a mixture of titanium ethoxide and oxide functionalities may have been attached to the polymer chains. The use of equipment specially designed to prevent the contact between water molecules present in the laboratory atmosphere and the alkoxy functionalities dangling from the cellulose acetate surface can greatly help to retain ethoxide functionalities in the polymer. Therefore, it is widely recommended to carry out the TiCl_4 reaction in a glove box or similar equipment whenever available. For the present research, this special equipment was not available and the best effort was made to avoid the formation of titanium oxides with the equipment at hand.

On the other hand, the water-solubility of the titanium-reacted cellulose acetate films suggested the presence of significant amounts of unreacted hydroxyl groups pending from the polymer chains. This finding indicates that only those hydroxyl functionalities more near to the polymer surface actually reacted with TiCl_4 and those underlying inside the network of random polymer chains were not reached by the reactive titanium centers. The hypothesis was strengthened by cross-sectional profile SEM images showing a significant change in the morphology of the layers near the surface of the polymer, and a very similar morphology to that of the unreacted polymer toward the center of the film.

The prolonged water-solubility of the films also motivated a further grafting reaction with aminosilanes for those samples prepared under the reaction conditions displaying higher CO_2 sorption capacities. Since higher sorption capacities are the result of more available hydroxyl reactive sites contributing with metal oxides to capture higher amounts of gas, only samples prepared under the optimum reaction conditions were subjected to the anhydrous grafting of aminosilanes. SEM images of the aminosilane grafted samples showed a change in the surface morphology of the films; however, negligible amounts of amines were found on the reaction products by elemental analysis and their infrared spectra did not show a definitive evidence of amine functionalities.

The different experimental conditions tested in the TiCl_4 reaction made it clear that to achieve the highest load of titanium functionalities grafted to the polymer chains a set of optimum reaction conditions exist. The main variables affecting the titanation

reaction are the amount of TiCl_4 added, the reaction time, the presence of water, and the chemical posttreatment.

The amount of TiCl_4 incorporated into the system and the reaction time have a profound impact on the amount of titanium functionalities loaded into the cellulose acetate polymer. In addition, both factors also deeply impact the level of surface degradation and loss of mechanical properties that the sorbent undergoes throughout the course of the reaction. Two amounts of TiCl_4 were tested for two different reaction times of 5 h and 48 h: 0.25 and 2.00 mL TiCl_4/g sample. Elemental analysis results indicate that for 5 h long reactions, the amount of titanium fixed into the polymer matrix reaches an optimum value of 2.08 wt% when adding 0.40 mL TiCl_4/g sample. This low titanium weight percentage corresponds to a functionalization with titanium ethoxides of only 10% of all the available hydroxyl reactive sites on a fully de-acetylated cellulose acetate polymer chain. The film with optimum amount of fixed titanium is also the one displaying best CO_2 sorption behavior. Further increase in the amount of TiCl_4 added does not yield higher titanium loadings. All films obtained after 5 h long reaction retained well its mechanical strength and increase its sorption capacity with respect to the pure polymer. On the other hand, the reaction of low-acetyl content cellulose acetate for about 48 h did not incorporate higher amounts of fixed titanium into the polymer matrix regardless of the TiCl_4 dose used. When adding either 0.25 or 2.00 mL TiCl_4/g sample, the titanium grafted into the polymer accounted for about 0.3 wt% of the modified polymer. However, all films subjected to long reaction times presented a significant decrease in the CO_2 sorption capacity with respect to the original polymer, a higher

degree of degradation and loss of mechanical properties. Degradation of the polymer may be due to prolonged exposure to HCl produced during the course of the reaction. The decomposition process may involve the removal of acetyl groups from the polymer backbone by reaction with a proton from dissociated HCl to form acetic acid. The acetic acid formed from degradation may take part in catalyzing further de-acetylation [100]. This process would explain the high brittleness of the films reacted during 48 h. The use of an acid acceptor or stabilizer compound that combines with HCl produced in the reaction might mitigate the polymer degradation problem.

Results from CO₂ sorption characterization revealed that the low-acetyl content cellulose acetate/titanium(IV) oxide film prepared by the reaction of 0.40 mL TiCl₄/g sample for 5h presented the higher improvement in sorption capacity. This sorbent showed a sorption capacity of 1.48 mmol CO₂/g sorbent at partial pressures of about 5 atm CO₂. This represented an additional capture of about 0.97 mmol CO₂/g sorbent after the titanium modification of cellulose acetate. It is interesting to note that all films reacted for 5h registered an enhanced CO₂ sorption capacity, while all films reacted during longer periods of time showed a decrease in the CO₂ sorption capacity. This phenomenon could also be due to the polymer degradation at extended periods of time. Significantly long sorption equilibration times, in the order of 3 to 4 days, were observed for the titanium-reacted films.

Sample *Q*, high-acetyl content cellulose acetate powder reacted with 0.40 mL TiCl₄/g CA, showed an increase in the CO₂ sorption capacity, reaching a value of 0.75 mmol CO₂/g sample and capturing about 0.19 mmol CO₂ additional per gram of sample *Q*.

Although the increase in sorption capacity was modest, it is important to note its advantages of water insolubility and a more straightforward method of preparation.

On the other hand, when sample *P*, low-acetyl content cellulose acetate/titanium(IV) oxide film with best sorption capacity enhancement, was subjected to a grafting reaction with aminosilanes under anhydrous conditions, the products showed a decrease in its sorption capacity, as can be observed in Figure 28. Sample *R*, grafted with $C_9H_{24}N_2OSi$ under anhydrous conditions decreased its sorption capacity from 1.48 mmol CO_2 /g sorbent to 1.39 mmol CO_2 /g sorbent. A similar behavior was observed for the grafting of sample *P* with $C_7H_{19}NOSi$ under dry conditions. This time, the sorption capacity presented a sharper decrease, from 1.48 mmol CO_2 /g sorbent to only 0.78 mmol CO_2 /g sorbent. Although the CO_2 sorption capacity of both films is still higher than that of pure high-acetyl content cellulose acetate, the objective of the grafting reaction was obviously to increase it further and this was not achieved.

Additional research is needed in order to overcome the water-solubility of the low-acetyl content cellulose acetate/titanium(IV) oxide sorbent films. The water sensitivity of these sorbents represents an important hurdle to overcome in order for them to be realistically considered for further industrial applications. It is believed that further investigation of set of reaction conditions allowing full reaction of all available hydroxyl functionalities in the polymer backbone and its subsequent substitution by titanium oxide and ethoxide functionalities will automatically hinder the water-solubility of the sorbents and further increment its CO_2 sorption capacity. Research orientated on finding a way to

carry out the TiCl_4 reaction with total dissolution of the reactants on a suitable aprotic solvent (instead of reacting the cast films as described here) will certainly allow a significant improvement of the reaction conversion and an increase of titanium functionalities loading into the polymer chains.

CHAPTER 7

GRAFTING OF AMINOSILANES ON HIGH-ACETYL CONTENT CELLULOSE ACETATE UNDER OPTIMUM REACTION CONDITIONS

Different experimental approaches have been attempted during the present research in order to increment the CO₂ sorption capacity of high-acetyl content cellulose acetate. The level of success in the improvement of cellulose acetate CO₂ sorption capacity achieved by the preparation of low-acetyl content cellulose acetate/titanium(IV) oxide, a deeper understanding of the polymer's chemical properties and a wider knowledge of some favorable reaction conditions for this particular material motivated an additional experimental pathway addressed in this chapter. In addition, a dose of curiosity to verify if some of the TiCl₄ conditions could work on a much simpler reaction framework encouraged this work.

This way, the conventional grafting method with aminosilanes under a set of optimum reaction conditions directly applied to high-acetyl content cellulose acetate was tested as a final approach to improve the sorption capacity through a more straightforward and reliable method. The main difference between the present and the first experimental pathway proposed in this study lays on the set of reaction conditions applied to the grafting procedure. The conditions proposed in this reaction framework arose from the learning curve experienced about the particular properties of the polymer and its chemical behavior on previous grafting reactions. It is important to note that there may be other conditions under which the CO₂ sorption capacity of cellulose acetate could

be improved to a higher extent, but time constraints on the present study did not allow further experimental testing. It is widely recommended to reserve a time in future projects for tuning the reaction conditions proposed in this experimental pathway.

7.1 Experimental

7.1.1 Materials

All materials were used as received. Cellulose acetate, anhydrous toluene, and xylenes were supplied by Sigma-Aldrich (St. Louis, MO, USA). Aminosilanes $C_9H_{24}N_2OSi$ and $C_7H_{19}NOSi$ were purchased from Gelest, Inc. (Morrisville, PA, USA). The typical physical and chemical properties of the cellulose acetate, $C_9H_{24}N_2OSi$ and $C_7H_{19}NOSi$ have been previously described.

7.1.2 Grafting of Aminosilanes on High-acetyl Content Cellulose Acetate

The deep impact that water, temperature, reactant amounts, reaction times and post-treatment methods had in the relative success of the previous approach motivated to test the grafting reactions with aminosilanes under a set of similar reaction conditions to the ones used in the $TiCl_4$ reaction with low-acetyl content cellulose acetate. These conditions included total anhydrous conditions for some experiments and the addition of

a controlled, minimum amount of water for others; a lower grafting temperature, a longer reaction time and a post-treatment procedure excluding water.

The as received high-acetyl content cellulose acetate powder was subjected to anhydrous and wet grafting of aminosilanes following a similar procedure to the ones applied in previous approaches, but under a set of different reaction conditions. 1 g of commercial, high-acetyl content cellulose acetate was dried overnight at 70 °C in a vacuum oven. All glassware used was dried overnight in a convection oven at 130 °C and torched right before its use. A 500 mL three-neck flask with a magnetic stirrer was connected to a condenser and, after introduction of the sample, the system was closed. A stream of dry nitrogen was run through the reaction system for 1 h. After this time, 150 mL of anhydrous toluene were injected into the system using a syringe. The powder and the solvent were allowed to mix for 30 min at room temperature under a nitrogen atmosphere. For wet grafting reactions, about 0.25 mL of water were incorporated at this point and the mixture was allowed to equilibrate for 3 h mixing at room temperature and keeping the nitrogen flow. For anhydrous grafting, the previous step was skipped and the temperature of the reaction solution was increased to 70 °C by placing it into a hot oil bath. 3 mL of the corresponding aminosilane were injected and the reaction was allowed to proceed during 24 h under a nitrogen atmosphere and constant temperature. After this time, the product was separated from the solvent by reduced pressure filtration and washed with 500 mL of anhydrous toluene and about 1 L of hexanes. The grafted samples were put into a vacuum oven at 70 °C overnight and stored afterwards in capped vials until further use. Table 15 present the samples obtained by the anhydrous and wet

grafting of aminosilanes on high-acetyl content cellulose acetate under optimal conditions.

Table 15. Reaction conditions for aminosilane-grafting of high-acetyl content cellulose acetate powder

Sample	Cellulose Acetate (g)	Toluene (mL)	Aminosilane Species	Aminosilane (mL)	H ₂ O (mL)	Amination Time (h)	Amination Temperature (°C)
<i>T</i>	1	150	C ₉ H ₂₄ N ₂ OSi	3	0.00	24	70
<i>U</i>	1	150	C ₉ H ₂₄ N ₂ OSi	3	0.25	24	70
<i>V</i>	1	150	C ₇ H ₁₉ NOSi	3	0.00	24	70
<i>W</i>	1	150	C ₇ H ₁₉ NOSi	3	0.25	24	70

Figure 49 provides a gallery of illustrations of the main reaction steps previously described.



Figure 49. Main experimental steps in the preparation of aminosilane functionalized cellulose acetate: (a) N₂ drying and purging of the reaction system (b) mixing of high-acetyl content cellulose acetate powder with toluene before grafting reaction, (c) aminosilane grafting reaction at 70°C for 24 h under N₂ atmosphere, (d) and (e) swollen aminosilane functionalized cellulose acetate after grafting reaction (sample *T*), (f) final product after drying and grinding (sample *T*)

7.1.3 Sorbent Sorption Characterization

The characterization of the CO₂ sorption capacities of the aminated cellulose acetate powder samples was carried out using the pressure decay method used in previous experimental approaches [55]. Detailed description of the method is provided before.

7.1.4 Instrumental Characterization of Sorbents

The composition and properties of the aminated cellulose acetate powder samples were also tested using Elemental Analysis (EA), density analysis, Attenuated Total Reflection Infrared Spectroscopy (ATR-IR), Thermogravimetric Analysis (TGA) and Scanning Electron Microscopy (SEM). A detailed description of each instrumental technique has been provided before.

7.2 Results

7.2.1 Sorbent Sorption Characterization

Figure 50 provides the isotherms obtained for samples *T–W*. Sample *T*, high-acetyl content cellulose acetate powder grafted with C₉H₂₄N₂OSi under anhydrous conditions, presented a significant improvement in its CO₂ sorption capacity after the

grafting reaction. At an equilibrium pressure of about 1 atm, sample *T* was capable of adsorbing about 27 cc (STP) CO₂/cc sorbent, while pure cellulose acetate captured about 6 cc (STP) CO₂/cc CA at very similar equilibration pressure. This represents an increment in the sorption capacity of about 4.5 times the sorption capacity of the unmodified polymer at low pressures. The increment in sorption capacity is equivalent to capture an additional 0.78 mmol CO₂ per gram of sample *T* or additional 0.15 mol CO₂ per mole of amines grafted. At high pressures of about 5 atm, sample *T* increased its sorption capacity up to 39.2 cc (STP) CO₂/ cc sorbent, capturing an additional amount of 0.84 mmol CO₂ per gram of sorbent. In addition, its sorption equilibration time during the first dry sorption cycle is about 2 h, very similar to that of pure cellulose acetate. It is a very short sorption equilibrium time in comparison to the 28 h equilibration time registered by sample *P*, low-acetyl content cellulose acetate/titanium(IV) oxide film that registered the highest improvement in sorption capacity after reaction with TiCl₄. At 1 atm, sample *U* grafted with C₉H₂₄N₂OSi under humid conditions was able to sorb about 11 cc (STP) CO₂/cc sample *U*, an increment of about 1.8 times the sorption capacity of the pure polymer. This means that sample *U* adsorbed additionally 0.17 mmol CO₂ per gram of sample at low pressures. On the other hand, both samples *V* and *W*, cellulose acetate grafted with C₇H₁₉NOSi under anhydrous and humid conditions respectively, decreased its CO₂ sorption capacity when compared to pure cellulose acetate.

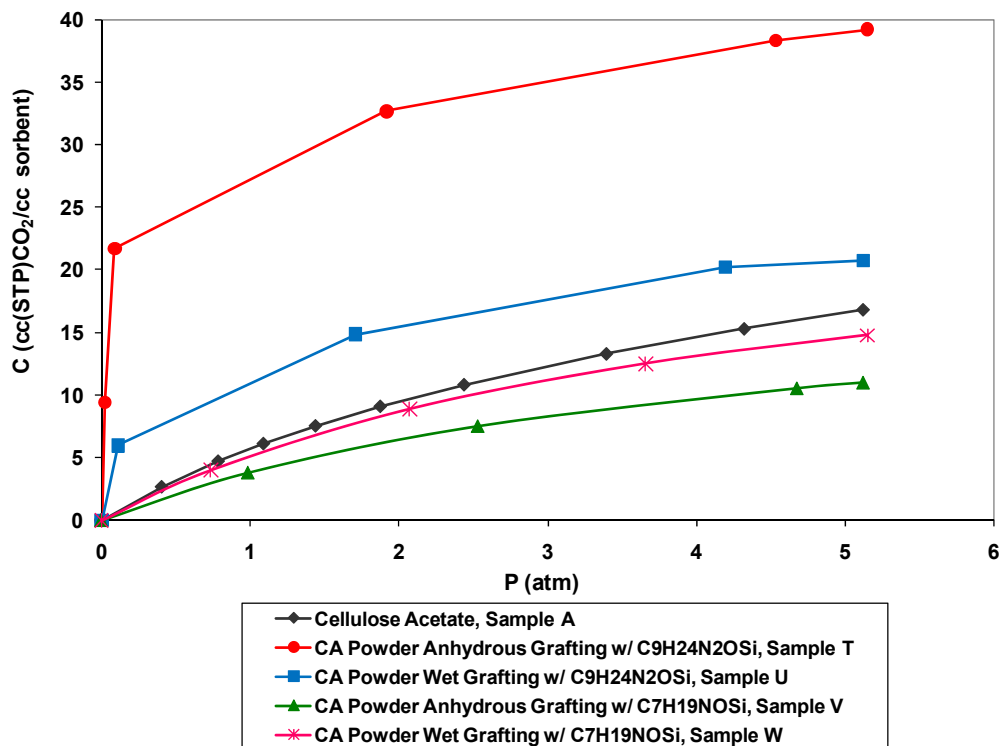


Figure 50. CO₂ sorption isotherms for samples *T*, *U*, *V* and *W*

Sample *T*, which presented the highest increment in CO₂ sorption capacity, was subjected to complete desorption of the CO₂ captured from its first exposure by increasing its temperature to about 120 °C under vacuum for 24 h. Half of the desorbed sample was subjected to a second CO₂ sorption cycle right after its desorption and was labeled as sample *X*. The other half of sample *T* was exposed to water vapor during 3 days and labeled as sample *Y*. This was performed by spreading the sample over a clean and dry Petri dish and introducing it into the top of a closed glass chamber with 500 mL of deionized water at its bottom. The water in the chamber remained heated to a temperature of about 50 °C during the experiment. After this time, hydrated sample *Y* was removed and put into a vacuum oven at 70 °C overnight. Afterwards, it was loaded into the pressure decay sorption system in order to test the sorption capacity on a second

sorption cycle after its exposure to water vapor. Figure 51 presents the isotherm for the first exposure to CO₂ of sample *T* already presented above, the isotherm for sample *X* recorded at its second CO₂ sorption cycle, and the isotherm for sample *Y* on a second sorption cycle after hydration with water vapor.

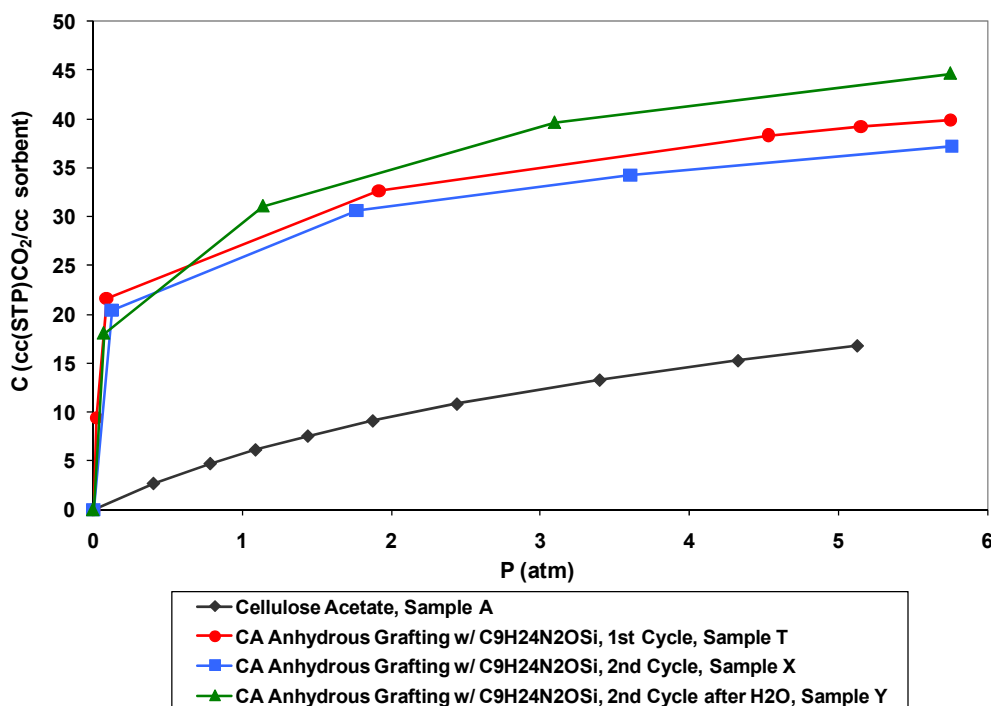


Figure 51. CO₂ sorption isotherms for samples *T*, *X* and *Y*

Sample *X*, obtained after a 24h-desorption process at 120 °C applied to sample *T*, presented a CO₂ equilibrium sorption capacity of 26 cc (STP) CO₂/cc sorbent at an equilibrium pressure of about 1 atm, slightly below the equilibrium sorption capacity of sample *T* at similar pressure (about 27 cc (STP) CO₂/cc sample *T*). This means that in its second dry sorption cycle, sample *T*'s sorption capacity decreased by about 4% at low pressures. However, when desorbed sample *T* was exposed to water vapor for about 3 days, subsequently dried at 70 °C overnight and loaded again into the sorption system, sample *Y* presented an increase of about 11% on the sorption capacity with

respect to its first sorption cycle. That is, the new sorption capacity of sample *Y* is about 30 cc (STP) CO₂/cc sorbent at 1 atm and 44.5 cc (STP) CO₂/cc sorbent at 5 atm. It was able to capture an additional 0.11 mmol CO₂ per gram of sample *Y* at low pressures and about 0.20 mmol CO₂ per gram of sample *Y* at 5 atm. On the other hand, it was observed that sample *X* had an average equilibration time of 4 h, while sample *Y* average time was about 15 h. It is important to note that these long equilibration times may have been caused by particle agglomeration, since after water exposure the average particle size may have been as twice as big as the initial powders. Therefore, further systematic kinetic studies using films are needed in order compare the kinetics of samples with same characteristic dimensions.

7.2.2 Elemental Analysis

Table 16 shows the results for the Elemental Analysis of cellulose acetate before and after dry and humid grafting reactions with aminosilanes under optimal reaction conditions.

Table 16. EA of pure and aminated cellulose acetate powder at dry and wet grafting optimum conditions

Sample		Elemental Analysis				
		% C	% H	% O	% N	% Si
<i>A</i>	High-acetyl content cellulose acetate (CA)	48.21	5.93	45.60	0.00	0.00
<i>T</i>	CA powder anhydrous grafting with C ₉ H ₂₄ N ₂ OSi	49.87	8.65	29.26	7.25	4.31
<i>U</i>	CA powder humid grafting with C ₉ H ₂₄ N ₂ OSi	49.13	6.31	40.22*	2.53	1.81
<i>V</i>	CA powder anhydrous grafting with C ₇ H ₁₉ NOSi	48.66	6.72	40.35	2.01	1.98
<i>W</i>	CA powder humid grafting with C ₇ H ₁₉ NOSi	48.61	6.91	37.86*	3.09	3.53

*Instrument could not accurately measure the oxygen amount. Estimated amounts by difference.

Elemental analysis has been a useful tool to analyze the effect that water and type of aminosilane have on the amount of amines loaded into high-acetyl content cellulose

acetate. The grafting of $C_9H_{24}N_2OSi$ on cellulose acetate powder under anhydrous conditions registered the highest loading of amine functionalities, with 7.25 wt% nitrogen. This amount is equivalent to graft about 5.18 mmol amine(nitrogen)/g sample *T*. Estimated theoretical values of molecular weight composition shows that the grafting of one molecule of $C_9H_{24}N_2OSi$ to one OH group per glucoside unit of the polymer yields a nitrogen amount of 6.70 wt%. As the amount of nitrogen obtained from EA results is a bit larger, it is suggested that at least one molecule of $C_9H_{24}N_2OSi$ was grafted to each glucoside unit in cellulose acetate, and for some repeating units, more than one was actually attached. The addition of a controlled amount of water to the grafting reaction drastically decreased the loading of amines functionalities and the sorption capacity of sample *U*. On the other hand, the sample with the least amount of grafted amines is *V*, corresponding to the anhydrous grafting of $C_7H_{19}NOSi$ on high-acetyl content cellulose acetate powder. The amount of nitrogen in this sample was reduced to 2.01 wt% or about 1.44 mmol amine(nitrogen)/g sample *V*. Surprisingly, while the addition of water decreased the amount of amine fixation for the grafting reactions with $C_9H_{24}N_2OSi$, humid conditions had the opposite effect when working with $C_7H_{19}NOSi$. The wet grafting of $C_7H_{19}NOSi$ on cellulose acetate increased the amount of amine loadings and its CO_2 sorption capacity.

7.2.3 Density Analysis

Densities of pure polymer and of aminated samples are showed in Table 17.

Table 17. Densities of high-acetyl content cellulose acetate and aminated cellulose acetate samples

Sample		Density (g/mL)
<i>A</i>	Acetone-soluble cellulose acetate powder (CA)	1.4205
<i>T</i>	CA powder anhydrous grafting with C ₉ H ₂₄ N ₂ OSi	1.1951
<i>U</i>	CA powder humid grafting with C ₉ H ₂₄ N ₂ OSi	1.2931
<i>V</i>	CA powder anhydrous grafting with C ₇ H ₁₉ NOSi	1.3134
<i>W</i>	CA powder humid grafting with C ₇ H ₁₉ NOSi	1.2548

Densities of the cellulose acetate grafted samples are expected to decrease with increasing amines content. The bulky aminosilane molecules grafted to the cellulose acetate backbone in substitution of hydroxyl groups decrease the packing of the polymer chains and the total weight per unit volume of sample. In agreement with this criterion, sample *T* with highest amine content presented the largest decrease in absolute density of about 15.8%. The sample with the lowest amount of grafted amines was sample *V*, which showed the smallest decrease in its density value (~7.5% decrease). These results confirm the significant change in the morphology of the polymer chains due to aminosilane grafting.

7.2.4. Attenuated Total Reflection Infrared Spectroscopy

ATR-IR spectrum of sample *T* is presented in Figure 52. The Si-CH₃ group has been reported to be easily recognizable for a strong, sharp band at about 1250 cm⁻¹, together with one or more strong absorption bands in the range of 750-865 cm⁻¹ [86]. Both characteristic absorptions bands are clearly visible in the spectrum of sample *T*, confirming the grafting of polysiloxane functionalities into the polymer backbone. In addition, the functionality [(CH₃)₂SiO]_x, present in the molecule of C₉H₂₄N₂OSi, is characterized by the strong band at 1020 cm⁻¹, also visible in the present spectrum. The

band of medium intensity at $\sim 1400\text{ cm}^{-1}$ corresponds to aliphatic amines, while the doublet of bands at 1550 and 1650 cm^{-1} are widely assigned to deformation vibrations of secondary amines [88]. Kanan et al. have assigned the 1650 cm^{-1} absorption band to free amine functionalities [87]. The appearance of the broad band around $2800\text{--}2970\text{ cm}^{-1}$ may correspond either to stretching C-H vibrations. Finally, the range from 3300 to 3550 cm^{-1} has been assigned to free amine functionalities [79]. Therefore, it can be concluded that the anhydrous grafting of $\text{C}_9\text{H}_{24}\text{N}_2\text{OSi}$ worked very well under the reaction conditions applied and the present spectrum can be used as the reference for the characteristics of the desired sorbent.

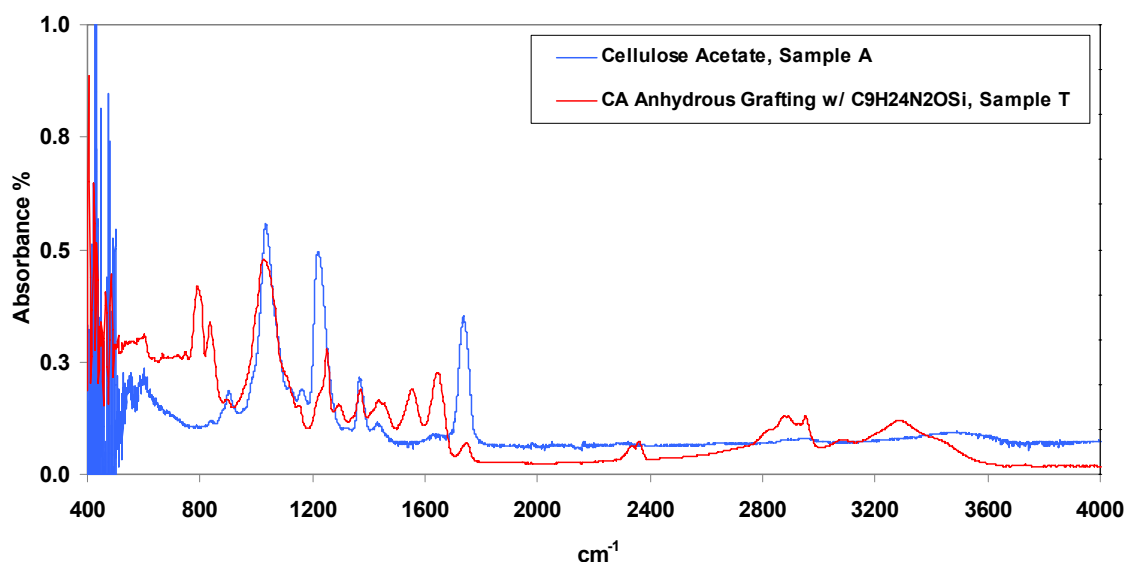


Figure 52. ATR-IR of CA and anhydrous grafting of CA with $\text{C}_9\text{H}_{24}\text{N}_2\text{OSi}$, sample *T*

The spectrum of sample *U*, $\text{C}_9\text{H}_{24}\text{N}_2\text{OSi}$ -grafted cellulose acetate under wet conditions, is shown in Figure 53. It confirms the grafting of a smaller amount of aminosilane functionalities. The couple of absorption bands around $750\text{--}865\text{ cm}^{-1}$ and

$\sim 1020\text{ cm}^{-1}$, characteristic of polysiloxanes, are weaker in comparison with the rest of the spectrum, as well as the bands at 1550 and 1650 cm^{-1} , corresponding to amine vibrations. The decrease in free amine functionalities is more evident in the region of $3400\text{--}3500\text{ cm}^{-1}$. The weaker absorption bands typical of organosilanes and amine functionalities confirm a smaller amount of $\text{C}_9\text{H}_{24}\text{N}_2\text{OSi}$ grafted in sample *U* under wet conditions. The same conclusions can be done for the spectrum of Sample *V*, grafted under anhydrous conditions with $\text{C}_7\text{H}_{19}\text{NOSi}$ and presented in Figure 54.

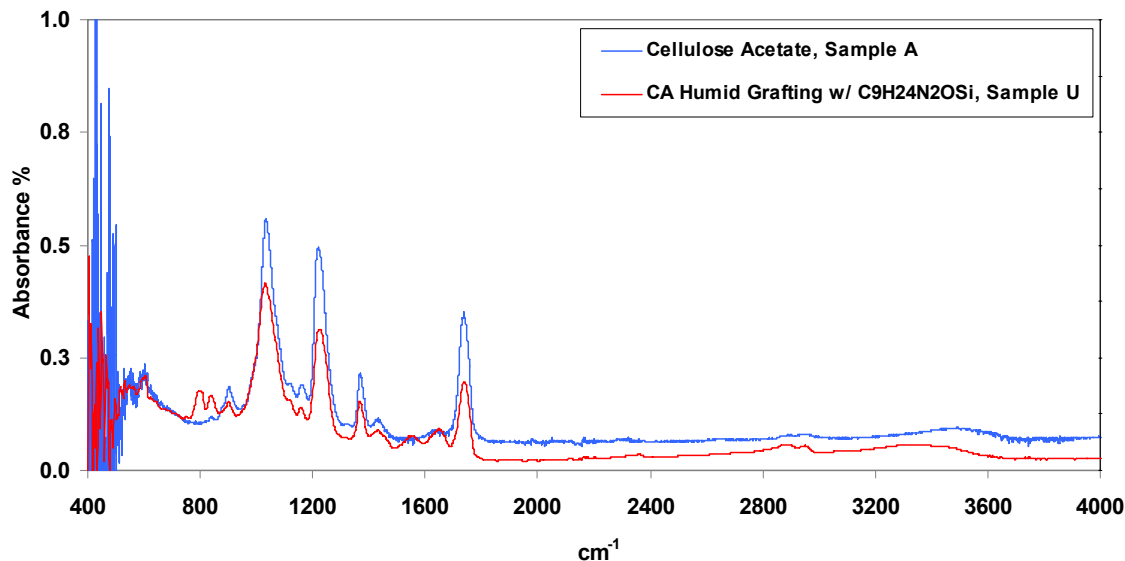


Figure 53. ATR-IR of CA and humid grafting of CA with $\text{C}_9\text{H}_{24}\text{N}_2\text{OSi}$, sample *U*

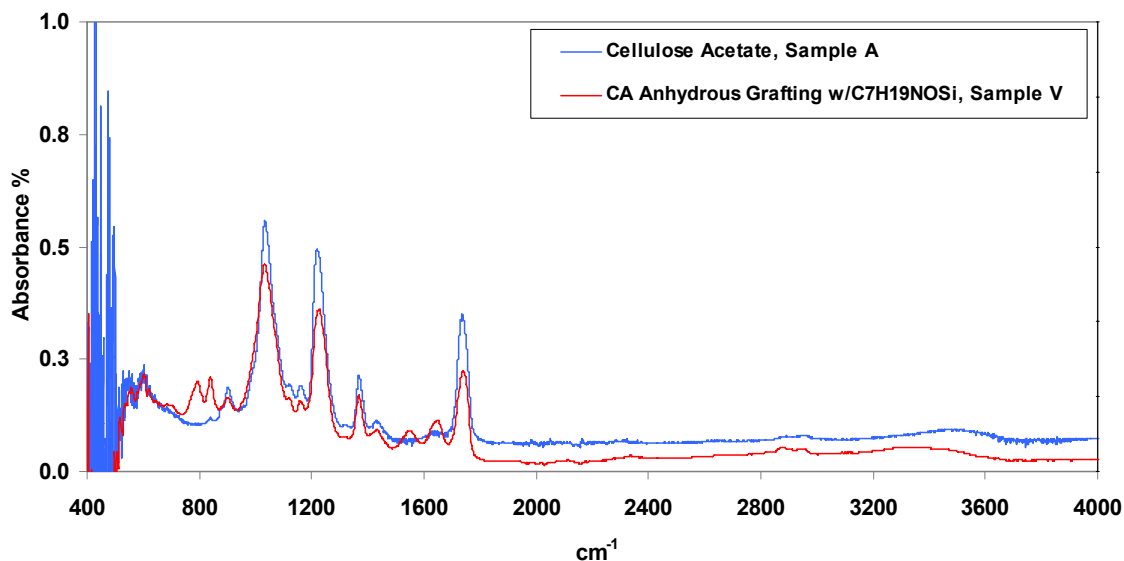


Figure 54. ATR-IR of CA and anhydrous grafting of CA with $C_7H_{19}NOSi$, sample *V*

However, an increase in absorption intensities is registered by sample *W*, $C_7H_{19}NOSi$ grafted under humid conditions. Its spectrum is presented in Figure 55. The absorption bands are $750\text{--}865\text{ cm}^{-1}$ indicate a higher presence of $Si\text{--}CH_3$ bonds in the grafted molecule, and the strong intensities of the 1550 cm^{-1} and 1650 cm^{-1} peaks suggests an increase in the amines grafting.

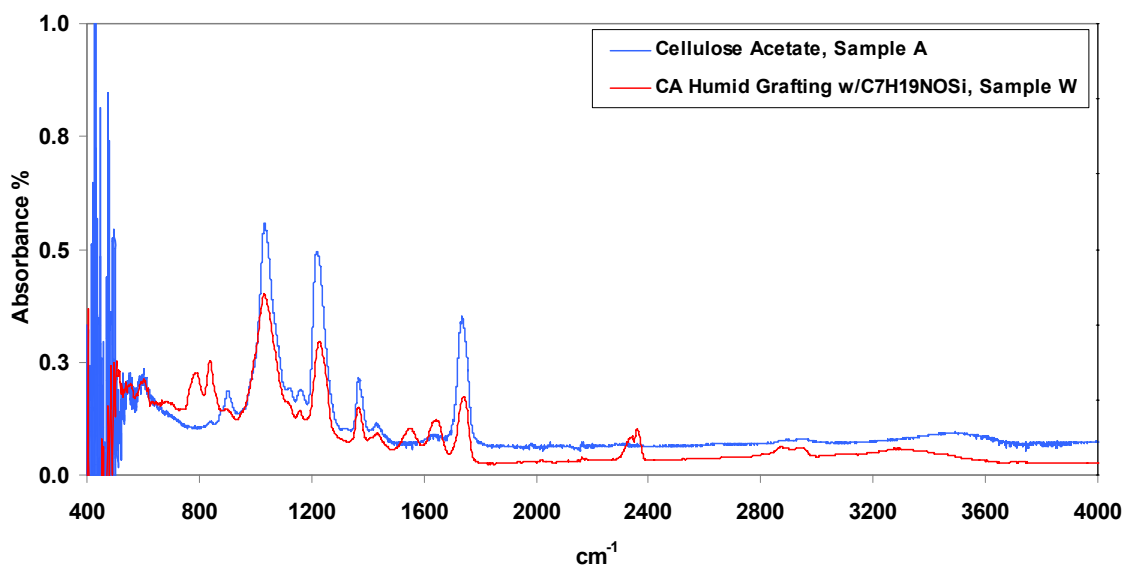


Figure 55. ATR-IR of CA and humid grafting of CA with $C_7H_{19}NOSi$, sample *W*

7.2.5 Thermogravimetric Analysis

The TG curves for aminosilane grafted cellulose acetate powder with $C_9H_{24}N_2OSi$ under anhydrous and humid conditions are shown in Figure 56. The thermal stability of both amine grafted samples decreased after the grafting reaction. Sample *T*, which presents the highest improvement in CO_2 sorption capacity, decreased its thermal stability from 310 °C to about 200 °C. The mass loss during this degradation step was about 82%, with a slower rate of thermal decomposition than commercial cellulose acetate. After 140 min and at a temperature of about 760 °C, the residual char amounted about 15% of the original sample weight. Similarly, cellulose acetate powder grafted with the same aminosilane species but under humid conditions presented a decreased on thermal stability to about 200 °C. The weight loss step was about of 73% and the amount of char residue increased to 25% of the original weight. The TG curve for sample *Y*, CO_2 -desorbed sample *T* after one sorption cycle and exposed to water for 3 days, was introduced into the TGA instrument right after its removal from water exposure. It registered a weight loss of about 7% its initial weight of 85 mg, that is, a mass of around 5.95 mg of water was removed from the sample at the beginning of the program. Around 180 °C, the sample lost its thermal stability and registered a degradation step where it lost about 79% its weight. Therefore, although sample *Y* increased its CO_2 sorption capacity after exposure to water, its thermal stability was slightly reduced after prolonged exposure to humid conditions.

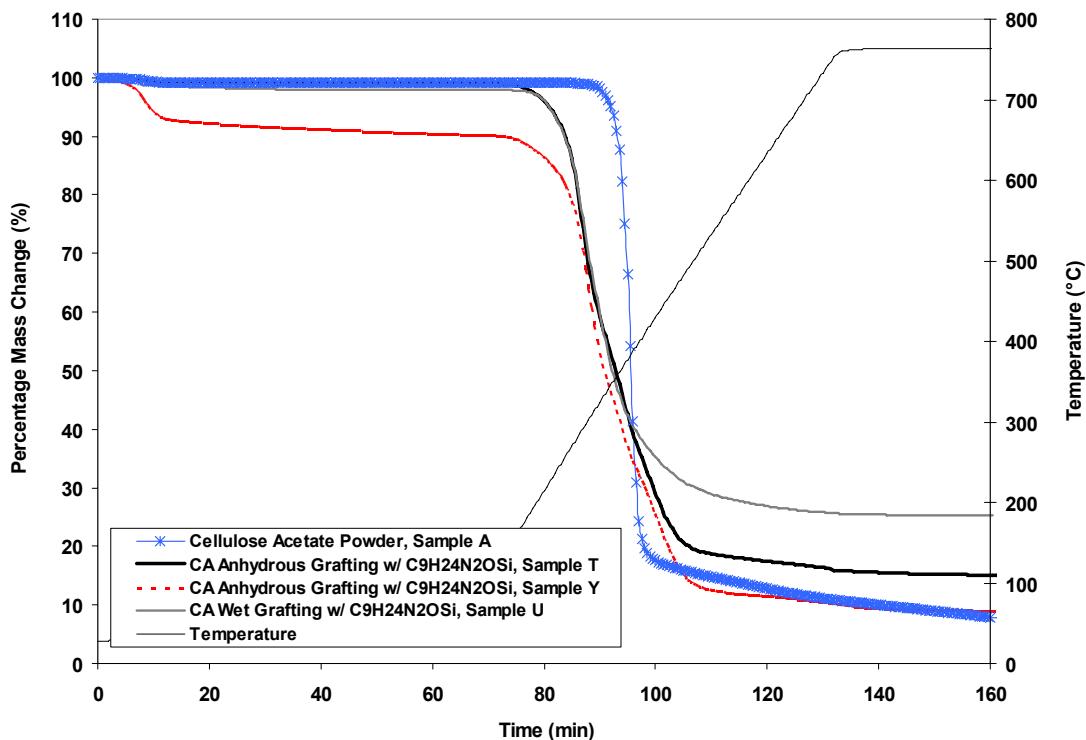


Figure 56. TG curves of CA, anhydrous and wet grafting of CA with $C_9H_{24}N_2OSi$ and sample Y

On the other hand, Figure 57 presents the TG curves of cellulose acetate samples grafted with $C_7H_{19}NOSi$ under dry and humid conditions. The anhydrous grafting reaction registered a weight loss of 81% at a degradation temperature of 200 °C and about 15% of the sample remained as char residue at the end of the test. The cellulose acetate sample grafted under humid conditions showed a smaller decrease in its thermal stability, starting to degrade at about 260 °C with a weight loss of about 74%. The rate of decomposition was a slightly faster than the dry grafted sample and yielded residual char of about 21%.

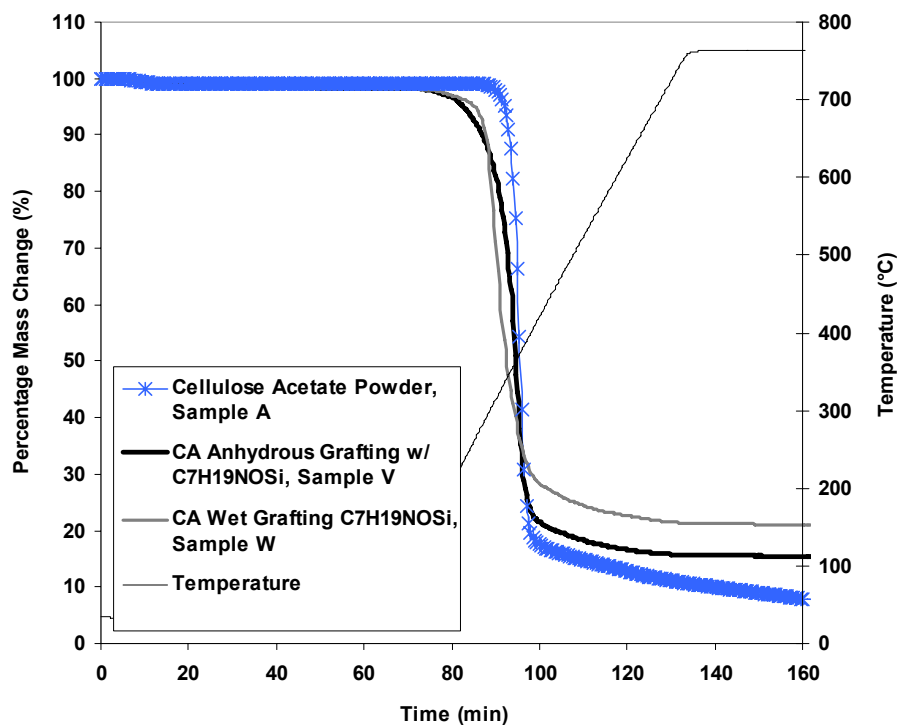


Figure 57. TG curves of CA, anhydrous and wet grafting of CA with $C_7H_{19}NOSi$

Overall, the thermal stability of all amine-grafted samples was affected to a similar extent by the introduction of aminosilane molecules in its molecular structure. However, the samples that presented the greater loss of thermal resistance were the ones grafted with $C_9H_{24}N_2OSi$. Particularly, sample *Y* obtained from prolonged water exposure and desorption of sample *T*, registered a further decreased in its thermal stability. It may be suggested that a trade-off exists between a high sorption capacity and thermal resistance. On the other hand, the presence of water during the grafting reaction did not influence degradation temperature, except for sample *W*, which degrades at a slightly higher temperature than the rest of amine-grafted species. It is inferred that the bulkier molecular structure of $C_9H_{24}N_2OSi$ dangling from the polymer chain affects the stability of the cellulose acetate molecular interactions, resulting in a new structure with less resistance to thermal treatments.

7.2.6 Scanning Electron Microscopy

Scanning electron micrographs of cellulose acetate and its aminosilane-grafted samples are presented in Figure 58. SEM images for high-acetyl content cellulose acetate powder grafted with $C_9H_{24}N_2OSi$ and $C_7H_{19}NOSi$ under anhydrous and humid conditions revealed a wide particle size distribution. Surface morphologies of the particles are very heterogeneous and rough. This may be the results of multiple reaction steps affecting the original particle size and homogeneity of the commercial polymer. Although the SEM images are not particularly revealing, they were included for consistency with the characterization analysis done to all samples.

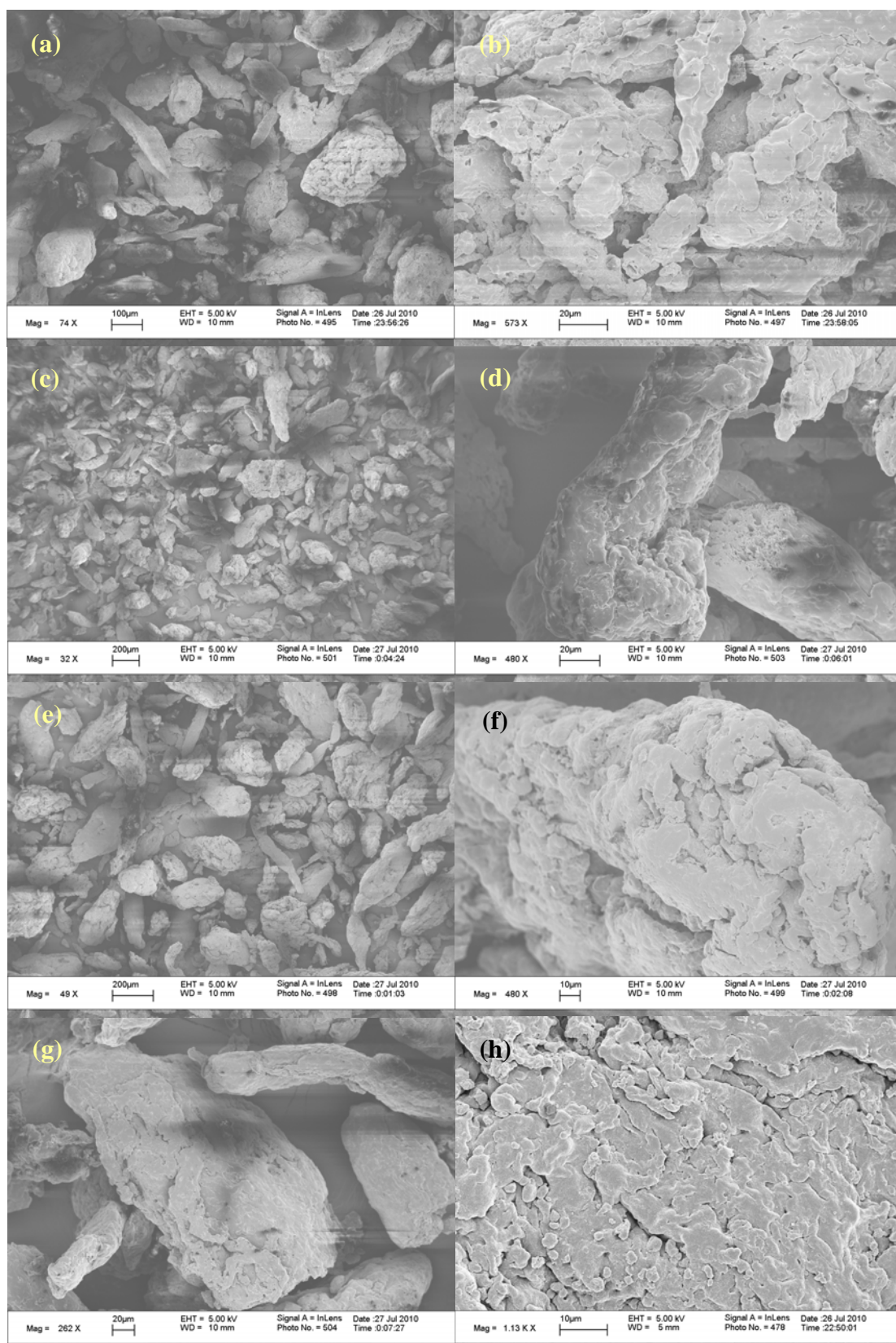


Figure 58. SEM images of (a) and (b): sample *T*; (c) and (d): sample *U*; (e) and (f): sample *V*; (g) and (h): sample *W*.

7.3 Discussion

The anhydrous and humid grafting of aminosilanes on high-acetyl content cellulose acetate powder under a set of optimum reaction conditions was addressed as the final approach of this research. Through this experimental pathway, it was discovered that the conventional procedure to graft amine functionalities into hydroxylated materials actually works well for high-acetyl content cellulose acetate if a set of special reaction conditions and the appropriate aminosilane species is used.

High-acetyl content, acetone-soluble cellulose acetate was subjected to a grafting reaction with two different types of aminosilanes, in the presence and absence of water. A diaminosilane ($C_9H_{24}N_2OSi$) and a monoaminosilane ($C_7H_{19}NOSi$) were reacted and characterized under the same reaction conditions in order to allow the comparison of amine loadings and improvement of CO_2 sorption capacity. The presence of two amine functionalities in $C_9H_{24}N_2OSi$ was useful to investigate the effect of multiple amine groups per aminosilane molecule on the cellulose acetate sorption capacity and overall stability. The existence of a single methoxy and ethoxy group in each molecule, respectively, should facilitate the controlled grafting of aminosilane functionalities. In addition, the grafting reactions were run under dry and humid conditions in order to determine the effect of water on the successful aminosilane grafting of the support.

The type and amount of solvent (anhydrous toluene), and the dose of aminosilane species employed were based on widely used literature values. The temperature of the reaction lowered to 70 °C and the drying procedures and inert conditions applied in anhydrous grafting reactions were based on previous experimental work from this study. These rigorous dry and inert conditions during the whole reactions were applied in order ensure the absence of any water other than those intentionally introduced. The reaction time was extended to 24 h in order to allow better diffusion of the reactants through the polymer chains. For humid grafting reactions, the amount of water used was based on the methodology previously used to find optimum amounts of specific reactants. The different solvent rising procedure was based on findings from the literature suggesting that rinsing with water impacts considerably the structure of the grafted aminosilanes, since water can completely remove some hydrogen bonded aminosilanes weakly attached to the supports before the drying step [25]. On this regard, it was found that drying procedures are also critical for ensuring covalent bond formation by condensation of hydrogen bonded silanol groups [21].

The described conditions were applied to as received commercial cellulose acetate with a degree of substitution of about 2.5, that is, acetate groups are occupying an average of 2.5 out of 3 available positions for acetyl substitution in each glucoside unit. The remaining positions are occupied by hydroxyl groups, averaging 3.5 wt% of the polymer. Elemental analysis results demonstrate that, when working at anhydrous conditions, diaminosilane $C_9H_{24}N_2OSi$ accommodated a higher amount of amine functionalities into the polymer backbone than the monoaminosilane used. However,

working under humid conditions, $C_7H_{19}NOSi$ grafted a higher amount of amino groups. This interesting finding could be explained by the fact that under anhydrous conditions the only available reactive hydroxyl groups are those dangling from the polymer backbone. Therefore, the reactivity of the alkoxy functionalities from the aminosilane molecule greatly influences the success of the reaction. According to Gelest, ethoxy silanes are essentially non-reactive in water-free environments and require catalysis for suitable reactivity. It has been found that the amine functionality in aminosilanes acts like a catalyst and enhances its reactivity [21]. However, the presence of only one amine group per $C_7H_{19}NOSi$ molecule decreases the overall amine loading. On the other hand, Gelest also suggests that only methoxysilanes are capable of reacting under anhydrous conditions [66]. Therefore, the highly reactive methoxy functionality in $C_9H_{24}N_2OSi$ and the presence of two amine functionalities per aminosilane molecule are responsible for the high amine loading achieved by $C_9H_{24}N_2OSi$ under anhydrous conditions. On the contrary, the presence of water in the reaction catalyzes the reactivity of the ethoxy functionality in $C_7H_{19}NOSi$ and increases its fixation into the polymer matrix. However, the opposite effect occurs when working with $C_9H_{24}N_2OSi$ under wet conditions, since the higher reactivity of the methoxy functionality increases its sensitivity to polymerization. Once polymerized, the diaminosilane species loses its reactivity toward cellulose acetate hydroxyl functionalities because of the loss of its only reactive methoxy group.

These findings highlight the relevance of understanding the chemical behavior of the selected aminosilane species for the grafting reactions in the presence or absence of

water. Several literature reports using triethoxy and trimethoxy-aminosilanes remark on the benefits of water presence during aminosilane grafting reactions on silica-base supports [18, 21, 34, 35]. Not all the three alkoxy ligands from these aminosilane species completely react with the surface hydroxyl groups from the silica support, so the presence of water molecules helps to consume the unreacted alkoxy ligands and complete the surface coverage. It is suggested that water increases the surface density of hydroxyl groups on the supports or initiates the hydrolysis of unreacted alkoxy groups with free aminosilanes still present in the solvent phase, starting a polymerization process that enhances the surface coverage when a free alkoxy functionality from these polymers finally gets linked to the silica surface. However, when working with aminosilanes with single methoxy/ethoxy functionalities, the polymerization effect induced by the presence of water in the reaction consumes the only reactive alkoxy functionality of the grafting agents and avoids further grafting of the aminosilanes polymers into the substrate.

Sample *T*, high-acetyl content cellulose acetate powder grafted with $C_9H_{24}N_2OSi$ under anhydrous conditions, achieved the highest amine loading and the highest improvement in CO_2 sorption capacity. The amine load achieved by this sample was 5.18 mmol amine(nitrogen)/g sample. Published work on amine-grafted silica-based adsorbents prepared under anhydrous conditions and applied for CO_2 adsorption have reported values of amine content in the range of 1.20-2.57 mmol amine(nitrogen)/g final material for monoamino-trialkoxysilanes, 3.07-3.76 mmol amine(nitrogen)/g final material for diamino-trialkoxysilanes, and 3.86-6.11 mmol amine(nitrogen)/g final material for triamino-trialkoxysilanes [4, 5, 16, 17, 21, 34, 47-49]. Water-aided amine-

grafted silica CO₂ adsorbents prepared with monoamino-trialkoxysilanes have reached amine contents in the range of 2.61-3.99 mmol amine(nitrogen)/g final material. When a diamino-trialkoxysilane has been used in this humid grafting procedures, a range of 2.64-4.61 mmol amine(nitrogen)/g final material has been reported, and the use of triamino-trialkoxysilanes has yielded amine contents of 5.80-7.98 mmol amine(nitrogen)/g final material [18, 21, 34, 35]. Therefore, the amine loading achieved by sample *T* surpassed by about 38% the highest amine content reported for silica-based sorbents grafted with diamino-trialkoxysilanes under anhydrous conditions. Likewise, it outranged by 12% the highest amine loading reported in the literature for wet grafting of diamino-trialkoxysilanes on silica-based supports. In addition, the amount of loaded amines on sample *T* is in good correspondence with the theoretical value of amine content resulting from the graft of one molecule of C₉H₂₄N₂OSi per glucoside unit (~ 6.70 wt%).

At a pressure of about 1 atm, sample *T* was capable of adsorbing about 27 cc (STP) CO₂/cc sorbent or about 1.01 mmol CO₂/g sorbent. At about 5 atm, sample *T* was able to sorb about 39.2 cc (STP) CO₂/cc sorbent or 1.46 mmol CO₂/g sorbent. These sorption capacities turn out to be very competitive when compared to literature values of dry sorption capacity from aminated silica-based supports. Dry sorption capacities reported for anhydrous grafting of monoamine-trialkoxysilanes grafted-silicas are reported to achieve capacities in the range of 0.41 to 1.59 mmol CO₂/g sample. Diamino-trialkoxysilane species grafted with similar procedures have reported sorption capacities of 0.87–1.66 mmol CO₂/g sample. Triamino-trimethoxysilane-grafted silicas sorption capacities for anhydrous grafting have a sorption capacity range of 0.97 to 1.55 mmol

CO₂/g sample. The addition of water to the grafting reactions in silica-based supports has not been of great aid in terms of sorption capacities, since monoamine-trialkoxysilanes grafted-silicas have reported values of sorption capacity of 0.10-0.66 mmol CO₂/g sample, while diamino-trialkoxysilane grafting has sorption capacities of 0.57-1.36 mmol CO₂/g sample. Triamino-trimethoxysilane-grafted silicas have increased their capacities under wet conditions up to 1.58-2.65 mmol CO₂/g sample [5, 16-18, 21, 34, 35, 47, 48]. The preliminary sorption equilibration time of sample *T* was about 3.5 h, very similar to that of pure cellulose acetate.

Sample *T* captured an additional amount of CO₂ in the order of 0.78 mmol CO₂ per gram of sample, that is, it achieved an amine efficiency of 0.15 mol CO₂ per mole of amines grafted. Amine-CO₂ interactions during the sorption tests are affected by the possibility of amine hydrogen bonding between amine groups or with the remaining hydroxyl groups, leading to a reduced amount of amine functionalities available for CO₂ sorption. Amine efficiencies values reported in the literature for anhydrous grafting of monoamine-trialkoxysilanes on silica-based adsorbents are in a range of 0.20-0.69 mol CO₂/mol amine, 0.23-0.46 mol CO₂/mol amine for diamino-trialkoxysilane grafted-silicas, and 0.17-0.31 mol CO₂/mol amine for triamino-trimethoxysilane graftings. On the other hand, water-aided graftings of monoamine-trialkoxysilanes on silica-based adsorbents has showed CO₂/N ratios of 0.02-0.25 mol CO₂/mol amine, 0.22-0.30 ratios for diamino-trialkoxysilane grafted-silicas, and 0.25-0.33 mol CO₂/mol amine for triamino-trimethoxysilane graftings [5, 16-18, 21, 33, 34, 46, 47].

Therefore, although there are other CO₂ sorbents with equal or higher sorption capabilities, it is believed that the improvement in cellulose acetate sorption capacity achieved here is promising. The simplicity of the preparation method and the low cost of the reactants make this procedure an attractive approach worth to be further developed.

Dissolution of the powdered sorbent samples is important in order to allow further practical applications in the form of films or fibers. Therefore, all the aminated samples were subjected to solubility tests in order to find a suitable solvent capable of dissolving them. Solubility tests were performed using common solvents like acetone, dichloromethane, chloroform, ethanol, methanol, tetrahydrofuran, and N-methyl-2-pyrrolidone. None of these solvents were capable of dissolving the grafted cellulose acetate powders. This may be evidence of polymer crosslinking due to the addition of aminosilanes. Further work is needed in order to overcome this issue.

CHAPTER 8

SUMMARY, CONCLUSIONS AND RECOMMENDATIONS

FOR FURTHER WORK

8.1 Summary

The objective of this research study has been the design and development of a suitable experimental strategy to improve the CO₂ sorption capacity of high-acetyl content cellulose acetate. The present report have described in detail and chronological order the different experimental approaches attempted in order to accomplish the objective.

The initial experimental approach pursued was the grafting of aminosilanes on high-acetyl content cellulose acetate powder under literature-based reaction conditions. A conventional humid grafting procedure was chosen as a starting point based on its extensive use and degree of success among the scientific community working in the area of aminosilane-modified silica supports. However, the set of reaction conditions utilized did not alter significantly the chemical structure of cellulose acetate and very low amounts of amines were loaded into the polymer chains. Sorption capacity characterization evidenced a decrease in the CO₂ sorption capacity of the reacted cellulose acetate samples. The analysis of the possible reasons for failure pointed out to

the lack of enough hydroxyl groups pending from the polymer backbone available for reaction with aminosilanes.

In order to increase the amount of hydroxyl functionalities dangling from the cellulose acetate chains and the reactivity of the polymer toward aminosilanes, a de-acetylation procedure was applied. The prolonged acidic hydrolysis yielded a highly hydroxylated polymer soluble in water. Dense films were solution-cast and subjected to a conventional anhydrous grafting method under the previous set of reaction conditions. Despite its high degree of hydroxylation, the films only incorporated a negligible amount of amines and its CO₂ sorption capacity was decreased considerably. It was found that hydroxyl groups from water-soluble cellulose acetate have a limited reactivity due to strong hydrogen bonding among them, preventing reaction with aminosilanes.

The following experimental pathway adopted to overcome the lack of reactivity of the polymer consisted in the preparation of a low-acetyl content cellulose acetate/titanium(IV) oxide sorbent based on published literature. At this stage of the research, it was envisioned that the reaction of the de-acetylated polymer with titanium tetrachloride would improve the reactivity of the material by breaking down the strong hydrogen bonding network and introducing titanium hydroxide functionalities in replacement. However, the persistent water-solubility of the films after the reaction forced us to follow different solvent rinsing procedures to exclude water from the post-treatment of the cellulosic\titanium(IV) hybrid polymer. At the same time, the discovery of a reaction intermediate with plenty of ethoxide functionalities attached to the titanium

centers determined the final course of the approach. In order to retain on the polymer chain the majority of the ethoxy functionalities with good potential for effectively CO₂ capture, a total anhydrous procedure was attempted. The objective was to avoid the hydrolysis of the ethoxy groups and further evolution into more stable titanium oxides functionalities. However, the elevated ease of hydrolyzation of titanium ethoxide functionalities led to the formation of a cellulose acetate/titanium(IV) oxide material. However, it was discovered that this new hybrid material can develop a significantly improved CO₂ sorption capacity when prepared under a set of optimum reaction conditions. The persistent water solubility of the titanium-reacted films suggested that the chemical treatment took place mainly at the surface of the polymer and its vicinity. A considerable amount of hydroxyl groups from the internal entangled polymer chains may remain unreacted. It has been suggested that longer reaction times are desirable in order to allow the penetration of the reactants to all regions of the polymer matrix. However, polymer degradation and a decrease in the CO₂ sorption capacity at extended reaction times suggested the existence of a trade-off between higher fixation of desirable functionalities and higher material degradation.

The relative success achieved by the previous approach motivated a last experimental pathway consisting in the grafting of aminosilanes into high-acetyl content cellulose acetate under a set of optimum reaction conditions. The conditions used in this approach derived from previous experimental approaches of the present study and from the literature. The use of a diamino-monomethoxysilane species as grafting agent under total anhydrous conditions greatly favored a high loading of amines into the polymer

structure. A significant increase in the CO₂ sorption capacity was registered for the sample with highest amine loading. In addition, exposure of the sorbent to water vapor did not negatively affect its sorption capacity, rather it enhances it. It was concluded that a set of optimum conditions exists for the successful aminosilane grafting of high-acetyl content cellulose acetate.

Two different types of cellulose acetate-based promising sorbents for CO₂ capture have been developed in the present research. On one hand, a low-acetyl content cellulose acetate/titanium(IV) oxide hybrid sorbent has been designed in the form of a film that is capable to adsorb up to 13.60 cc (STP) CO₂/ cc sorbent at 1 atm of pressure and 49.27 cc (STP) CO₂/ cc sorbent at equilibrium pressures of 5 atm. This represents an additional capture of about 0.22 mmol CO₂/g sorbent at 1 atm and 0.97 mmol CO₂/g sorbent at 5 atm after the titanium modification of cellulose acetate. However, the sorbent dissolves in water. On the other hand, an aminosilane functionalized cellulose acetate sorbent in powder form has been tailored to adsorb up to 27 cc (STP) CO₂/ cc sorbent at 1 atm and about 39.2 cc (STP) CO₂/ cc sorbent at 5 atm. Its amine loading is about 5.18 mmol amine(nitrogen)/g sorbent. The sorbent captured an additional amount of CO₂ in the order of 0.78 mmol CO₂ per gram of sorbent at 1 atm and 0.84 mmol CO₂ per gram of sorbent at 5 atm. The exposure of the sorbent to water vapor slightly increases its sorption capacity on a second CO₂ sorption cycle. The new capacity of the sorbent reached 30 cc (STP) CO₂/cc sorbent at 1 atm and 44.5 cc (STP) CO₂/cc sorbent at 5 atm. This sorbent represents a very promising option for further investigation. Moreover, in the presence of

humidity, further increases in sorption capacity are expected based on higher amine efficiencies known to occur in humid environments.

8.2 Conclusions

The present research has been a valuable and enriching learning experience that has opened the door to an interesting variety of research possibilities in the area of aminosilane functionalization of polymeric sorbents. Among the different findings encountered during the course of the study, the following are worth to be clearly reminded.

1. The CO₂ sorption capacity of commercial high-acetyl content cellulose acetate can be significantly improved by the grafting of aminosilanes functionalities to the polymer chains if a set of optimum reaction conditions is applied. These conditions can be significantly different to those widely used in the literature for similar materials and, therefore, it is important to reserve a time to find them.
2. For commercial cellulose acetate with acetyl content in the range of 39.8-40 wt%, it has been found that the optimum grafting conditions of 3.0 mL C₉H₂₄N₂OSi/g sample added, 150 mL toluene as solvent, 70 °C, 24 h of reaction, a total anhydrous and inert atmosphere and the use of toluene and hexanes for solvent rinsing yields an amount of grafted amines of about 7 wt%.

3. The chemical reactivity of the aminosilane species under anhydrous or humid grafting conditions has a deep impact in the amounts of amine loadings. Aminomethoxysilanes are among the most reactive organosilanes under anhydrous conditions, while aminoethoxysilanes have limited reactivity in the absence of water. Therefore, special attention has to be put on the aminosilane species elected for the grafting reactions.
4. An additional number of factors determine the success of the aminosilanes grafting reaction in cellulose acetate, namely, the presence of water, the amount of aminosilane species added, the reaction time and temperature, the solvent rinsing procedures and the drying of the grafted materials.
5. Cellulose acetate with the highest amine loading (~7 wt%) also registered the highest increment in CO₂ sorption capacity, reaching values of 27 cc (STP) CO₂/cc sorbent at 1 atm and about 39.2 cc (STP) CO₂/cc sorbent at 5 atm.
6. The aminosilane functionalized cellulose acetate presenting the higher amine loading and the higher increase in CO₂ sorption capacity did not degrade in the presence of water; on the contrary, its sorption capacity was enhanced to 30 cc (STP) CO₂/cc sorbent at 1 atm and 44.5 cc (STP) CO₂/cc sorbent at 5 atm. Therefore, it can be concluded that aminosilane functionalized cellulose acetate have potential for industrial application if transformed into a more suitable substrate form.
7. The aminosilane functionalized cellulose acetate sorbents displayed a relative short sorption equilibration time of about 2 h in the first sorption cycle and about 4 h in the second sorption cycle. After exposure to water vapor, the sorbents

sorption equilibration time increased, however this can be easily caused by particle agglomeration. Further systematic kinetics studies are needed. The equilibration time can presumably be reduced by using a highly porous fiber as opposed to dense particles or films.

8. Low-acetyl content cellulose acetate/titanium(IV) oxide films are alternative CO₂ sorbents with a sorption capacity of about 13.60 cc (STP) CO₂/ cc sorbent at 1 atm and 49.27 cc (STP) CO₂/ cc sorbent at 5 atm, but presents a rather long sorption equilibration time of about 48 h. Water-solubility, a much complex preparation method, and slow sorption kinetics make this sorbents less attractive for development on industrial applications.
9. The successful preparation of low-acetyl content cellulose acetate/titanium(IV) oxide films with enhanced CO₂ sorption capacity involves the application of a set of optimum reaction conditions; these are: addition of 0.40 mL TiCl₄/g sample, 100 mL of carbon tetrachloride as solvent, 70 °C, 5 h of reaction, a total anhydrous and inert atmosphere at all times and the use of carbon tetrachloride for solvent rinsing and 250 mL ethanol for prolonged immersion. The application of these conditions yields an amount of grafted titanium of about 2.08 wt%.
10. The preparation of low-acetyl content cellulose acetate/titanium(IV) oxide films with identical chemical characteristics is difficult to achieve, since several factors can affect the chemical composition of the products, like film defects, limited diffusion of the reactants through the film matrix, contact with atmospheric moisture, extent of degradation by hydrochloric acid, among others.

8.3 Recommendations for Further Work

Certainly, there is a lot of room for further investigation on both types of cellulose acetate derived sorbents. For the case of low-acetyl content cellulose acetate/titanium(IV) oxide film material, future work on the following issues is recommended:

1. Improvement of the reaction conditions to allow full substitution of the hydroxyl groups with titanium oxide and ethoxide functionalities in regions of the polymer where the effective transport and diffusion of the reactants may be hindered is important. In turn, this will suppress the present water-solubility property of the sorbent.
2. Research aimed to achieve the dissolution of low-acetyl content cellulose acetate in a solvent different than water, in order to investigate the efficiency of a TiCl_4 reaction in complete dissolution of the reactants also should be pursued.
3. Hindering of the water-solubility of the present sorbent by finding a solvent capable to swell the films and crosslink them with a suitable crosslinker agent is also important.
4. Finally, testing of the proposed TiCl_4 reaction procedure in fiber sorbents.

On the other hand, the amine-grafted high-acetyl content cellulose acetate powder sorbent is a very promising research option. Future work is recommended in the following areas:

1. Tuning up the optimal reaction conditions to find out further improvements in the CO_2 sorption capacity.

2. Investigation of the effects on the sorbent sorption capacity of a higher number of CO₂ sorption cycles.
3. Investigation of the sorbent sorption capacity when exposed to humid CO₂ cyclic sorption tests.
4. Research about the effectiveness of the aminosilanes grafting reaction in cellulose acetate fiber sorbents at optimal reaction conditions.

There are a number of obstacles to overcome in the development of the CO₂ sorbents described in this study. However, they are certainly a promising research area worth to be developed in the future. Success of the developed materials will depend on the effective improvement of the reaction conditions to synthesize them, on finding suitable pathways to transform the modified sorbents into useful substrate forms, like films or fibers, and its efficient performance over cyclic CO₂ sorption systems.

REFERENCES

1. West, P. (2005) *After Two Large Annual Gains, Rate of Atmospheric CO₂ Increase Retrurns to Average*. NOAA Magazine.
2. NOAA, *Mauna Loa CO₂ Annual Mean Data*. 2010, National Oceanic and Atmospheric Administration.
3. U.S. Energy Information Administration, D.o.E., *Emissions of Greenhouse Gases in the United States 1985-1990*. 1993, U.S. Department of Energy: Washington, D.C. p. 16.
4. Hiyoshi, N., Yogo, K., Yashima, T. , *Adsorption of Carbon Dioxide on Aminosilane-modified Mesoporous Silica* Journal of the Japan Petroleum Institute, 2005. **48**(1): p. 29-36.
5. Harlick, P.J.E., Sayari, A., *Applications of Pore-Expanded Mesoporous Silica. 3. Triamine Silane Grafting for Enhanced CO₂ Adsorption*. Industrial and Engineering Chemistry Research 2006. **45**: p. 3248.
6. Khatri, R.A., Chuang, S. S. C., Soong, Y., Gray, M. , *Thermal and Chemical Stability of Regenerable Solid Amine Sorbent for CO₂ Capture*. Energy & Fuels, 2006. **20**: p. 1514-1520.
7. Feng, B., Du, M., Dennis, T. J., Anthony, K., Perumal, M. J. , *Reduction of Energy Requirement of CO₂ Desorption by Adding Acid into CO₂-loaded Solvent*. Energy Fuels, 2010. **24**: p. 213–219.
8. Li, Y., *Study on Corrosion and Material Selection for Desulphurization Unit in Refinery*. Petroleum Refinery Engineering, 2008. **38**: p. 24-27.
9. Veltman, K., Singh, B., Hertwitch, E.G., *Human and Environmental Impact Assessment on Postcombustion CO₂ Capture Focusing on Emissions from Amine-*

based Scrubbing Solvents to Air. Environmental Science and Technology 2010. **44**: p. 1496–1502.

10. Bredesen, R., Jordal, K., Bolland, O., *High-temperature Membranes in Power Generation with CO₂ Capture*. Chemical Engineering and Processing 2004. **43**(9): p. 1129-1158.
11. Kim, S., Ida, J., Guliants, V. V., Lin, Y. S., *Functionalised Mesoporous Silica Membrane for the Separation of Carbon Dioxide*. International Journal of Environment Technology and Management, 2004. **4**(1-2): p. 21.
12. Lively, R.P., Chance, R. R., Kelley, B. T., Deckman, H. W., Drese, J. H., Jones, C. W., Koros, W. J. , *Hollow Fiber Adsorbents for CO₂ Removal from Flue Gas*. Industrial and Engineering Chemistry Research, 2009. **48**: p. 7314–7324.
13. Su, F., Lu, C., Kuo, S. C., Zeng, W. , *Adsorption of CO₂ on Amine-functionalized Y-type Zeolites*. Energy Fuels, 2010. **24**: p. 1441–1448.
14. Plaza, M.G., Pevida, C., Arias, B., Casai, M. D., Martin, C. F., Fermoso, J., Rubiera, F., Pis, J. J. , *Different Approaches for the Development of Low-cost CO₂ Adsorbents*. Journal of Environmental Engineering, 2009. **135**: p. 426–432.
15. Czakkel, O., Onyestyák, G., Pilatos, G., Kouvelos, V., Kanellopoulos, N., László, K. , *Kinetic and Equilibrium Separation of CO and CO₂ by Impregnated Spherical Carbons*. Microporous and Mesoporous Materials 2009. **120**: p. 76–83.
16. Huang, H.Y., Yang, R. T., Chinn, D., Munson, D. L., *Amine-Grafted MCM-48 and Silica Xerogel as Superior Sorbents for Acidic Gas Removal from Natural Gas*. Industrial and Engineering Chemistry Research 2003. **42**(2427).
17. Knowles, G.P., Delaney, S. W., Chaffee, A. L., *Amine-Functionalised Mesoporous Silicas as CO₂ Adsorbents*. Studies in Surface Science and Catalysis, 2005. **156**: p. 887.
18. Zheng, F., Tran, D. N., Busche, B. J., Fryxell, G. E., Addleman, R. S., Zemanian, T. S., Aardahl, C. L., *Ethylenediamine-Modified SBA-15 as Regenerable CO₂ Sorbent*. Industrial and Engineering Chemistry Research, 2005. **44**: p. 3099.

19. Yue, M.B., Chun, Y., Cao, Y., Dong, X., Zhu, J. H., *CO₂ Capture by As-prepared SBA-15 with an Occluded Organic Template*. *Advanced Functional Materials* 2006. **16**: p. 1717–1722.
20. Knöfel, C., Martin, C., Hornebecq, V., Llewellyn, P. L., *Study of Carbon Dioxide Adsorption on Mesoporous Aminopropylsilane-Functionalized Silica and Titania Combinig Microcalorimetry and in Situ Infrared Spectroscopy*. *Journal of Physical Chemistry C*, 2009. **113**: p. 21726-21734.
21. Harlick, P.J.E., Sayari, A., *Applications of Pore-Expanded Mesoporous Silica. 5. Triamine Grafted Material with Exceptional CO₂ Dynamic and Equilibrium Adsorption Performance*. *Industrial & Engineering Chemistry Research*, 2007. **46**(2): p. 446-458.
22. Couck, S., Denayer, J. F. M., Baron, G. V., Remy, T., Gascon, J., Kapteijn, F. , *An Aminefunctionalized MIL-53 Metal-organic Framework with Large Separation Power for CO₂ and CH₄*. *Journal of the American Chemical Society*, 2009. **131**: p. 6326–6327.
23. Yazaydin, A.O., Snurr, R. Q., Park, T. H., Koh, K., Liu, J., LeVan, M. D., Benin, A. I., Jakubczak, P., Lanuza, M., Galloway, D. B., Low, J. J., Willis, R. R. , *Screening of Metal-organic Frameworks for Carbon Dioxide Capture from Flue Gas Using a Combined Experimental and Modeling Approach*. *Journal of the American Chemical Society*, 2009. **131**(18198–18199).
24. Rosenholm, J., Penninkanga, A., Linden, M., *Amino-functionalization of Large-pore Mesoscopically Ordered Silica by a One-step Hyperbranching Polymerization of a Surface-grown Polyethyleneimine*. *Chemical Communications* 2006: p. 3909–3911.
25. Serna-Guerrero, R., Belmabkhout, Y., Sayari, A. , *Modeling CO₂ Adsorption on Amine-functionalized Mesoporous Silica: 1. A Semi-empirical Equilibrium Model*. *Chemical Engineering Journal*, 2010. **161**: p. 173–181.
26. Jung, C.H., Kim, G. W., Han, S. H., Lee, Y. M., *Gas Separation of Pyrolyzed Polymeric Membranes: Effect of Polymer Precursor and Pyrolysis Conditions*. *Macromolecular Research*, 2007. **15**(6): p. 565-574.

27. Prabhakar, R.S., Freeman, B. D. , *Fluoropolymer/hydrocarbon Polymer Composite Membranes for Natural Gas Separation*. Advanced Materials for Membrane Separations, ACS Symposium Series, 2004. **876**: p. 106-128.
28. Long, V.T., Minhas, B. S., Matsuura, T., Sourirajan, S. , *Gas Chromatographic Method for the Measurement of Gas Sorption on Polymeric Materials* Journal of Colloid and Interface Science, 1988. **125**(2): p. 478-483
29. Denisova, G.P., Rakhlevskaya, M. N., Kuznetsova, S. L., *Sorption of Vapors and Gases by Cellulose Acetate Films*. Fibre Chemistry, 1996. **27**(6): p. 427-430.
30. Sada, E., Kumazawa, H., Yoshio, Y., Wang, S. T., Xu, P., *Permeation of Carbon Dioxide Through Homogeneous Dense and Asymmetric Cellulose Acetate Membranes*. J. Polym. Sci., Part B: Polym. Phys. , 1988. **26**(5): p. 1035-1048.
31. Stern, S.A., De Meringo, A. H., *Solubility of Carbon Dioxide in Cellulose Acetate at Elevated Pressures*. Journal of Polymer Science: Polymer Physics Edition, 2003. **16**(4): p. 735 - 751.
32. Seoane, B., Valladares, J. G., Aguilar,, *Permeabilidad de Gases a Presiones Subatmosféricas en Membranas de Acetato de Celulosa*. J. Anales de Fisica, Serie B: Aplicaciones, Metodos e Instrumentos, 1985. **81**: p. 80-87.
33. Pusch, W., Tanioka, A., Desalinisation, 1983. **46**: p. 425.
34. Raucher, D., Sefcik, M. D., *Gas Transport in Glassy Polymers as Predicted by the Matrix Model*. Polymer Preprints. , 1983. **24**: p. 87.
35. Daus, P.A., Pauley, C. R. , *Carbon Dioxide and Methane Separation from Natural Gas Streams, Especially in Enhanced Oil Recovery*. 2000.
36. Saji, A., Sakai, M., Ichikawa, M., *Separation and Recovery of Carbon Dioxide from Boiler Flue Gases*. 1994: Japan.
37. Mansson, P., Westfelt, L., Journal of Polymer Science Part A: Polymer Chemistry 1981. **19**: p. 1509.

38. Nie, L., Narayan, R. , *Grafting Cellulose Acetate with Poly(styrene-co-maleic anhydride) for Improved Dimensional Stability of Cellulose Acetate*. Journal of Applied Polymer Science, 1994. **54**: p. 601.
39. Abdel-Razik, E.A., *Grafting of Dichlorodimethylsilane onto Cellulose Acetate as a Model System in Homogeneous Media*. Polymer International, 1996. **40**: p. 1739.
40. Vidéki, B., Klébert, S., Pukánszky, B. , *Grafting of Caprolacton to Cellulose Acetate by Reactive Processing*. European Polymer Journal, 2005. **41**: p. 1699.
41. Guruprasad, K., H., Shashidhara, G. M . *Grafting, Blending, and Biodegradability of Cellulose Acetate*. Journal of Applied Polymer Science, 2004. **91**: p. 1716.
42. Liesiene, J., *Synthesis of Water-soluble Cationic Cellulose Derivatives with Tertiary Amino Groups*. Cellulose, 2010. **17**: p. 167.
43. Khidoyatov, A.A., Rogovin, Z. A., *Synthesis of Graft Copolymers of Cellulose Acetate with Polymers Containing Tertiary Amino Groups*. Fibre Chemistry, 1969. **1**(3): p. 70-71.
44. Babadzhanova, E.N., Bank, A. S., Askarov, M. A., Aikhodzhaev, B. I., Pogosov, Yu. L. , *Modification of Cellulose Acetates*. 1968.
45. Zhao, J.S., Yang, Z. Y., Zhang, Y. H., Yang, Z. Y., *Immobilization of Glucose Oxidase on Cellulose/Cellulose Acetate Membrane and its Detection by Scanning Electrochemical Microscope (SECM)*. Chinese Chemical Letters, 2004. **15**: p. 1361.
46. Bank, A.S., Askarov, M. A., Shakirova, E. N. , *Uzbekskii Khimicheskii Zhurnal* , 1968. **12**: p. 42.
47. Hestekin, J.A., Bachas, L. G., Bhattacharyya, D. , *Poly(amino acid)-Functionalized Cellulosic Membranes: Metal Sorption Mechanisms and Results*. Industrial & Engineering Chemistry Research, 2001. **40**: p. 2668-2678.

48. Biermann, C.J., Narayan, R., *Grafting of Poly(ethylenimine) onto Mesylated Cellulose Acetate, Poly(methyl methacrylate) and Poly(vinyl chloride)* Carbohydrate Polymers, 1990. **12**: p. 323.
49. Arockiasamy, D.L., Nagendran, A., Shobana, K. H., Mohan, D. , *Preparation and Characterization of Cellulose Acetate/Aminated Polysulfone Blend Ultrafiltration Membranes and their Application Studies* Separation Science and Technology, 2009. **44**(2): p. 398 - 421
50. Arockiasamy, D.L., Nagendran, A., Mohan, D. , *Studies on Cellulose Acetate/Aminated Poly(ether imide) Blend Ultrafiltration Membranes.* International Journal of Polymeric Materials, 2008. **57**(11): p. 997-1018
51. Lapenko, V.L., Slivkin, A. I., Smirnov, D. N., Zakharova, O. V., Suntsova, N. S., Dmitriev, L. A. , *Preparation of Amine-containing Cellulose Derivatives using Triethylenetetramine Copolymer.* 1990.
52. Liu, C.W., S. T., Lesch, D. A. , *High Plasticization-resistant Cross-linked Polymeric Membranes for Gas Separations.* 2010.
53. Friesen, D.T., Obligin, A. S., *Preparation and Uses of Semipermeable Siloxane-grafted Cellulosic Membranes.* 1989.
54. Puleo, A.C., Paul, D.R., Kelley, S.S. , *The Effect of Degree of Acetylation on Gas Sorption and Transport Behavior in Cellulose Acetate* Journal of Membrane Science, 1989. **47**: p. 301-332.
55. Koros, W.J., Paul, D. R., *Design Considerations for Measurement of Gas Sorption in Polymers by Pressure Decay.* Journal of Polymer Science Part B: Polymer Physics 1976. **14**: p. 1903.
56. Meng, L.Z., Du, C. Q., Chen, Y. Y., He, Y. B., *Preparation, Characterization, and Behavior of Cellulose-Titanium(IV) Oxide Modified with Organosilicone.* Journal of Applied Polymer Science, 2002. **84**: p. 61-66.
57. Da Silva, L.R.D., Gushikem, Y., Goncalves, M., D., C., Rodrigues Filho U., P., De Castro, S., C. , *Highly Dispersed Titanium(IV) Oxide on alpha-Cellulose*

- Surface: An XPS, SEM, and XRD Study*. Journal of Applied Polymer Science, 1995. **58**: p. 1669-1673.
58. Wada, M., Nishiyama, Y., Chanzy, H., Forsyth, T., Langan, P., *The Structure of Celluloses* Advances in X-Ray Analysis, 2008. **51**: p. 138-144.
 59. Tanghe, L.J., Genung, L. B., Mench, J. W., *Methods in Carbohydrate Chemistry*, ed. R.L. Whistler, Ed. Vol. 3. 1963, New York: Academic Press.
 60. Kamidem, K.S., M. , *Advances in Polymer Science*, 1987. **83**: p. 1.
 61. Fischer, S., Thümmel, K., Volkert, B., Hettrich, K., Schmidt, I., Fischer, K. , *Properties and Applications of Cellulose Acetate* Macromolecular Symposia, 2008. **262**(Structure and Properties of Cellulose): p. 89-96.
 62. Kiso, Y., Kitao, T. Nishimura, K., *Journal of Applied Polymer Science*, 1998. **71**: p. 1657.
 63. Takahashi, T., *Adsorption of N-methylcarbamates on Membrane Filters* Hokkaidoritsu Eisei Kenkyushoho, 2000. **50**: p. 75-77.
 64. Yartseva, N.M., Ryabukhova, T. O., Okisheva, N. A., Ramazaeva, L. F., Surkova, A. N., *Fibre Chemistry*, 2006. **30**: p. 260.
 65. Miura, M., Cole, C. A., Monji, N., Hoffman, A. S., *Temperature-dependent Adsorption/desorption Behavior of Lower Critical Solution Temperature (LCST) Polymers on Various Substrates* Journal of Biomaterials Science Polymer Edition 1994. **5**(6): p. 555-68.
 66. Gelest, *Silicon Compounds: Silanes and Silicones*, in *A Survey of Properties and Chemistry*, Gelest, Editor. 2008: Morrisville, PA.
 67. Lapenko, V.L., Slivkin, A. I., Smirnov, D. N., Zakharova, O. V., Suntsova, N. S., Dmitriev, L. A., *Preparation of Amine-containing Cellulose Derivatives using Triethylenetetramine Copolymer*, in *Otkrytiya, Izobret.* 1990, USSR USSR

68. Engelhardt, H., Orth, P. , *Alkoxy Silanes for the Preparation of Silica Based Stationary Phases with Bonded Polar Functional Groups* Journal of Liquid Chromatography, 1987. **10**(8-9): p. 1999-2022.
69. Caravajal, G.S., Leyden, D. E., Quinting, G. R., Maciel, G. E., *Structural Characterization of (3-aminopropyl)triethoxysilane-modified Silicas by Silicon-29 and Carbon-13 Nuclear Magnetic Resonance*. Analytical Chemistry, 1988. **60**(17): p. 1776-86.
70. Zhang, F.S., M. P., *Self-Assembled Molecular Films of Aminosilanes and Their Immobilization Capacities* Langmuir, 2004. **20**(6): p. 2309-2314.
71. Smith, E.A., Chen, W. , *How to Prevent the Loss of Surface Functionality Derived from Aminosilanes* Langmuir, 2008. **24**(21): p. 12405-9.
72. Joensson, U., Olofsson, G., Malmqvist, M., Ronnberg, I., *Chemical Vapor Deposition of Silanes*. Thin Solid Films, 1985. **124**(2): p. 117-23.
73. Everett, D.H., *Manual of Symbols and Terminology For Physicochemical Quantities and Units*, in *Definitions, Terminology and Symbols in Colloid and Surface Chemistry, Appendix II, Part I*, L.K. Koopal, Editor. 1971, International Union of Pure and Applied Chemistry, Division of Physical Chemistry: Washington, D.C.
74. Vannice, M.A., *Kinetics of Catalytic Reactions*. 2005, USA: Springer Science + Business Media, Inc.
75. Tsujita, Y., *Gas Sorption and Permeation of Glassy Polymers with Microvoids*. Progress in Polymer Science, 2003. **28**: p. 1377-1401.
76. Missouri, U.o. *Infrared Spectroscopy*. 1997 12/08/1997 [cited 2010 July 28, 2010]; Available from: <http://www.umsl.edu/~orglab/documents/IR/IR2.html>.
77. Clark, C., *IR Review Sheet*. 2006: Vancouver, WA.

78. Suthar, J.N., Patel, M. J., Patel, K. C., Patel, R. D. , *Studies on Structural Aspects of Cellulose Acetate*. Die Angewandte Makromolekulare Chemie, 1985. **130**: p. 125-136.
79. Lawrence-Berkeley, N.L., *Characteristic IR Band Positions*, U.S.D.o. Energy, Editor. 2009, ALS Infrared Beamlines: Berkeley, CA, USA.
80. Shinoda, S., Saito, Y. , *Journal of Colloid and Interface Science* 1985. **103**: p. 554.
81. White, L.D., Tripp, C. P. , *Reaction of (3-Aminopropyl)dimethylethoxysilane with Amine Catalysts on Silica Surfaces*. *Journal of Colloid and Interface Science*, 2000. **232**(2): p. 400-407.
82. Malm, C.J., Tanghe, L. J., Laird, B. C., Smith, G. D. , *Re-esterification during the Hydrolysis of Cellulose Acetate*. *Industrial and Engineering Chemistry Research* 1952. **74**: p. 4106.
83. Olaru, N., Olaru, L., *Cellulose Acetate Deacetylation in Benzene/Acetic Acid/Water Systems*. *Journal of Applied Polymer Science*, 2004. **94**: p. 1965–1968.
84. Baltrusaitis, J.J., J. H.; Grassian, V. H., *FTIR Spectroscopy Combined with Isotope Labeling and Quantum Chemical Calculations to Investigate Adsorbed Bicarbonate Formation Following Reaction of Carbon Dioxide with Surface Hydroxyl Groups on Fe₂O₃ and Al₂O₃* *Journal of Physical Chemistry B* 2006. **110**: p. 12005.
85. Wang, H., Li, B., Shi, B., *Porous Cellulose Acid-Base Properties*. *BioResources*, 2008. **3**(1): p. 3-12.
86. Launer, P.J. (1987) *Infrared Analysis of Organosilicon Compounds: Spectra Structure Correlations*. *Silicon Compounds Register and Review*, 100-103.
87. Kanan, S.M., Tze, W. T. Y., Tripp, C. P. , *Method to Double the Surface Concentration and Control the Orientation of Adsorbed (3-*

Aminopropyl)dimethylethoxysilane on Silica Powders and Glass Slides Langmuir, 2002. **18**(17): p. 6623-6627.

88. *Spectra-Structure Correlation, Qualitative Analysis*. 190-213.
89. Miyamoto, T., Sato, Y., Shibata, T. , ¹³C-NMR Spectral Studies on the Distribution of Substituents in Water-Soluble Cellulose Acetate. Journal of Polymer Science: Polymer Chemistry Edition, 1985. **23**(5): p. 1373-1381.
90. Busca, G., Lorenzelli, V., *Infrared Study of CO₂ Adsorption on Haematite*. Materials Chemistry, 1980. **5**: p. 213-224.
91. Vimont, A., Traver, A., Bazin, P., Lavalley, J. C., Daturi, M., Serre, C., Ferey, G., Bourrelly, S., Llewellyn, L., *Evidence of CO₂ Molecule Acting as an Electron Acceptor on a Nanoporous Metal–Organic-Framework MIL-53 or Cr³⁺(OH)(O₂C–C₆H₄–CO₂)*. Chemical Communications, 2007: p. 3291–3293.
92. Alfaya, R.V.S., Gushikem, Y. , 1999. **203**.
93. Kakos, G.A., Winter, G., *C-O and Ti-O Vibration Frequencies in Alkyltitanates*. Australian Journal of Chemistry 1968. **21**: p. 793-795.
94. Kriegsmann, H., Light, K., *Spektroskopische Untersuchungen an Titan- und Kieselsaure-Estern*. Zeitschrift für Elektrochemie, 1958. **62**(10): p. 1163-1174.
95. Ramadan, A.R., Yacoub, N., Amin, H., Ragai, J. , *The Effect of Phosphate Anions on Surface and Acidic Properties of TiO₂ Hydrolyzed from Titanium Ethoxide*. Colloids and Surfaces A: Physicochemical and Engineering Aspects, 2009. **352**: p. 118-125.
96. Barraclough, C.G., Bradley, D. C. Lewis, J., Thomas, I. M. , *The Infrared Spectra of Some Metal Alkoxides, Trialkylsilyloxides, and Related Silanols*. 1961. **510**: p. 2601.

97. Murashkevich, A.N., Lavitskaya, A. S., Barannikova, T. I., Zharskii, I. M., *Infrared Absorption Spectra and Structure of TiO₂–SiO₂ Composites*. Journal of Applied Spectroscopy, 2008. **75**(5): p. 730-734.
98. Turevskaya, E.P., Yanovskaya, M. I., Turova, N., Inorganic Materials, 2000. **36**: p. 260.
99. Wu, S.F., Zhu, Y. Q., *Behavior of CaTiO₃/Nano-CaO as a CO₂ Reactive Adsorbent* Industrial & Engineering Chemistry Research, 2010. **49**(6): p. 2701-2706.
100. Acetate, A.N.f.I.i.C. (2001) *Appendix 4: Deterioration Pathway of Cellulose Acetate* Assessment Guidelines **2010**.